Supplementary material to the EMEP Status Report 1/2015
Date: August 2015

METEOROLOGISK INSTITUTT
Norwegian Meteorological Institute

EMEP/MSC-W model performance for acidifying and eutrophying components, photo-oxidants and particulate matter in 2013

EMEP/MSC-W: Michael Gauss, Svetlana Tsyro and Anna C. Benedictow

EMEP/CCC: Anne-Gunn Hjellbrekke and Sverre Solberg

Supplementary material to EMEP Status Report 1/2015

Contents

CHAPTER 1

Introduction

This report is a supplement to the EMEP Status Report 1/2015 and presents a more detailed evaluation of the EMEP/MSC-W model. This report is available from the EMEP website (www.emep.int).

The EMEP/MSC-W model is evaluated with respect to acidifying and eutrophying components, photo-oxidants and particulate matter. Model results for 2013 are validated against measurements collected from the EMEP monitoring network for 2013.

Tables of model skill and time series plots are presented for different chemical species at individual EMEP measurement stations, along with scatter-plots and maps covering the EMEP domain.

As in previous evaluations, data from some measurement stations have been excluded from this evaluation for either of the following reasons:

- Problems have been identified in regard to the measurements (during Quality Control by EMEP-CCC).
- The measurement site is located in a mountain area, and the difference between its height above sea level and the mean elevation in the respective EMEP/MSC-W model grid cell is larger than 500m.

The agreement between model results and observations depends on a combination of several factors - the measurement accuracy (sampling and analysis), the representativeness of the measurement sites, the adequacy of emissions, and the model performance. Thus, any model underestimation or overestimation in the evaluation presented in the following chapters only implies that the modelled values are different from the observations, but is not necessarily an indication of model deficiency.

Chapter 2 deals with acidifiying and eutrophying components (sulphur and nitrogen species), Chapter 3 with photooxidants (ozone), and Chapter 4 with particulate matter.

CHAPTER 2

Acidifying and eutrophying components

M. Gauss, S. Tsyro, A. C. Benedictow and A.-G. Hjellbrekke

In this chapter the EMEP/MSC-W model is evaluated with respect to acidifying and eutrophying components. Section 2.1 includes an overview table of the model performance and scatter plots for acidifying and eutrophying components. In Section 2.2 we present time series plots for all EMEP stations with measurements in year 2013, while Section 2.3 contains combined maps of modelled and measured air concentrations and of concentrations in precipitation for selected species in 2013.

2.1 Scatter plots and tables

Evaluations of the EMEP/MSC-W model performance for acidifying and eutrophying components have been presented earlier in numerous EMEP reports (e.g. Gauss et al. 2014, Nyíri et al. 2013, Fagerli and Hjellbrekke 2008, Fagerli and Aas 2008).

In addition, an overview study of how the model performance has changed over the years was presented in Chapter 3 of EMEP Status Report 1/2013 (Simpson et al. 2013). The main conclusions of that study were:

- Year-to-year variations in model evaluation can be large, so evaluation statistics determined for one year cannot be assumed to be representative for general model performance;
- Model performance varies strongly among pollutants, often in an uncorrelated way. For example, model changes that improved SO_4^{2-} were associated with reduced performance for SO_2;
- Model performance is (as expected) generally better for secondary than for primary pollutants;

Component	N_{stat}	Obs.	Mod.	Bias (%)	RMSE	Corr.	IOA
NO_2 (μg(N) m^{-3})	73	2.03	1.90	-7	0.73	0.87	0.93
SO_2 (μg(S) m^{-3})	71	0.42	0.37	-11	0.36	0.53	0.70
SO_4^{2-}, sea salt corrected (μg(S) m^{-3})	23	0.40	0.30	-27	0.13	0.95	0.90
SO_4^{2-}, including sea salt (μg(S) m^{-3})	40	0.53	0.42	-22	0.16	0.89	0.88
NH_3 (μg(N) m^{-3})	14	0.70	0.77	11	0.44	0.69	0.81
NH_4^+ (μg(N) m^{-3})	22	0.74	0.60	-19	0.29	0.78	0.84
NH_3+NH_4^+ (μg(N) m^{-3})	36	1.32	1.39	5	0.58	0.81	0.88
NO_3^- (μg(N) m^{-3})	21	0.39	0.34	-13	0.20	0.88	0.88
HNO_3 (μg(N) m^{-3})	11	0.19	0.10	-45	0.20	0.42	0.52
NO_3^-+HNO_3 (μg(N) m^{-3})	42	0.51	0.45	-12	0.16	0.83	0.89
SO_4^{2-} wd (μg(S)m^{-2})	47	9353	8827	-6	94	0.69	0.82
SO_4^{2-} cp (μg(S)l^{-1})	47	0.28	0.25	-11	0.13	0.72	0.83
NH_4^+ wd (μg(N)m^{-2})	47	12185	13641	12	129	0.82	0.89
NH_4^+ cp (μg(N)l^{-1})	47	0.35	0.37	5	0.17	0.58	0.75
NO_3^- wd (μg(N)m^{-2})	47	10549	10390	-2	125	0.69	0.81
NO_3^- cp (μg(N)l^{-1})	47	0.29	0.28	-6	0.12	0.59	0.77
precipitation (mm)	47	39526	40471	2	236	0.81	0.88

Table 2.1: Comparison of model results and observations for 2013. Annual averages over all EMEP sites with measurements. N_{stat}= number of stations, wd=wet deposition, cp= concentration in precipitation, Corr. = spatial correlation coefficient, RMSE = root mean square error, IOA = index of agreement.

- A more systematic evaluation is needed, with all inputs and observations held constant while the model version is changed, in order to identify key factors behind changes in model performance (benchmarking);
- The latest model version shows a good level of performance across pollutants and years, generally better than older codes when all pollutants are considered together.

This year we present results from EMEP/MSC-W model version rv4.7, which is slightly different from model version rv4.5, which was used for last year's evaluation (Gauss et al. 2014). Recent changes in the model are described in Simpson et al. (2015). As last year, the meteorological input data are based on data from the ECMWF-IFS model.

Table 2.1 shows for each component the number of stations where measurements were available and data coverage criteria were satisfied (N_{stat}), measured yearly average over all stations (Obs), modelled yearly average over all stations (Mod), bias ($\frac{Mod-Obs}{Obs} \times 100\%$), correlation between observation and model for station yearly averages (Corr), root mean square error, Rmse ($\sqrt{\frac{1}{n}\sum_{i=1}^{n}(m_i - o_i)^2}$ where m_i and o_i are modelled and measured concentration at monitoring station *i*), and index of agreement (Willmott 1981, 1982). The index of agreement is calculated as follows: IOA= $1 - \frac{\sum_{i=1}^{N_{stat}}(m_i-o_i)^2}{\sum_{i=1}^{N_{stat}}(|m_i-Obs|+|o_i-Obs|)^2}$). It varies between 0 (theoretical minimum) and 1 (perfect agreement between observed and predicted values) and gives the degree to which model predictions are error free.

The scatter plots in Figures 2.1–2.3 are based on yearly averages of observed data at

EMEP stations with measurements in 2013. The lines on the scatter plots display deviations in the scatter of 30% ('30% line') and 50% ('50% line') relative bias, respectively. Relative bias is defined here as $\frac{Mod-Obs}{0.5\,(Mod+Obs)} \times 100\%$, where 'Mod' refers to yearly averaged modelled concentrations, while 'Obs' refers to yearly averaged measured concentrations.

In contrast to last year, we have also included daily means of available hourly measurements in this year's analysis. Thus, a much larger number of stations is taken into account this year, as compared to previous reports.

Sulphur dioxide in air

On average, SO_2 is somewhat underestimated (-11%) compared to measurements. Time series for SO_2 are shown in Figures 2.4–2.11. In 2012, several modifications to reduce the overestimation during the cold season were implemented (Fagerli et al. 2012). One of these was improved seasonal variation of the emissions implying a 10% displacement per decade from winter to summer in the model (Simpson et al. 2012) to better account for the fact that nowadays a larger part of emissions is released during the summer time with increasing use of air condition, and more importantly, the growth of telecommunications and computer hardware use.

Figure 2.1(a) shows that the largest overestimations for SO_2 occur at stations FR15, SE14, GB48 and RU18. One of these sites, Råö (SE14), is situated on the coast of southern Sweden. The overestimation of SO_2 at this site might indicate that the ship emissions included in the EMEP inventory are somewhat too high, or that the model resolution is too low for this area. FR15 is also located not too far from the coast.

For the Russian site, Danki (RU18), high discrepancies between the modelled and observed values have been identified also for other components and in previous years. Danki lies relatively close to Moscow, and this local influence might be the reason of the poor performance for this site.

Sulphate in air

Figures 2.1(b)–2.1(c) show EMEP model results compared to measurements for, respectively, sea salt-corrected sulphate, and sulphate including sea salt. In comparisons with measurements including sea salt, 7% of modelled sea salt[1] have been added to modelled suphate. The modelled and observed sulphate levels are in somewhat better agreement when sea salt sulphate is taken into account (e.g. the bias is -22% in the comparison where sea salt sulphate is added to chemically produced sulphate, while it is -27% without sea salt sulphate). Still, sulphate is generally somewhat underestimated in both comparisons.

In previous years there were several measurement sites where SO_4^{2-} was underestimated while there was an overestimation of SO_2, and other sites where the model underestimated both SO_4^{2-} and SO_2, with a higher under-prediction for sulphate. As the bulk production of SO_4^{2-} results from the oxidation of SO_2 to sulphuric acid in liquid clouds, these observations indicated that there was too little oxidation of SO_2 to sulphate in the model. In 2012 a change in the scheme for the oxidation of SO_2 to SO_4^{2-} was implemented in the EMEP model (Fagerli et al. 2012, Simpson et al. 2012) resulting in higher oxidation rate and, consequently, less underestimation of sulphate concentrations in air.

Time series for sulphate in air are shown in Figures 2.12–2.19.

[1] Sea salt is assumed to consist of approximately 7 % sulphate.

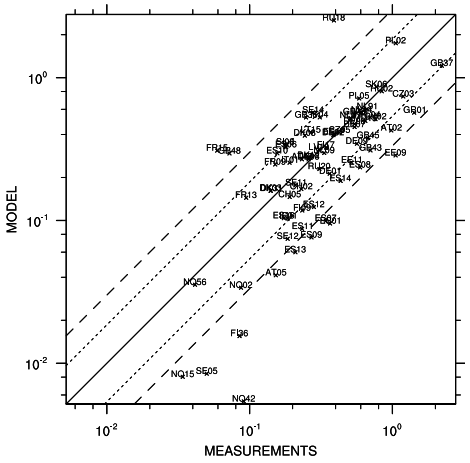

(a) SO_2

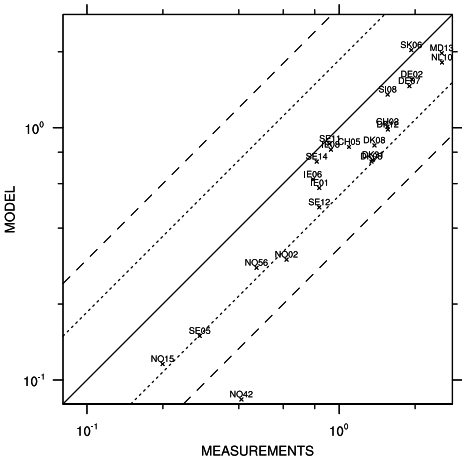

(b) SO_4^{2-}, measurements corrected for sea salt

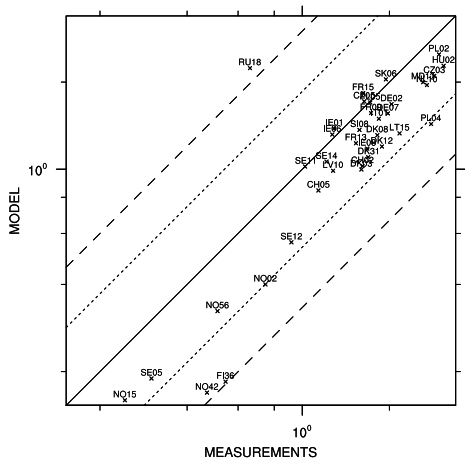

(c) SO_4^{2-}, including sea salt SO_4^{2-}

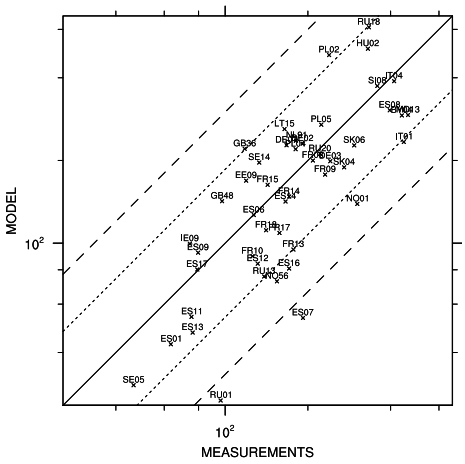

(d) SO_4^{2-} wet dep.

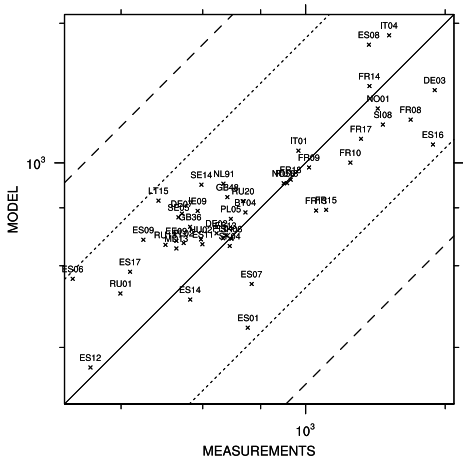

(e) Precipitation

Figure 2.1: Scatter plots of model results versus observations of a) sulphur dioxide [μg(S) m^{-3}], b+c) sulphate [μg(S) m^{-3}], d) wet deposition of sulphur [μg(S)m^{-2}], and e) precipitation [mm]. For sulphate concentrations, panel (b) shows a comparison of model results to sea salt corrected sulphate measurements, while panel (c) shows model results of sulphate plus 7 % sea salt in comparison to non-corrected measurement data.

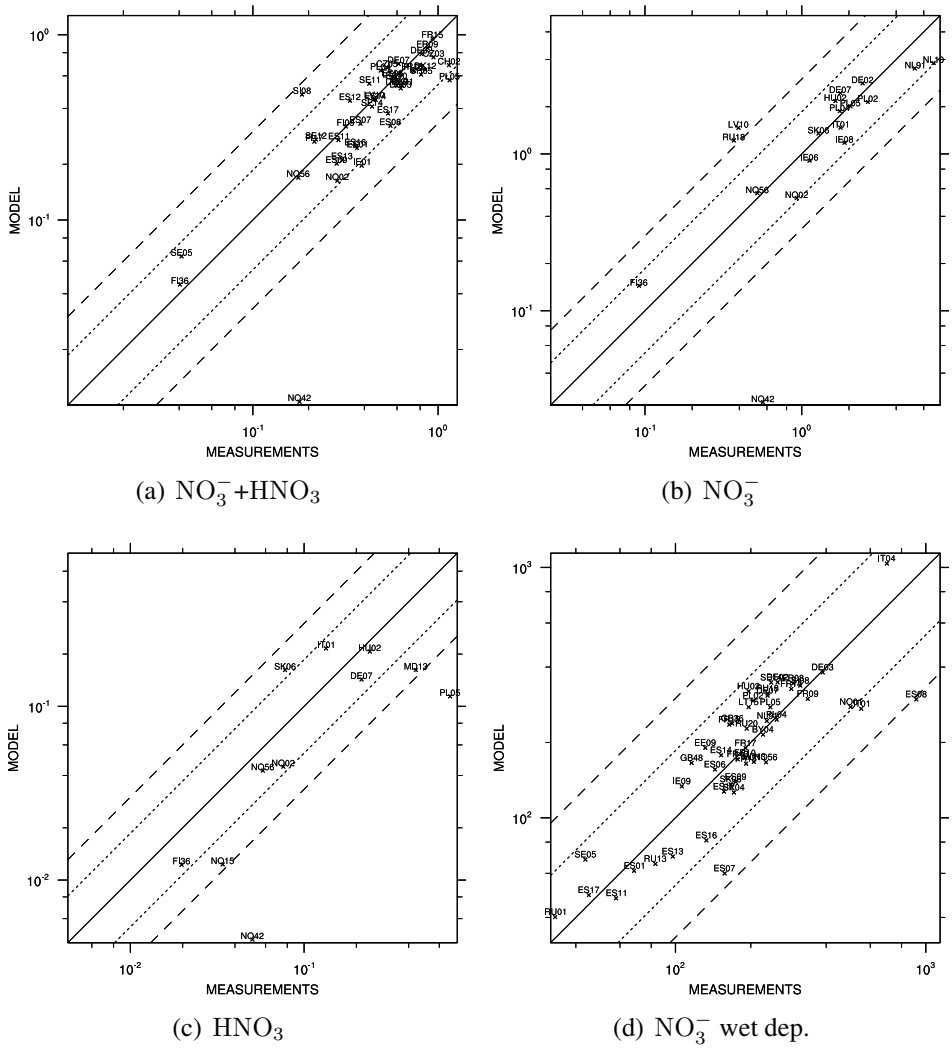

(a) NO_3^-+HNO_3 (b) NO_3^-

(c) HNO_3 (d) NO_3^- wet dep.

Figure 2.2: Scatter plots of modelled versus observed concentrations of total nitrate, nitrate aerosol, nitric acid [μg(N) m^{-3}] and wet deposition of oxidized nitrogen [μg(N)m^{-2}].

Nitrate and nitric acid in air

Measurements of airborne nitrate are expected to have a rather large uncertainty due to the very different physical characteristics of the compounds making up total nitrate. Whilst nitric acid is a spatially variable volatile gas with fast dry deposition, particulate nitrate dry deposits only slowly and hence concentrations are more determined by long range transport.

In Figure 2.2 we show scatter plots for total nitrate, particulate nitrate and nitric acid in air. Time series for total nitrate in air are shown in Figures 2.20–2.24.

Normally, the results for nitrate aerosol and nitric acid are somewhat worse than for total nitrate, because the monitoring data quality for these components are in general not as good as for total nitrate. The reason for this is that the individual concentrations of nitrate and nitric acid are biased when using the common filter-pack method. This has also been shown in the evaluation of the EMEP model performance for nitrogen compounds using intensive measurement data from two sampling periods, June 2006 and January 2007 (Fagerli and Aas 2008).

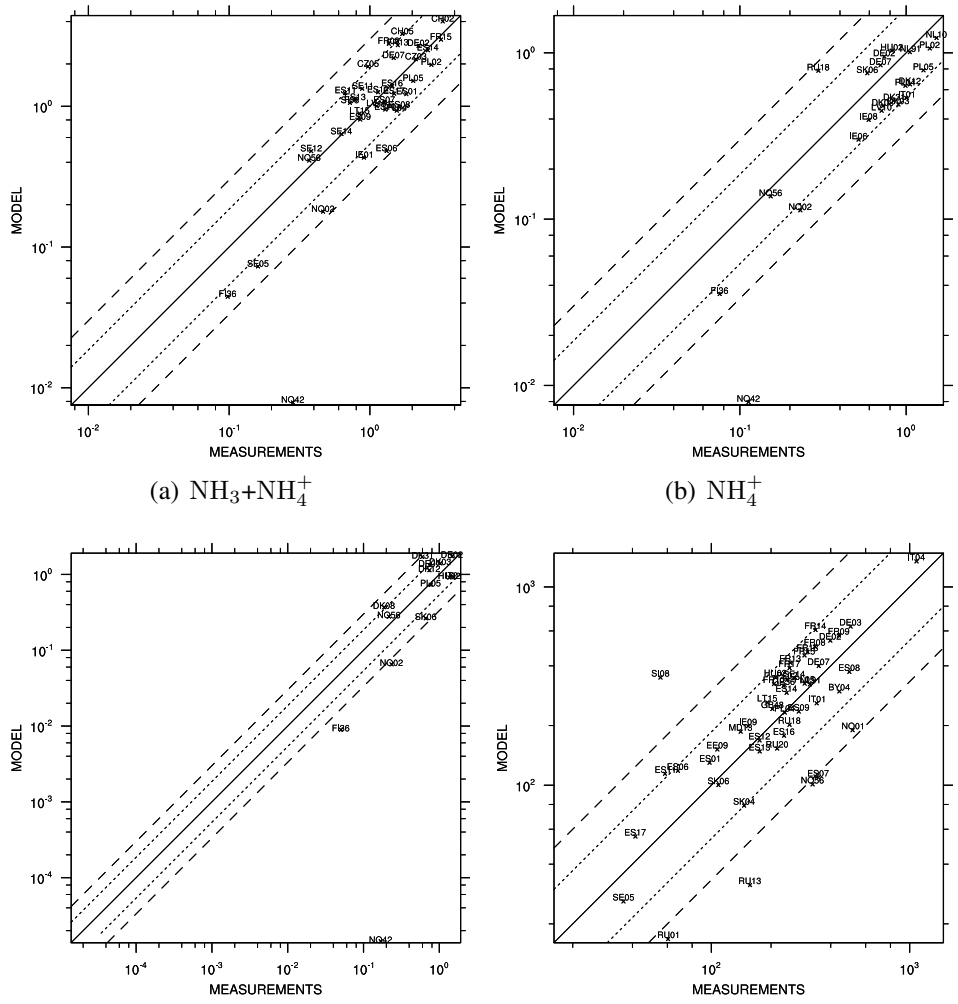

(a) NH_3+NH_4^+ (b) NH_4^+

(c) NH_3 (d) NH_4^+ wet dep.

Figure 2.3: Scatter plots of modelled versus observed concentrations of total ammonium+ammonia, aerosol ammonium and ammonia in air [μg(N) m^{-3}] and wet deposition of reduced nitrogen [μg(N)m^{-2}].

In this year's model results, HNO_3 was underestimated by 45%, while NO_3^- was underestimated by 13%. The sum of NO_3^-+HNO_3 was slightly underestimated by 12%. The spatial correlation is best for nitrate aerosol (Corr = 0.88), slightly worse for the sum of aerosol and gas (Corr = 0.83) and the lowest for nitric acid (Corr = 0.42). However, one should keep in mind that the stations used in the comparison for the different components are not exactly the same, thus the results are only indicative and not strictly comparable.

Ammonia and ammonium aerosol in air

In order to evaluate the model performance for NH_x (NH_3+NH_4^+) properly, ammonia and ammonium should be studied separately. However, the number of measurements for 2013 where the gaseous and particle phase are analyzed both separately and at the same time is limited, e.g. NH_3 measurements are available only from 14 sites (though this is an improvement from last year).

Normally, the results for NH_3 and NH_4^+ are somewhat worse than for total reduced ni-

trogen (NH_x), because the monitoring data quantity and quality for these components are in general not as good as for NH_3+NH_4^+. The reason for this is that the individual concentrations of ammonia and ammonium are biased when using the common filter-pack method due to the volatile nature of ammonium nitrate. Separation of these gases and particles by a simple aerosol filter is unreliable, and to obtain better quality data it is necessary to use denuders. However, this is a much more demanding method and several sites in the EMEP network are still using the filter-pack method and report the individual concentrations of ammonia and ammonium based on this.

The modelled yearly averages of the concentrations of ammonia, ammonium and the sum of ammonia and ammonium have biases of +11%, -19% and +5%, respectively, compared to the monitoring data. The spatial correlations for NH_4^+ and NH_3+NH_4^+ are high (0.78 and 0.81), while NH_3 has a lower spatial correlation (Corr=0.69).

Scatter plots for modelled versus measured concentrations for total ammonium+ammonia, aerosol ammonium and ammonia in air in 2013 are presented in Figures 2.3(a), 2.3(b) and 2.3(c), respectively, while time series for NH_3+NH_4^+ are shown in Figures 2.25–2.29.

Concentrations in precipitation / wet depositions

The ability of the model to predict concentrations in precipitations and wet depositions is limited by the accuracy of the precipitation fields used in the model. The precipitation field pattern is very patchy (e.g. influenced by local topographic effects), and the regional scale model is unable to resolve this sub grid scale distribution. A typical problem arises with small scale showers. In reality precipitation is high in a small area of a given grid, but a large fraction of the grid should remain dry. Within the model, however, this precipitation is averaged out to cover the whole grid at a lower intensity. Thus, even though average precipitation amounts may be simulated well, the model experiences precipitation more often, but in lower amounts, than occur in reality. On a shorter time scale, e.g on daily basis, this may lead to too high concentrations in precipitation for episodes when it rains only in a small part of the grid square. For a regional scale model it is more sensible to compare the bulk concentrations, i.e the sum of the wet deposited compounds divided by the sum of precipitation.

The correlation between model and measurements for concentrations in precipitation and wet depositions will to a large extent depend on the model precipitation field.

A scatter plot for modelled versus observed precipitation is shown in Figure 2.1(e). In average, the observed and modelled precipitation is very similar (bias=+2%) and the spatial correlation coefficient is high (0.81). This also contributes to the relatively good model performance in terms of reduced nitrogen in precipitation and sulphur in precipitation (low biases and good correlations).

Scatter plots for modelled versus observed wet depositions of sulphur, oxidized nitrogen and reduced nitrogen are shown in Figures 2.1(d), 2.2(d) and 2.3(d), respectively.

Time series for wet deposition of sulphur, oxidized nitrogen and reduced nitrogen are shown in Figures 2.30–2.35, Figures 2.36–2.41 and Figures 2.42–2.47, respectively.

2.2 Time series

In this section we present time series plots for a selection of stations that have supplied data on acidifying and eutrophying components to EMEP CCC for 2013. The plots show daily model

results and measurements, where available. Time series are shown also for those measurement sites which were excluded from the scatter plots. Time series for sulphur dioxide in air are shown in Figures 2.4–2.11, for sulphate in air in Figures 2.12–2.19, for total nitrate in air in Figures 2.20–2.24 and for ammonia+ammonium in air in Figures 2.25–2.29. In addition, time series are shown for wet deposition of sulphur, oxidized nitrogen and reduced nitrogen in Figures 2.30–2.35, Figures 2.36–2.41 and Figures 2.42–2.47, respectively.

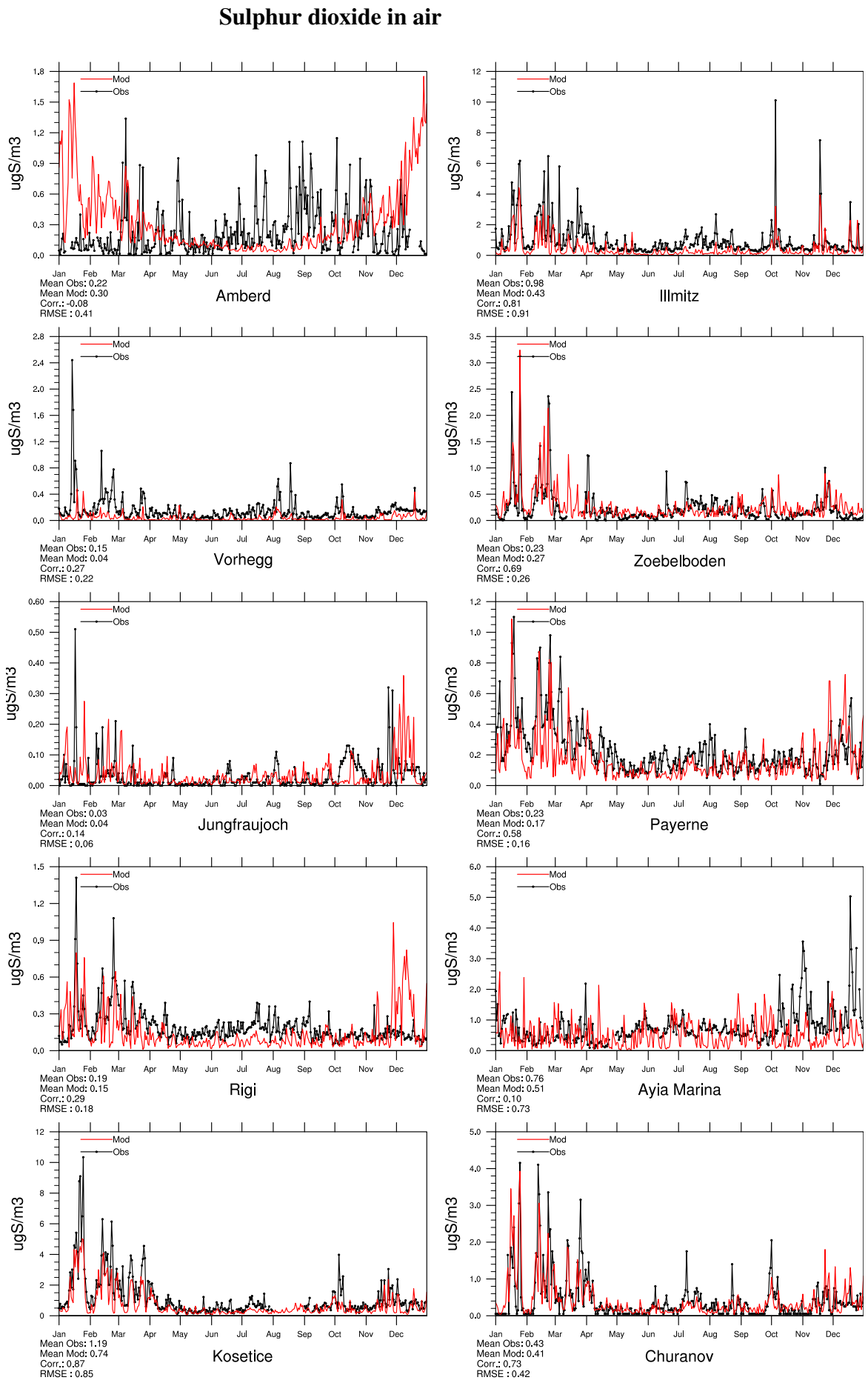

Figure 2.4: Comparison of model results and measurements (daily) for SO_2 in air [ugS] for stations that have measured SO_2 in 2013.

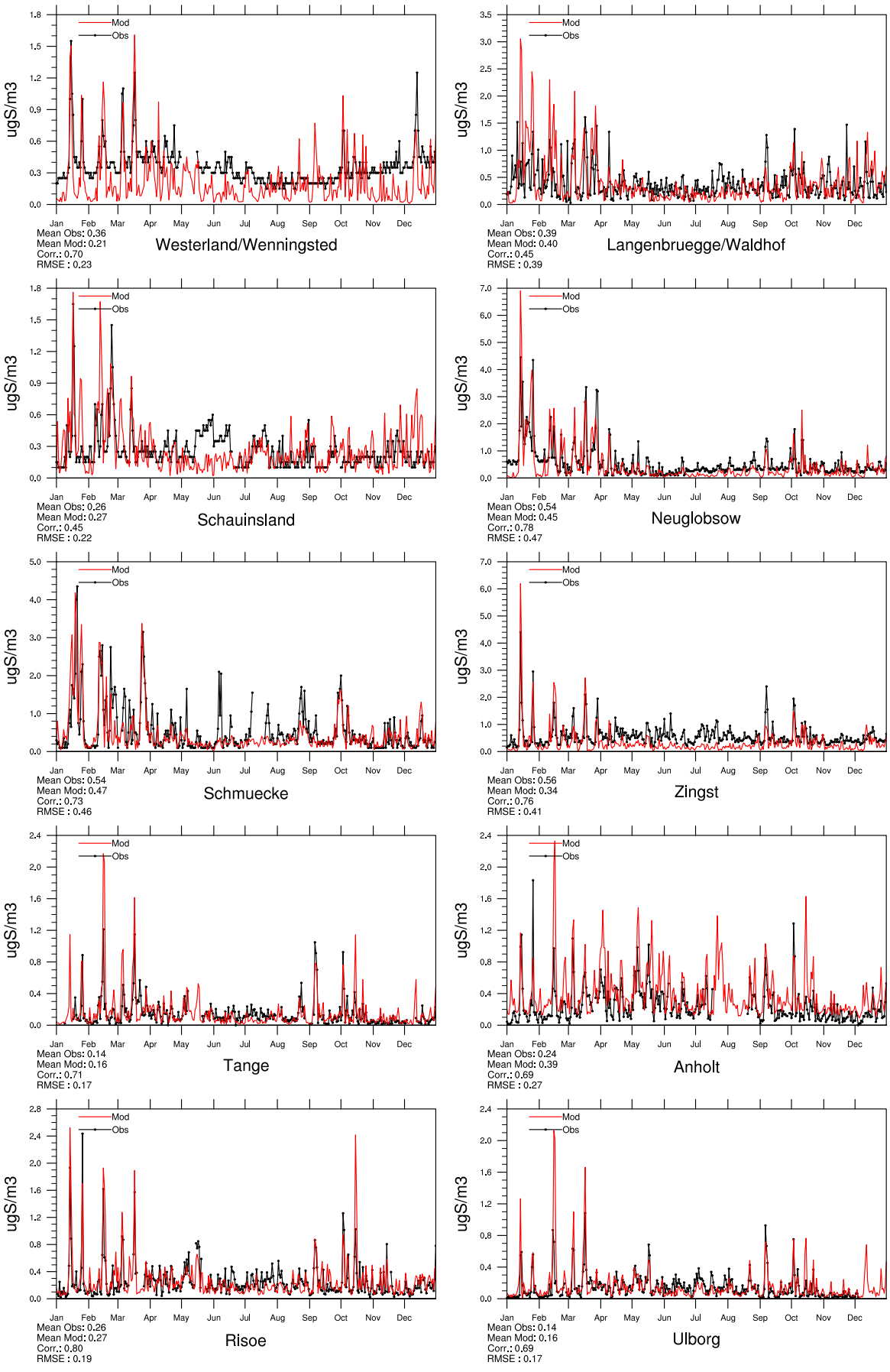

Figure 2.5: Comparison of model results and measurements (daily) for SO_2 in air [ugS] for stations that have measured SO_2 in 2013.

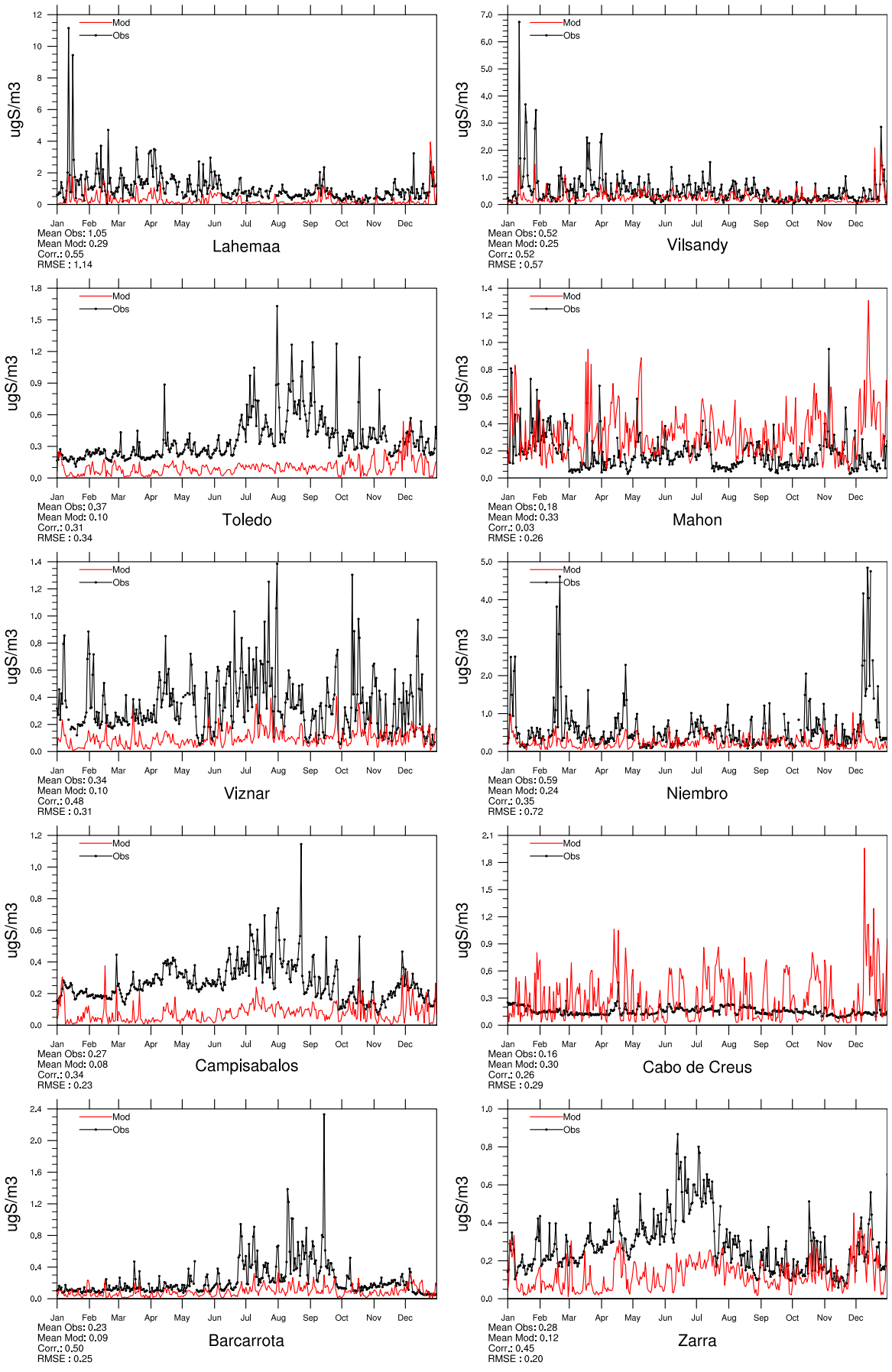

Figure 2.6: Comparison of model results and measurements (daily) for SO_2 in air [ugS] for stations that have measured SO_2 in 2013.

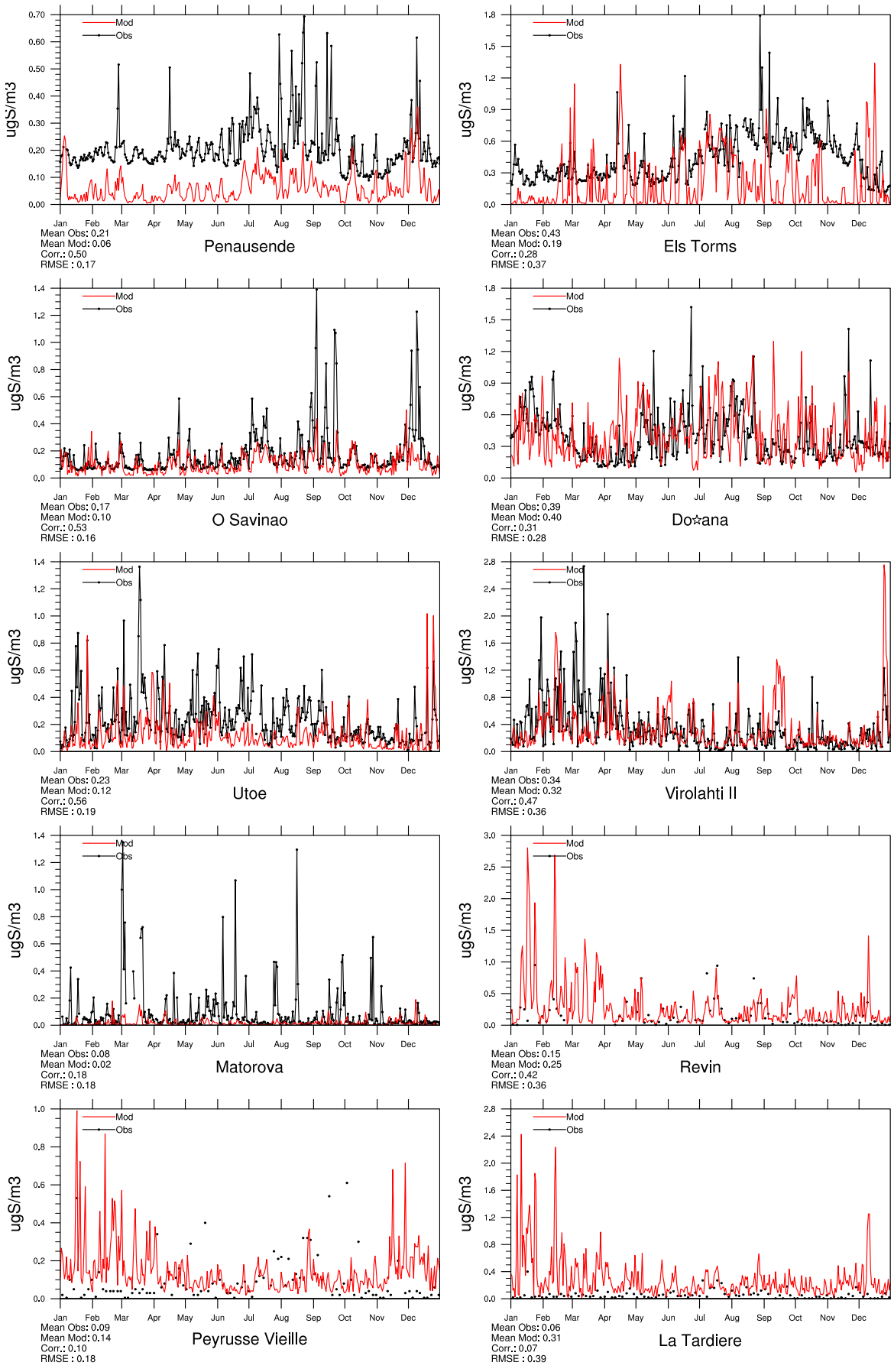

Figure 2.7: Comparison of model results and measurements (daily) for SO_2 in air [ugS] for stations that have measured SO_2 in 2013.

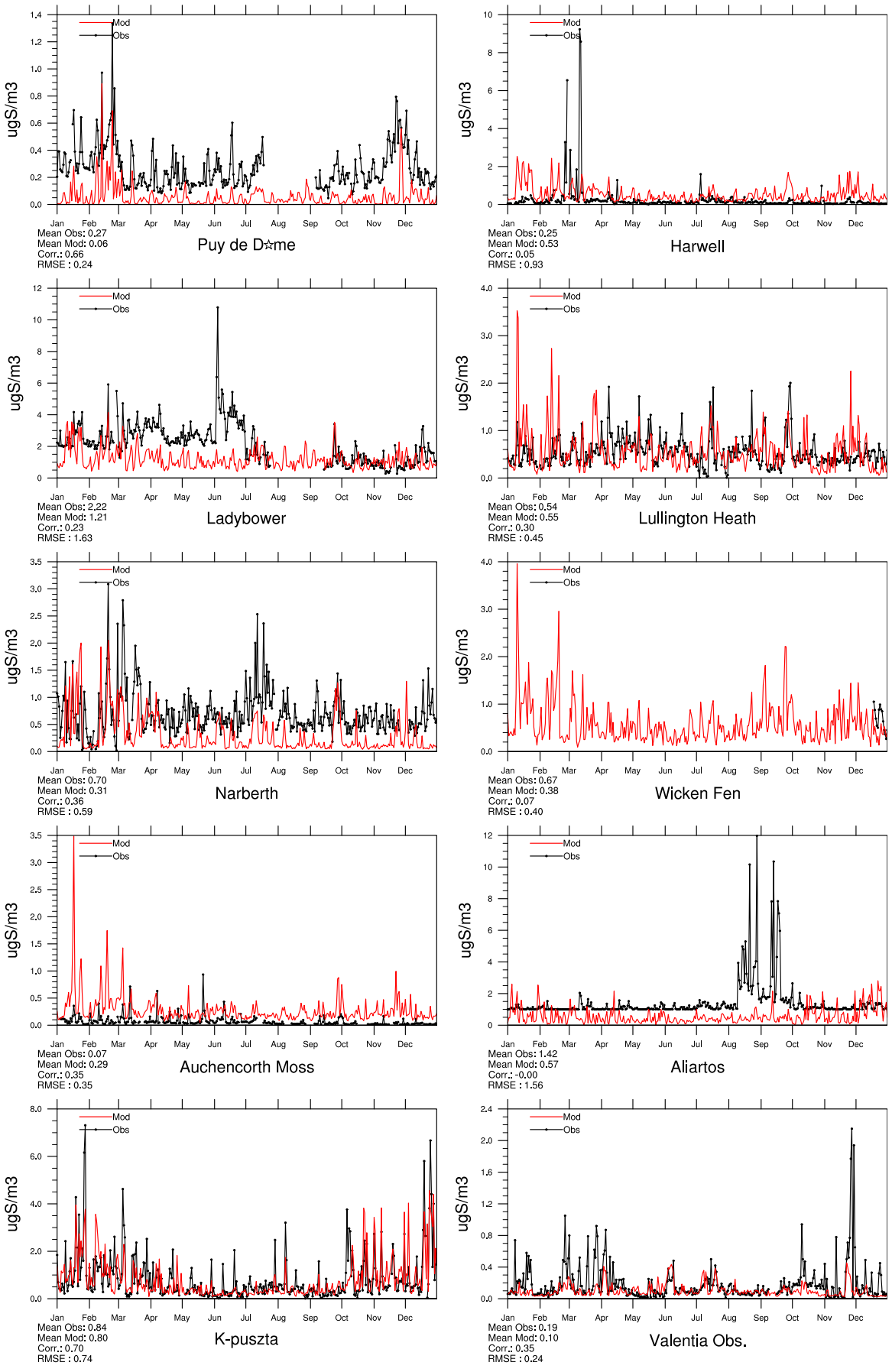

Figure 2.8: Comparison of model results and measurements (daily) for SO_2 in air [ugS] for stations that have measured SO_2 in 2013.

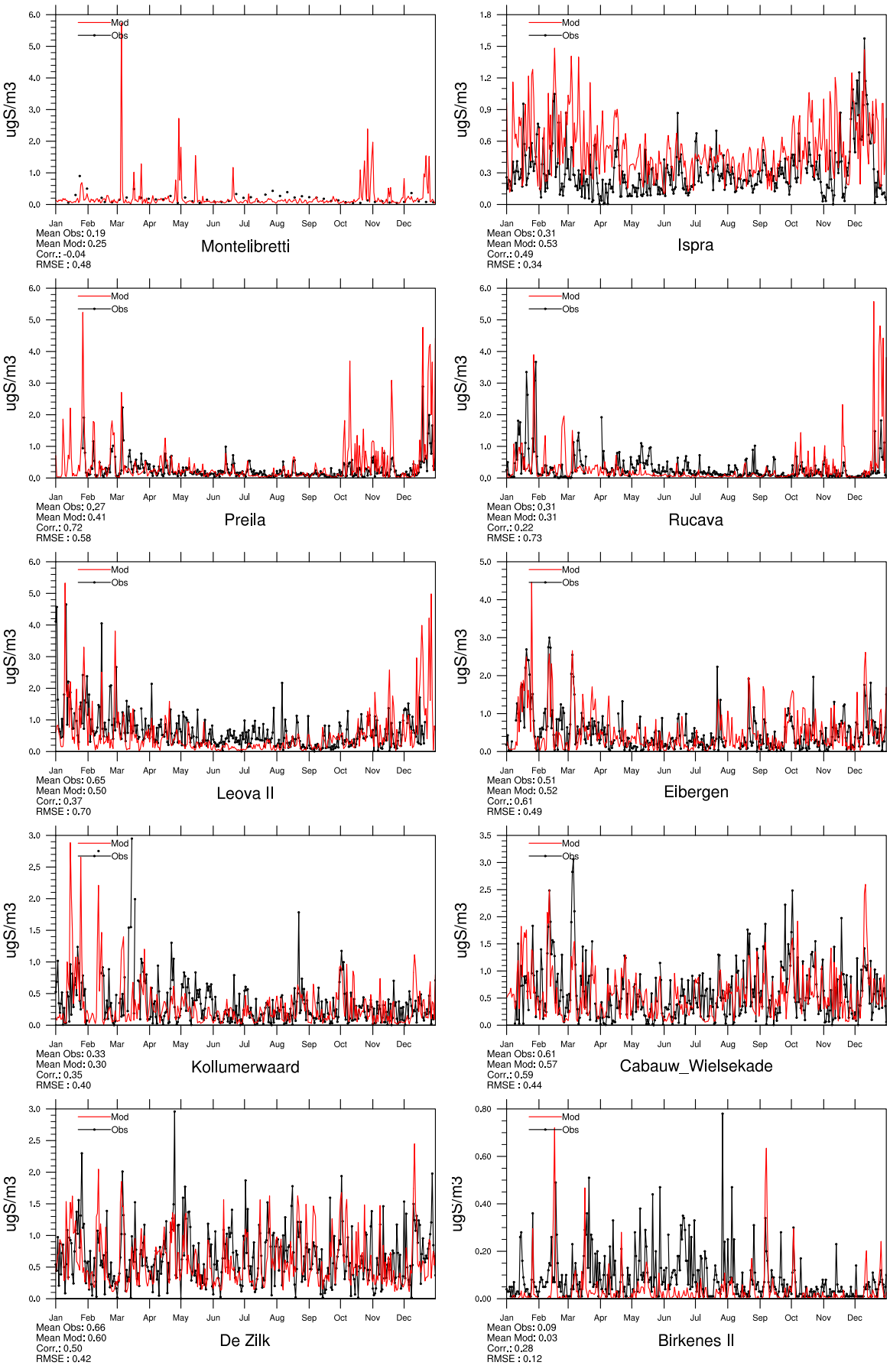

Figure 2.9: Comparison of model results and measurements (daily) for SO_2 in air [ugS] for stations that have measured SO_2 in 2013.

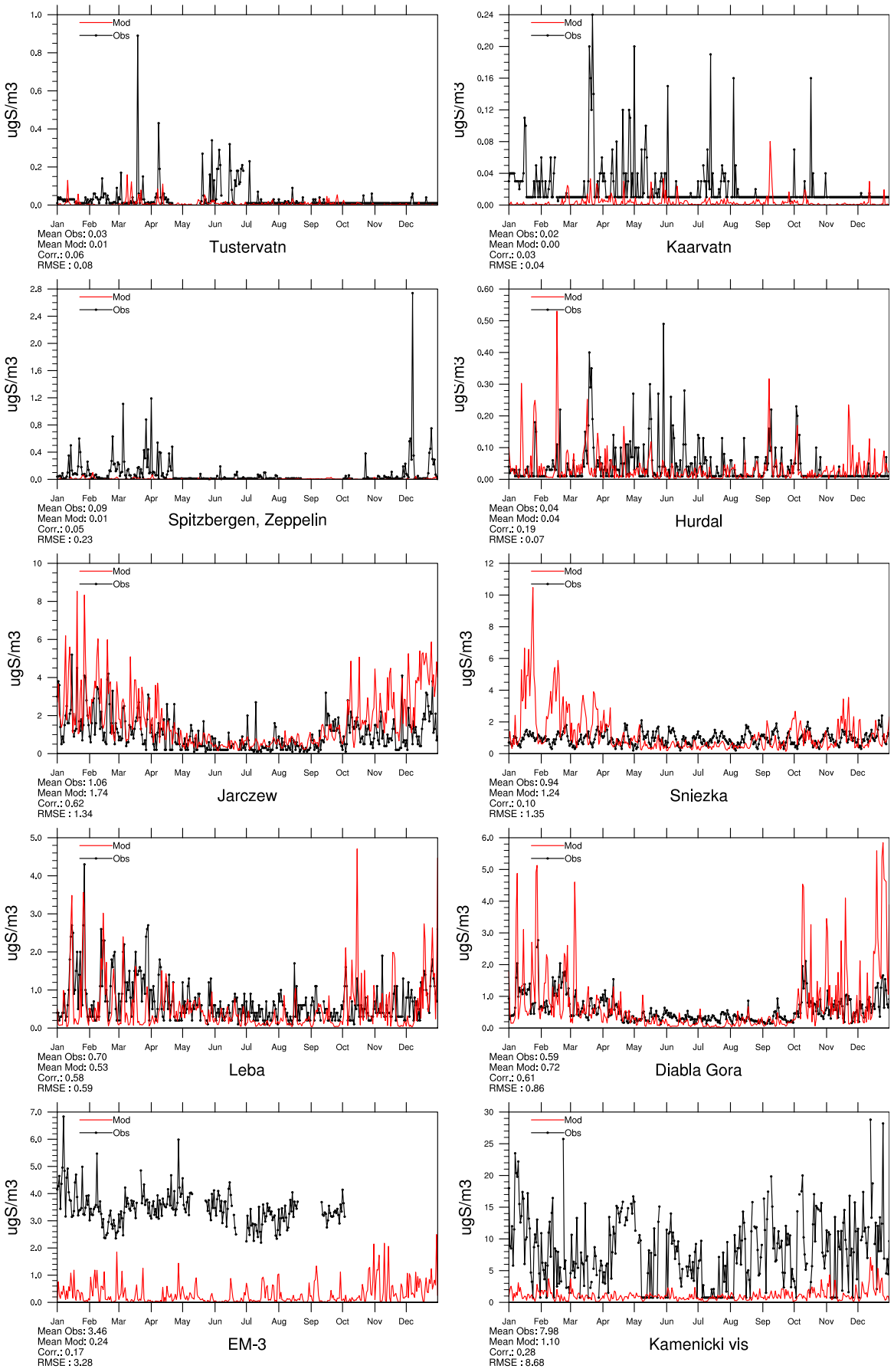

Figure 2.10: Comparison of model results and measurements (daily) for SO_2 in air [ugS] for stations that have measured SO_2 in 2013.

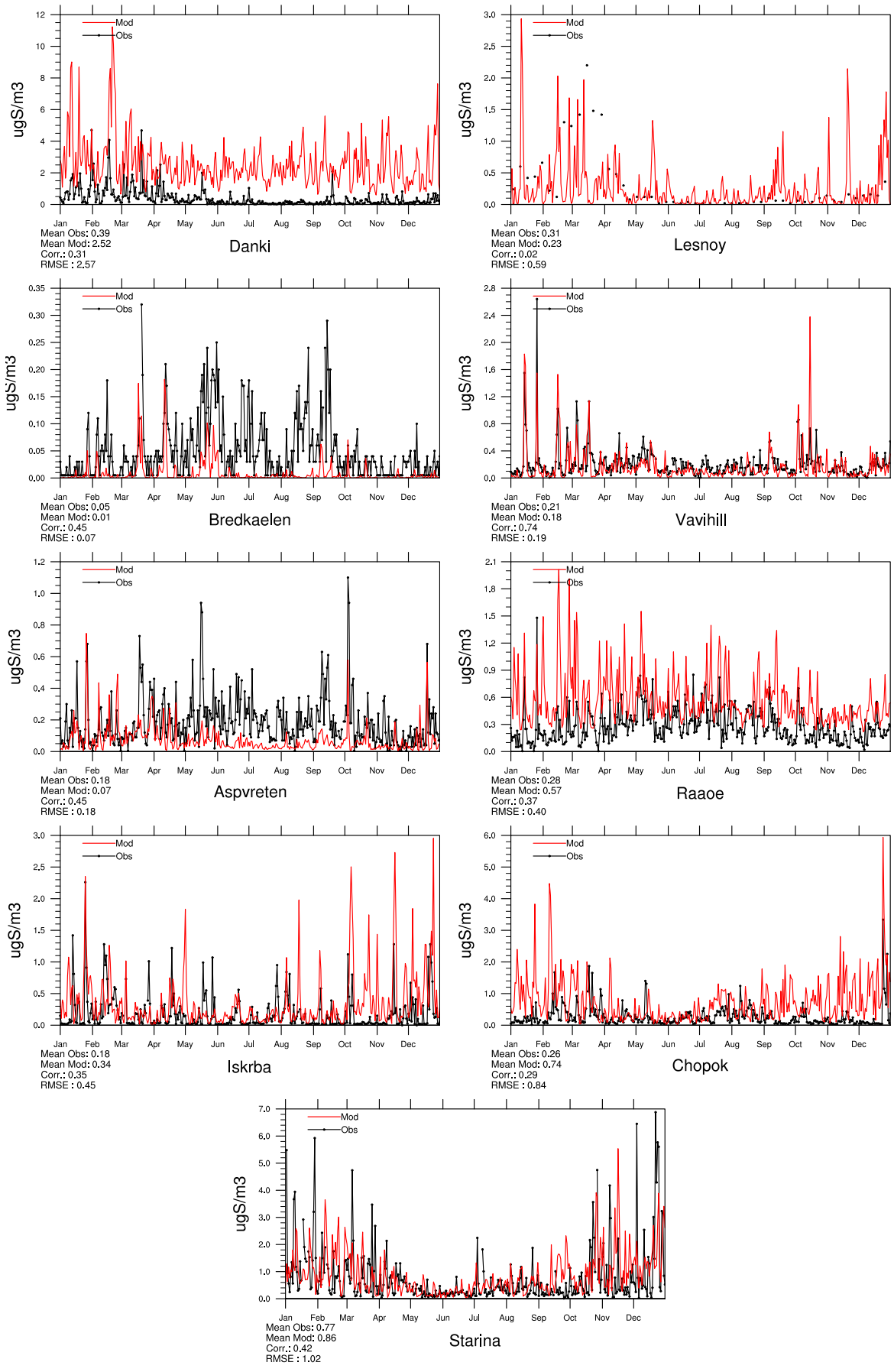

Figure 2.11: Comparison of model results and measurements (daily) for SO_2 in air [ugS] for stations that have measured SO_2 in 2013.

Sulphate in air – sea salt corrected

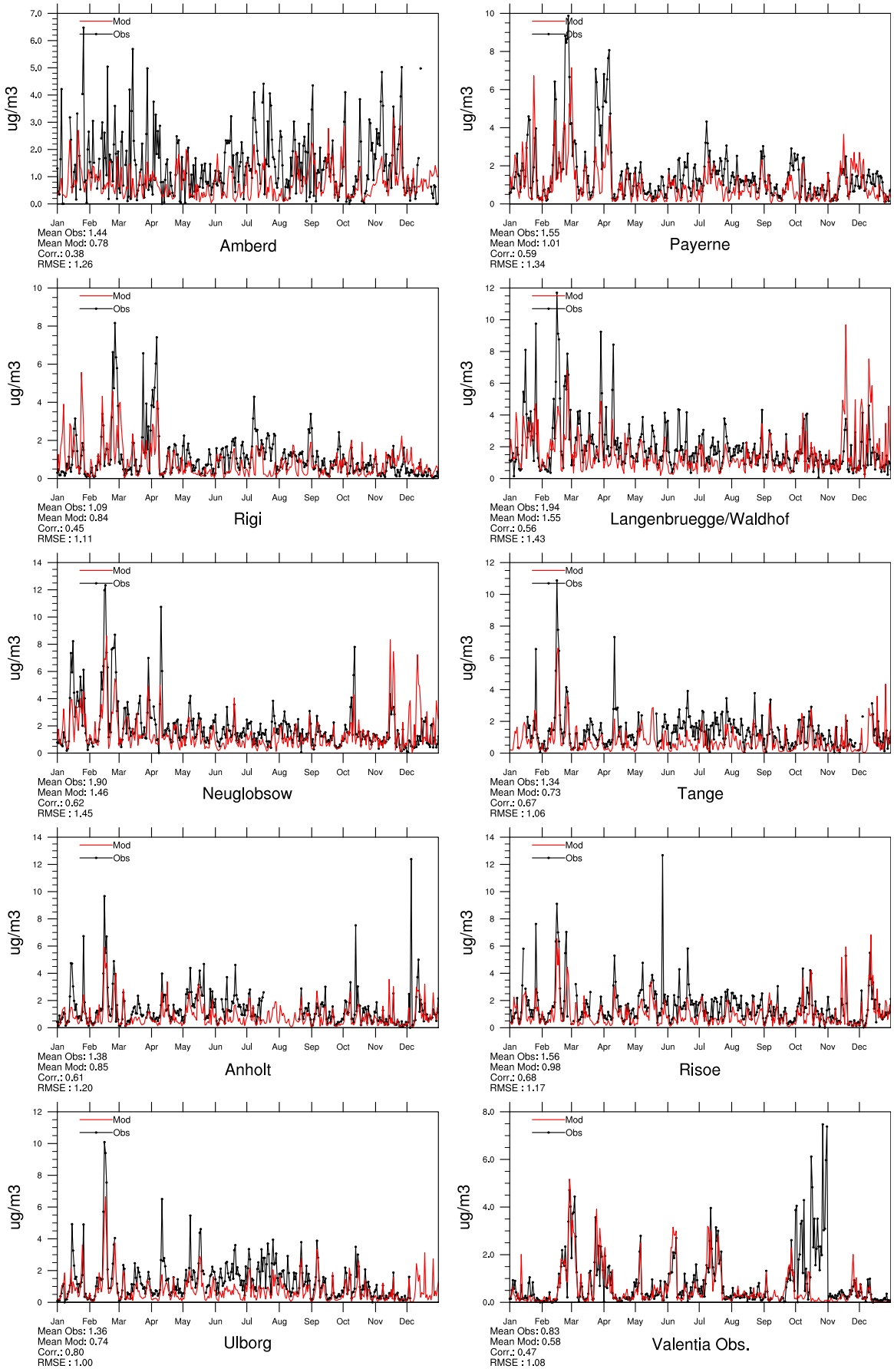

Figure 2.12: Comparison of model results and measurements (daily) for sea salt corrected sulphate in air [ugS] for stations that have measured sulphate in 2013.

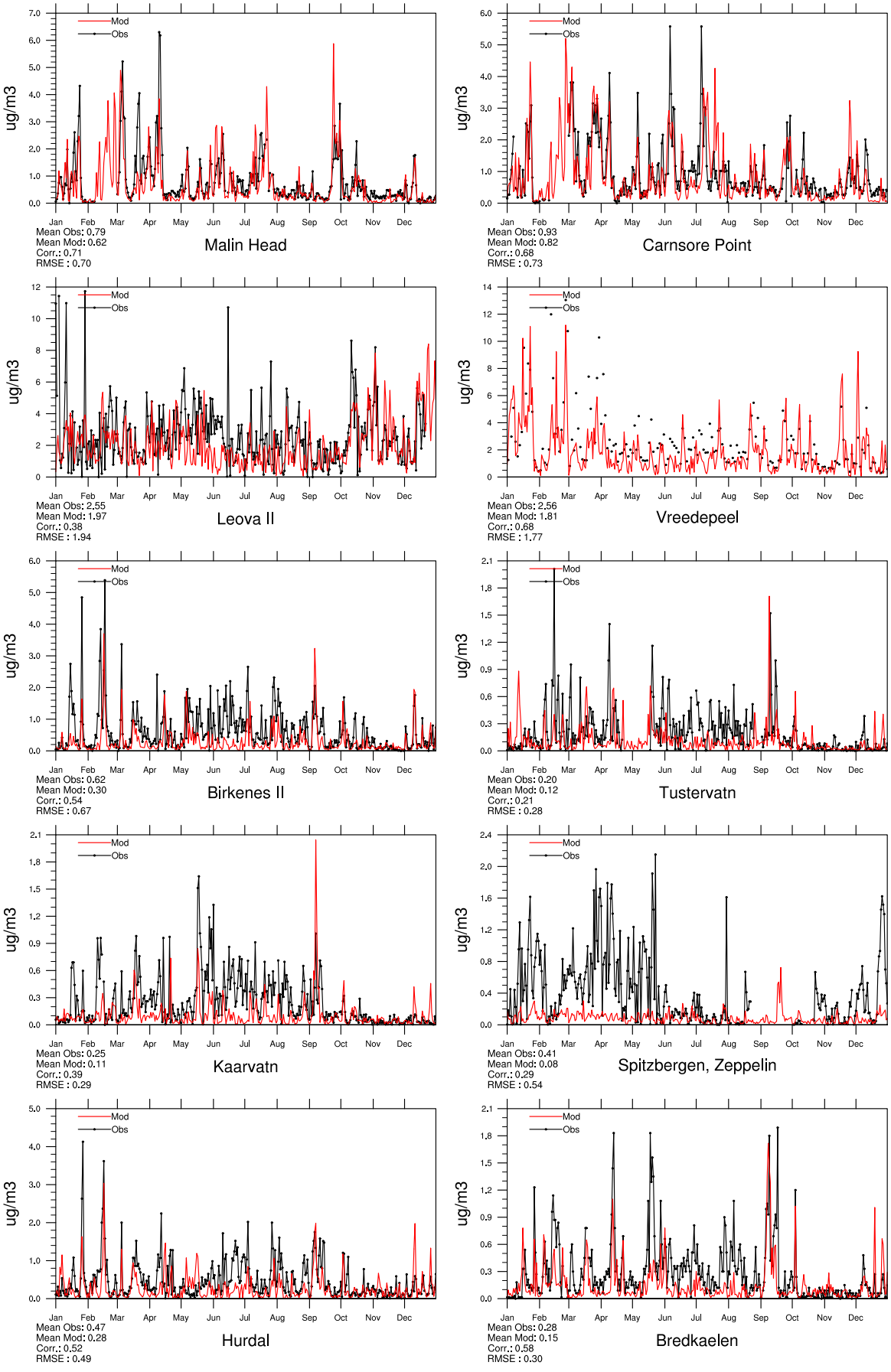

Figure 2.13: Comparison of model results and measurements (daily) for sea salt corrected sulphate in air [ugS] for stations that have measured sulphate in 2013.

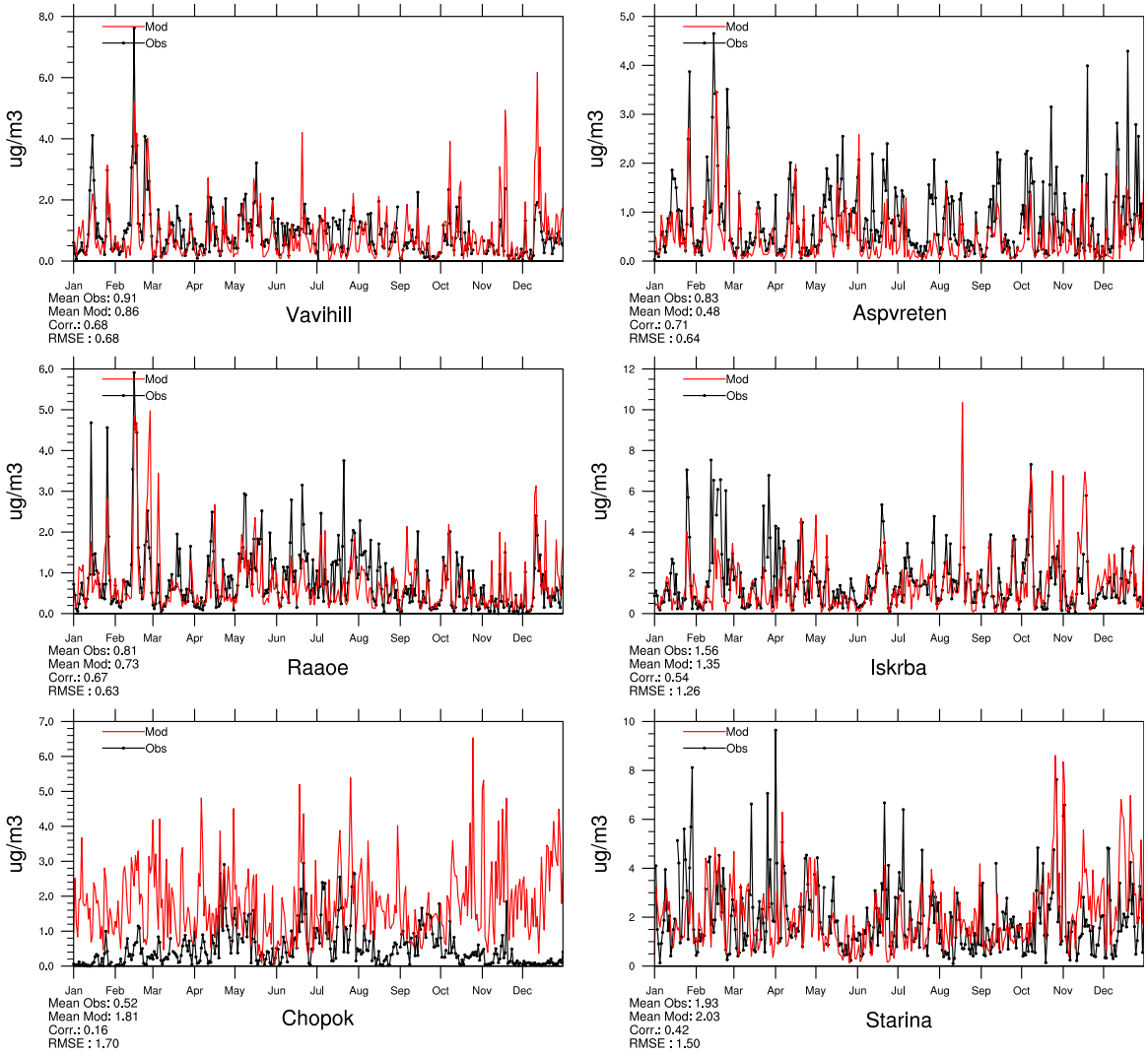

Figure 2.14: Comparison of model results and measurements (daily) for sea salt corrected sulphate in air [ugS] for stations that have measured sulphate in 2013.

Sulphate in air – sea salt included

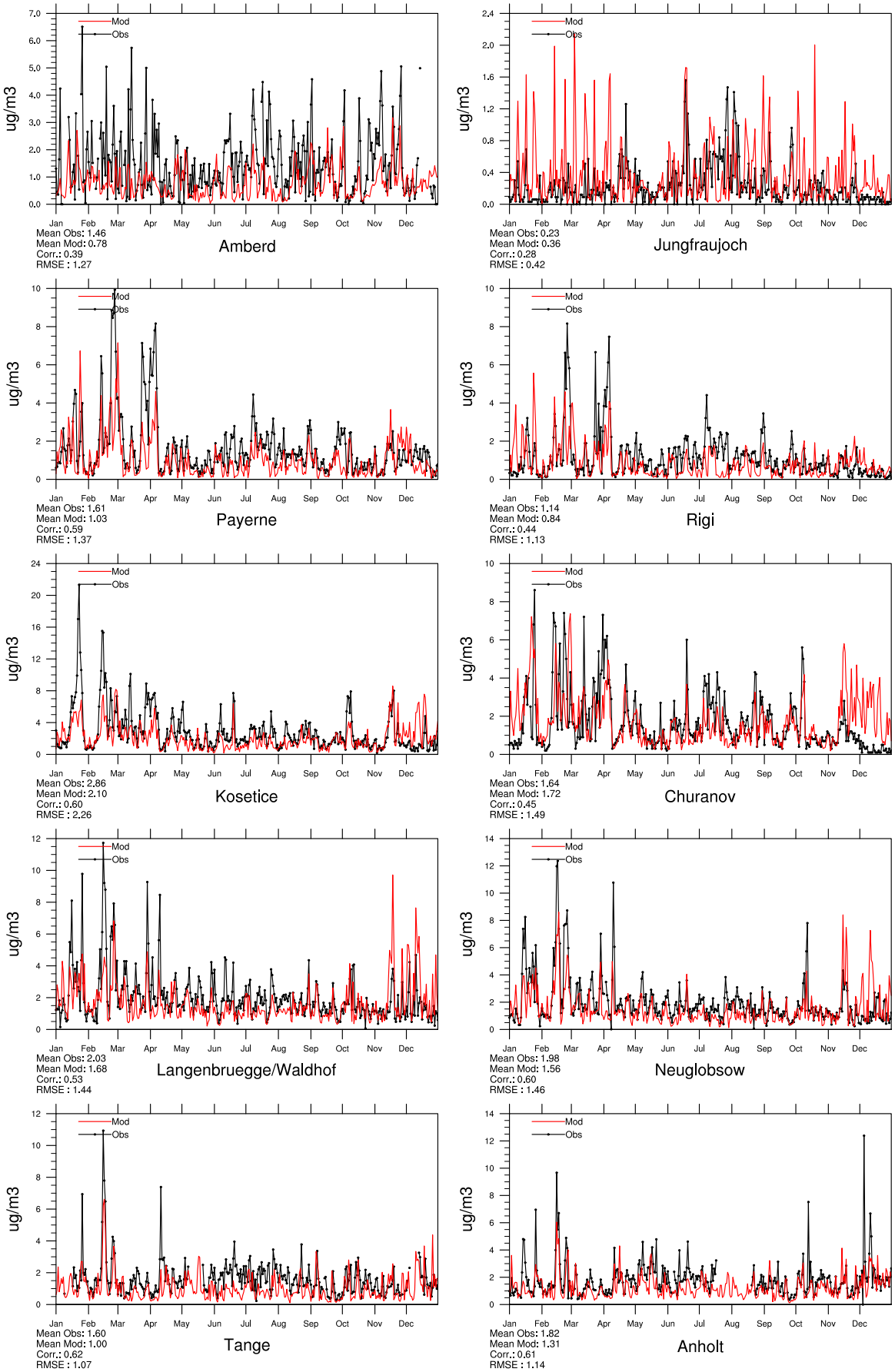

Figure 2.15: Comparison of model results and measurements (daily) for sulphate (including sea salt) in air [ugS] for stations that have measured sulphate in 2013.

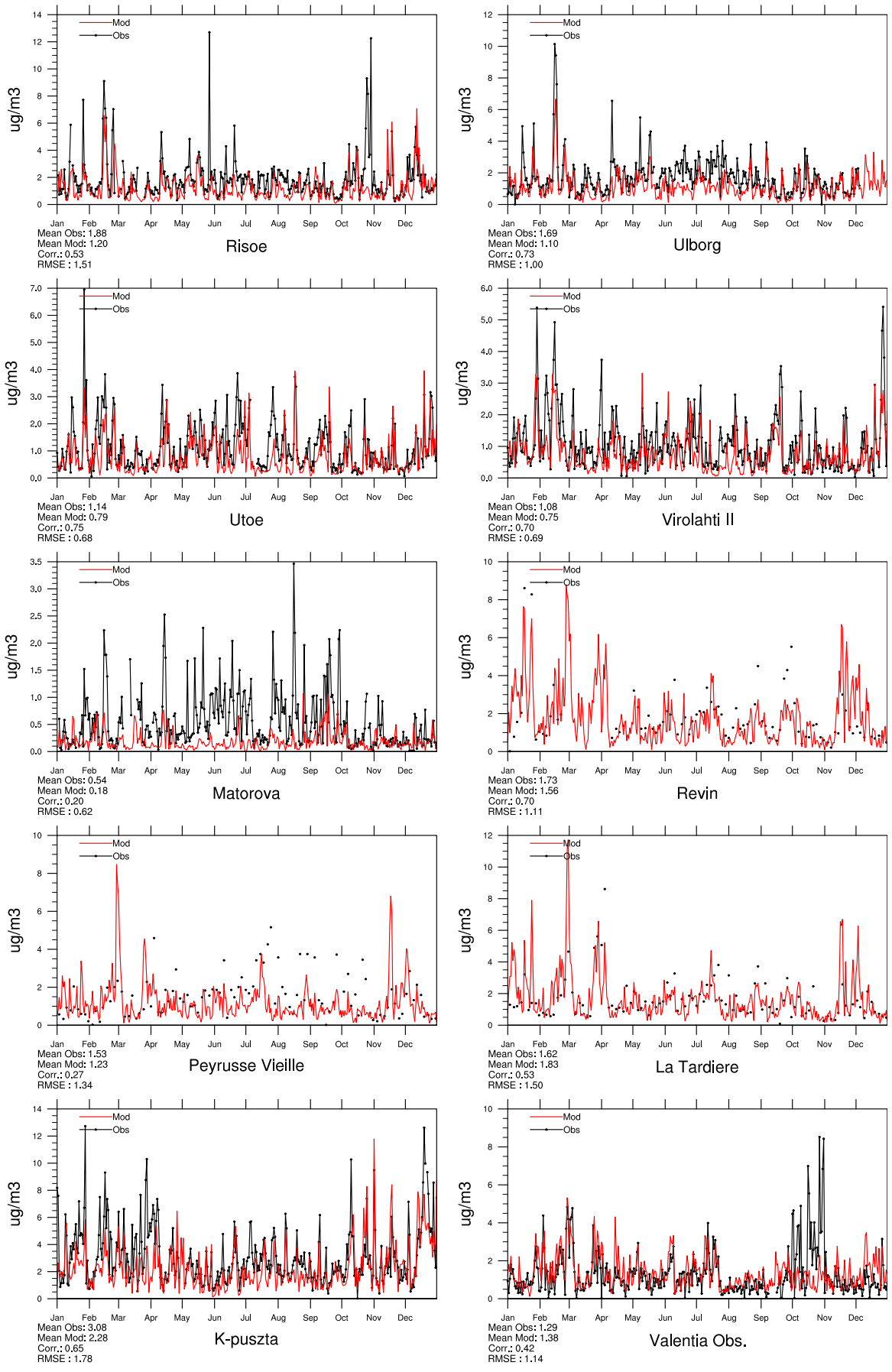

Figure 2.16: Comparison of model results and measurements (daily) for sulphate (including sea salt) in air [ugS] for stations that have measured sulphate in 2013.

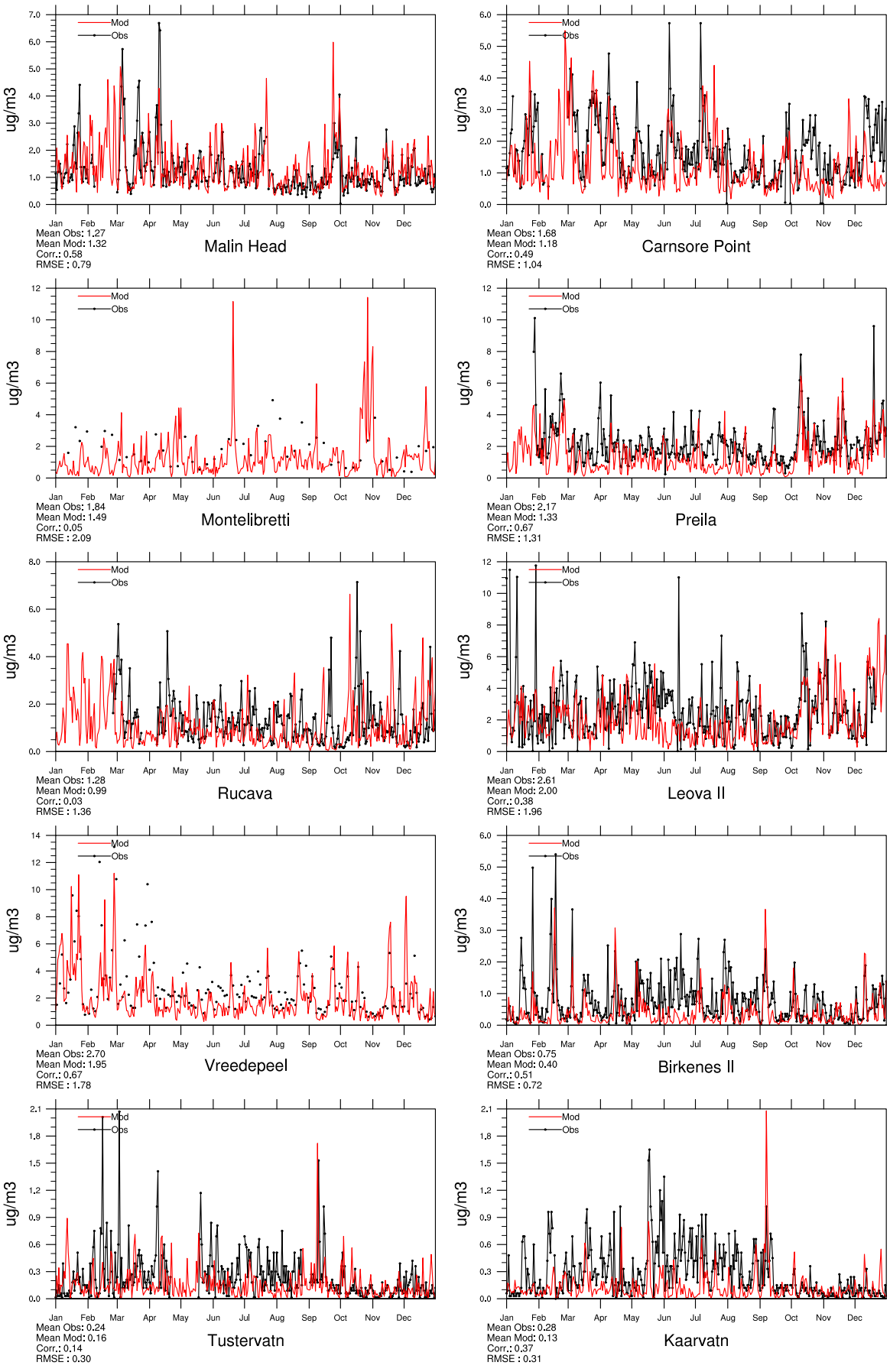

Figure 2.17: Comparison of model results and measurements (daily) for sulphate (including sea salt) in air [ugS] for stations that have measured sulphate in 2013.

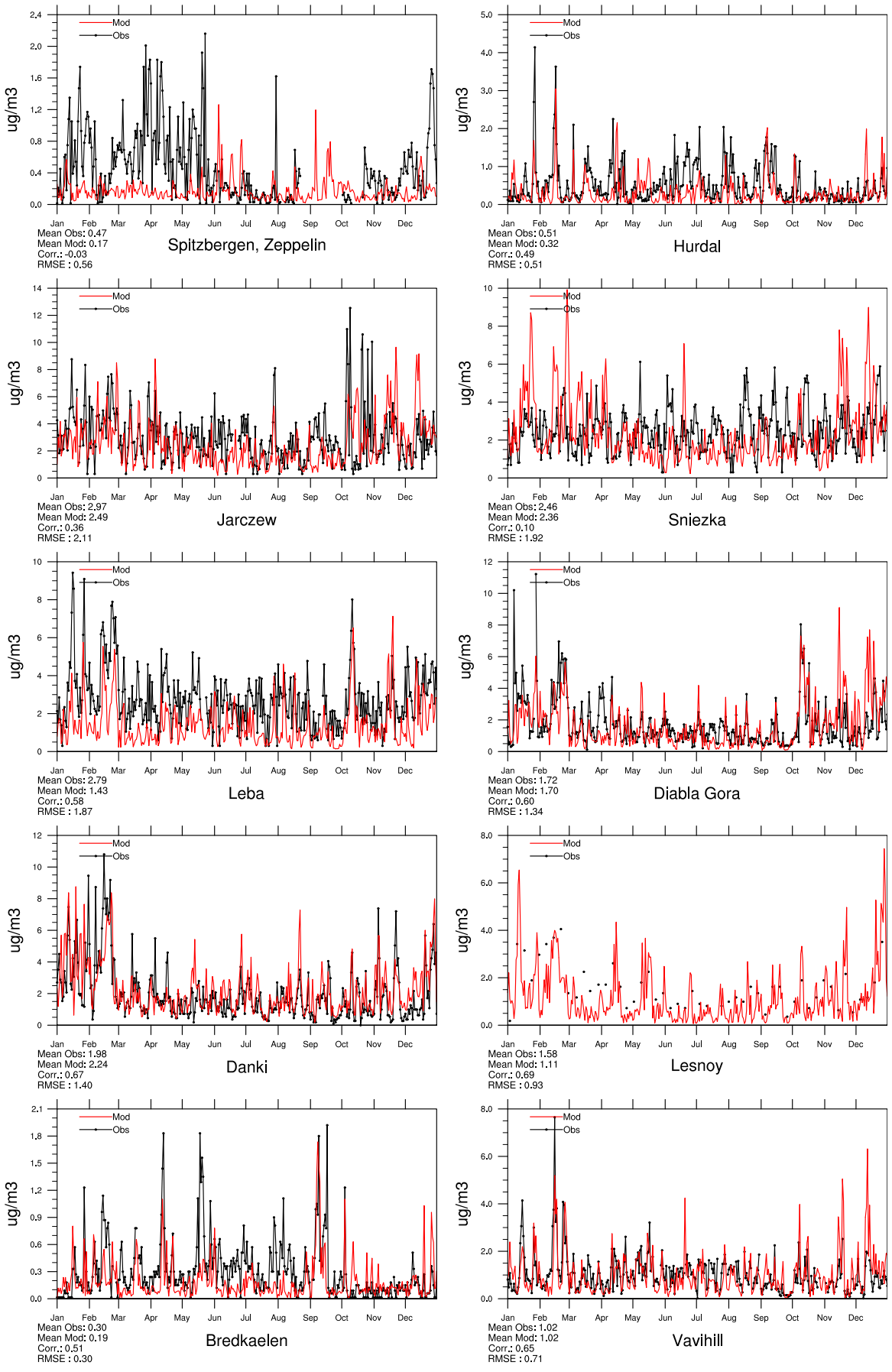

Figure 2.18: Comparison of model results and measurements (daily) for sulphate (including sea salt) in air [ugS] for stations that have measured sulphate in 2013.

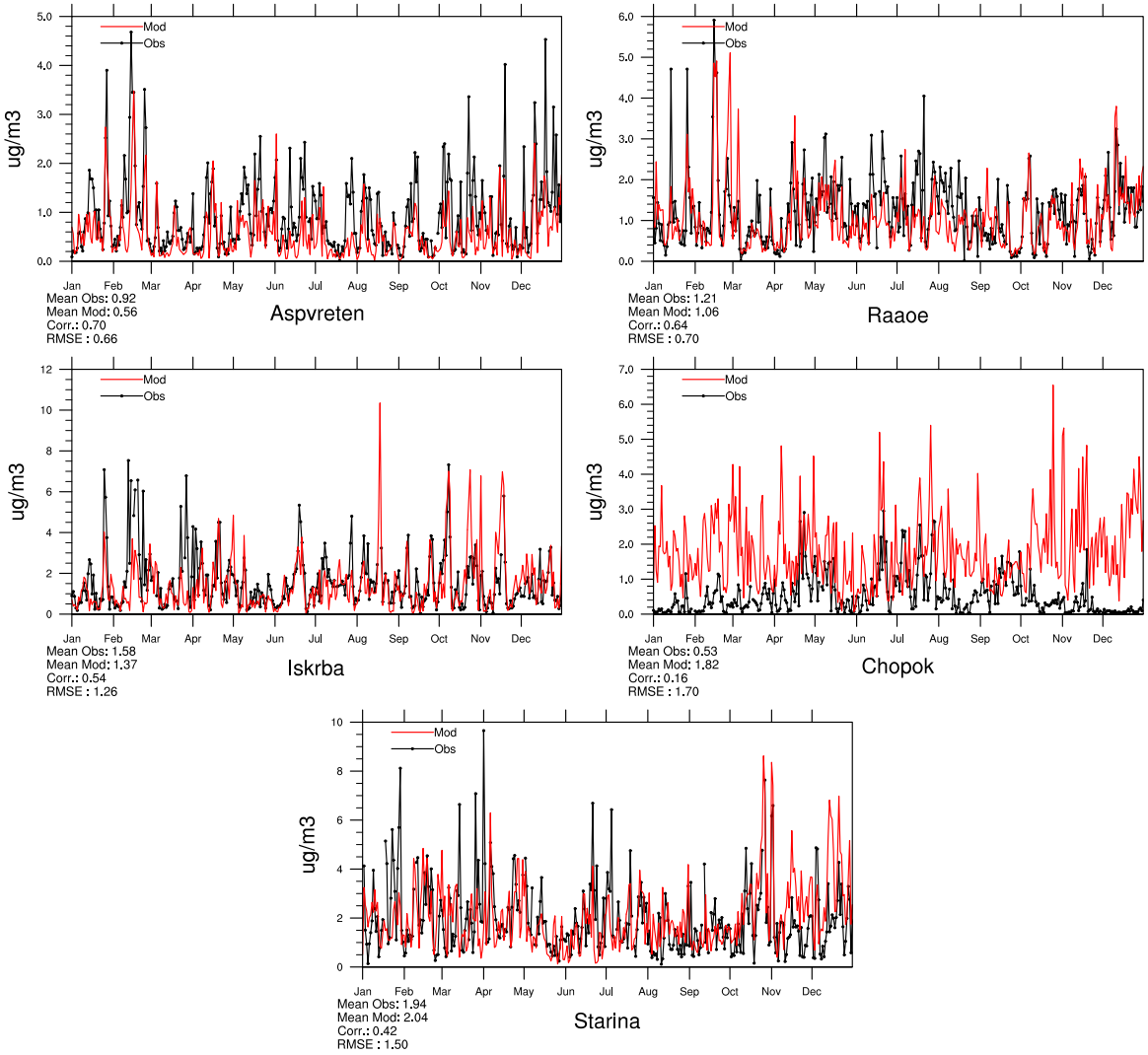

Figure 2.19: Comparison of model results and measurements (daily) for sulphate (including sea salt) in air [ugS] for stations that have measured sulphate in 2013.

Total nitrate in air

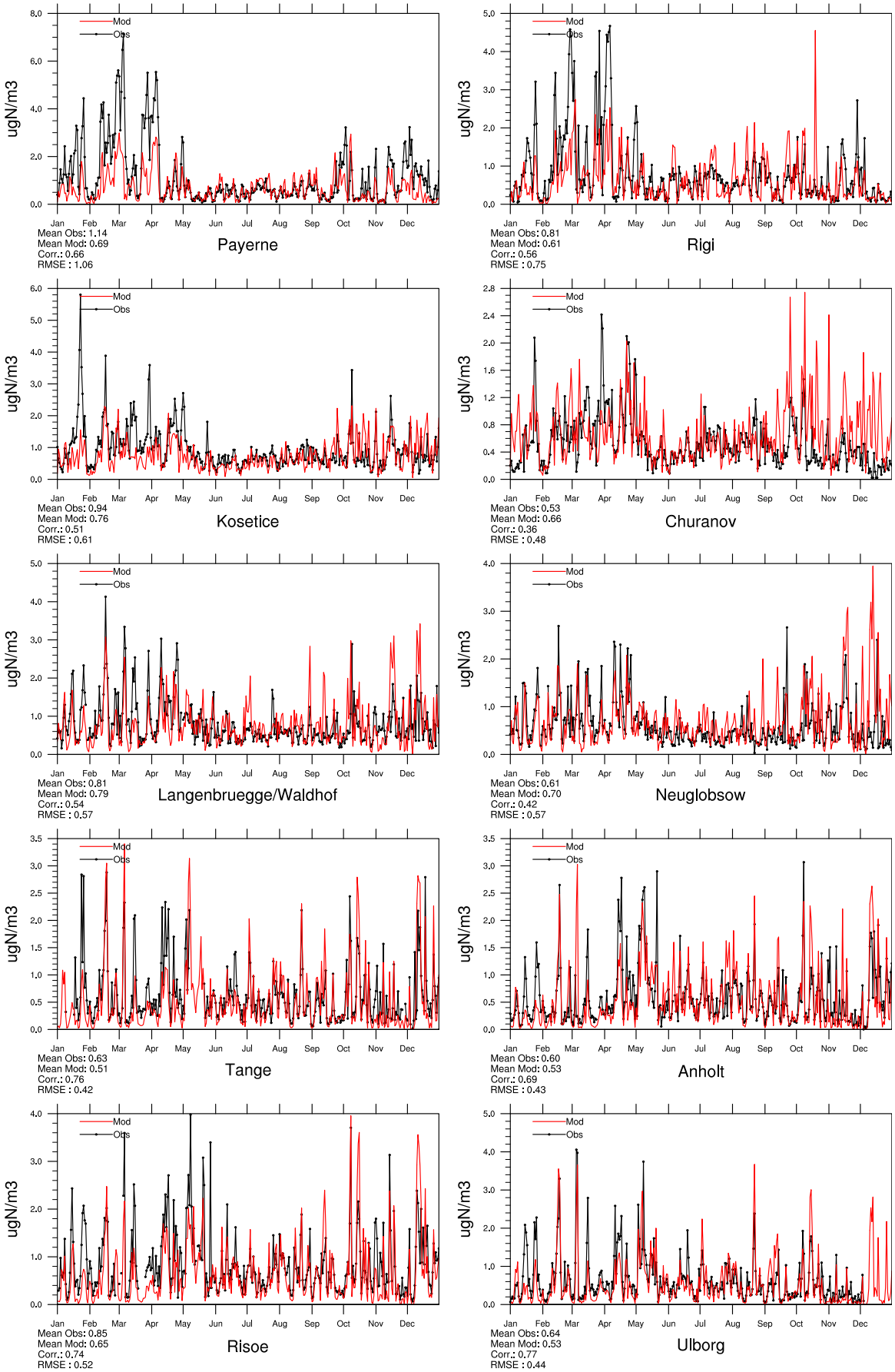

Figure 2.20: Comparison of model results and measurements (daily) total nitrate concentrations [μg(N) m^{-3}] for stations that have measured total nitrate in 2013.

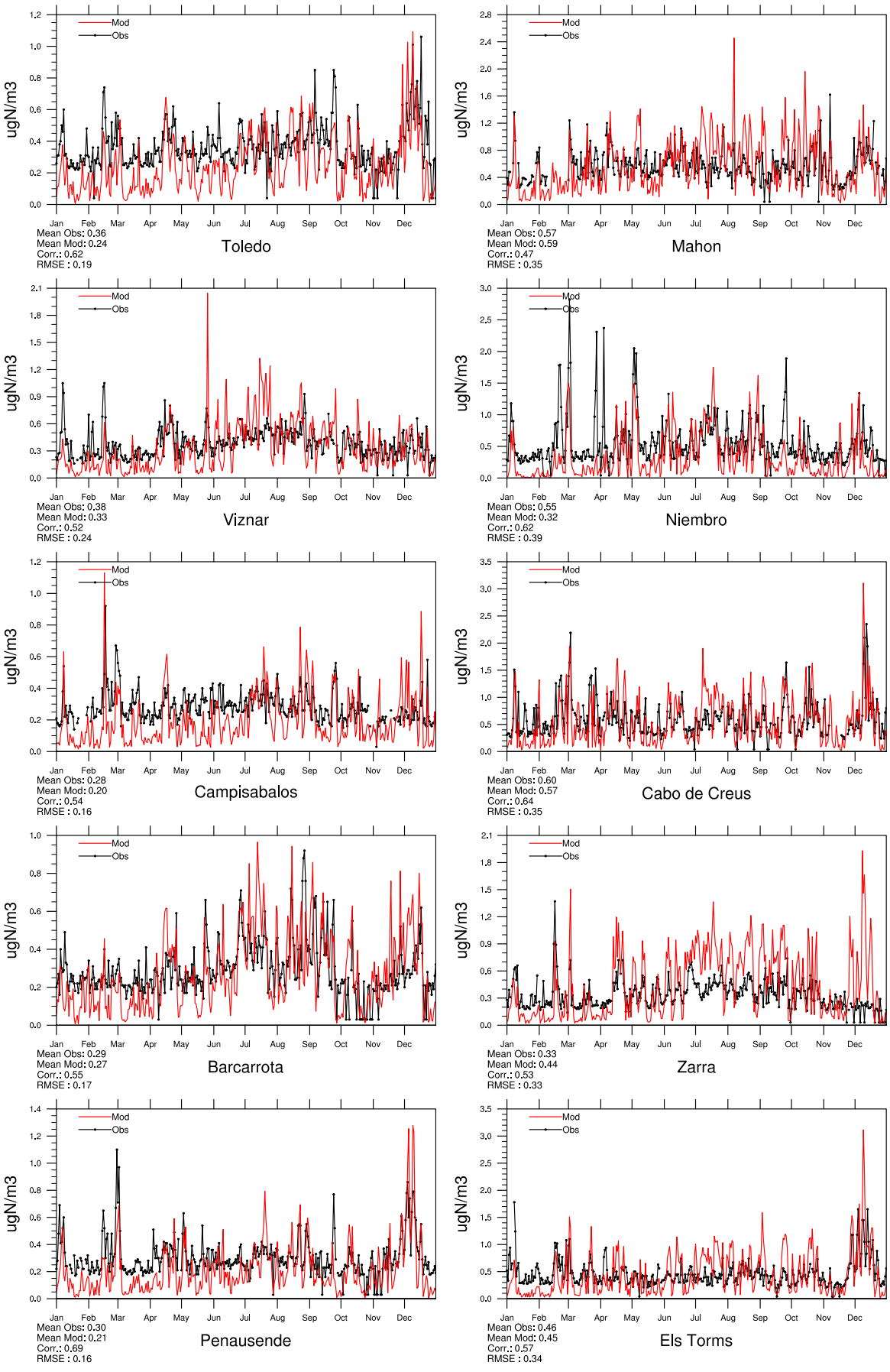

Figure 2.21: Comparison of model results and measurements (daily) total nitrate concentrations [μg(N) m^{-3}] for stations that have measured total nitrate in 2013.

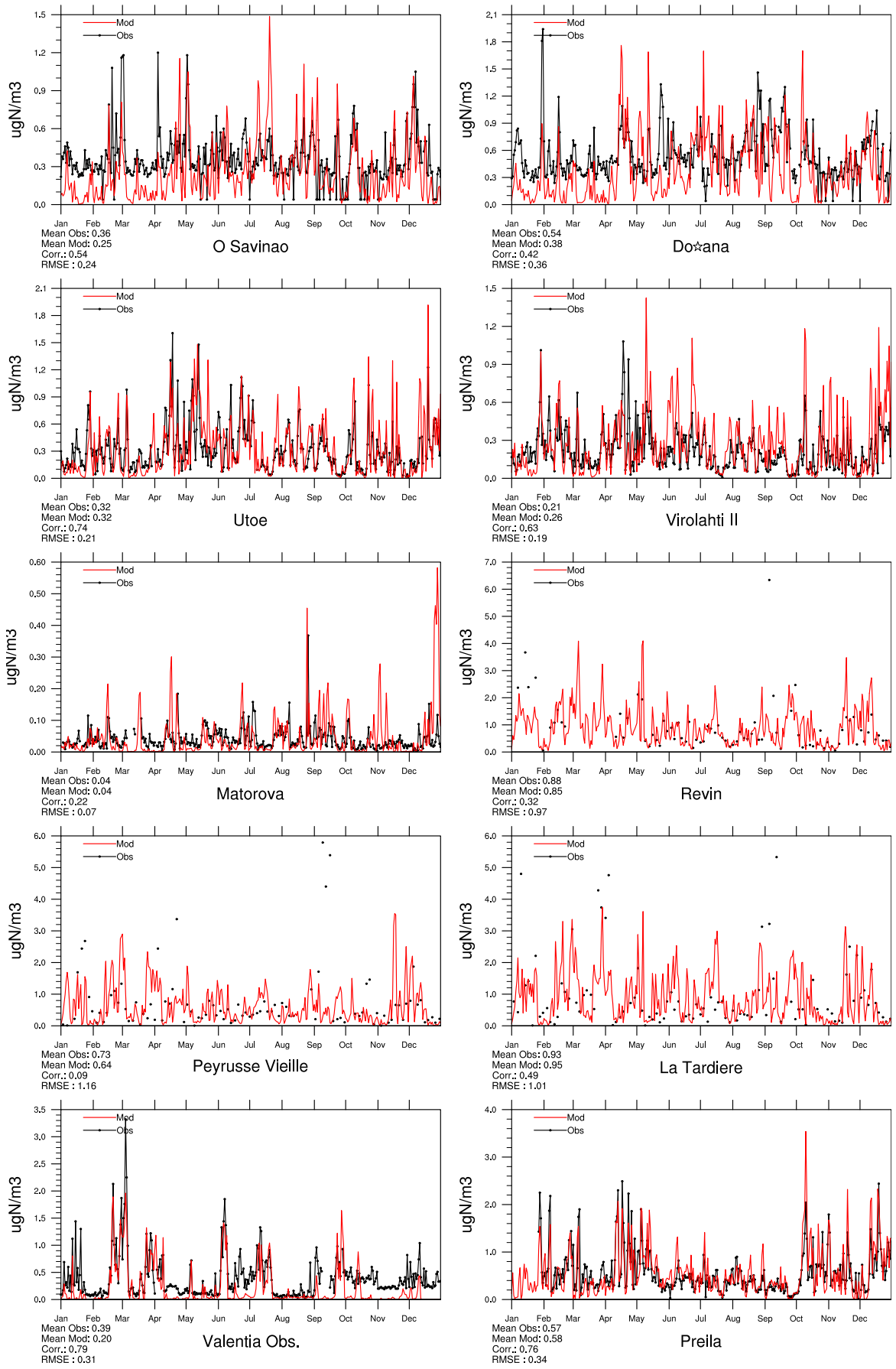

Figure 2.22: Comparison of model results and measurements (daily) total nitrate concentrations (μg(N) m^{-3}) for stations that have measured total nitrate in 2013.

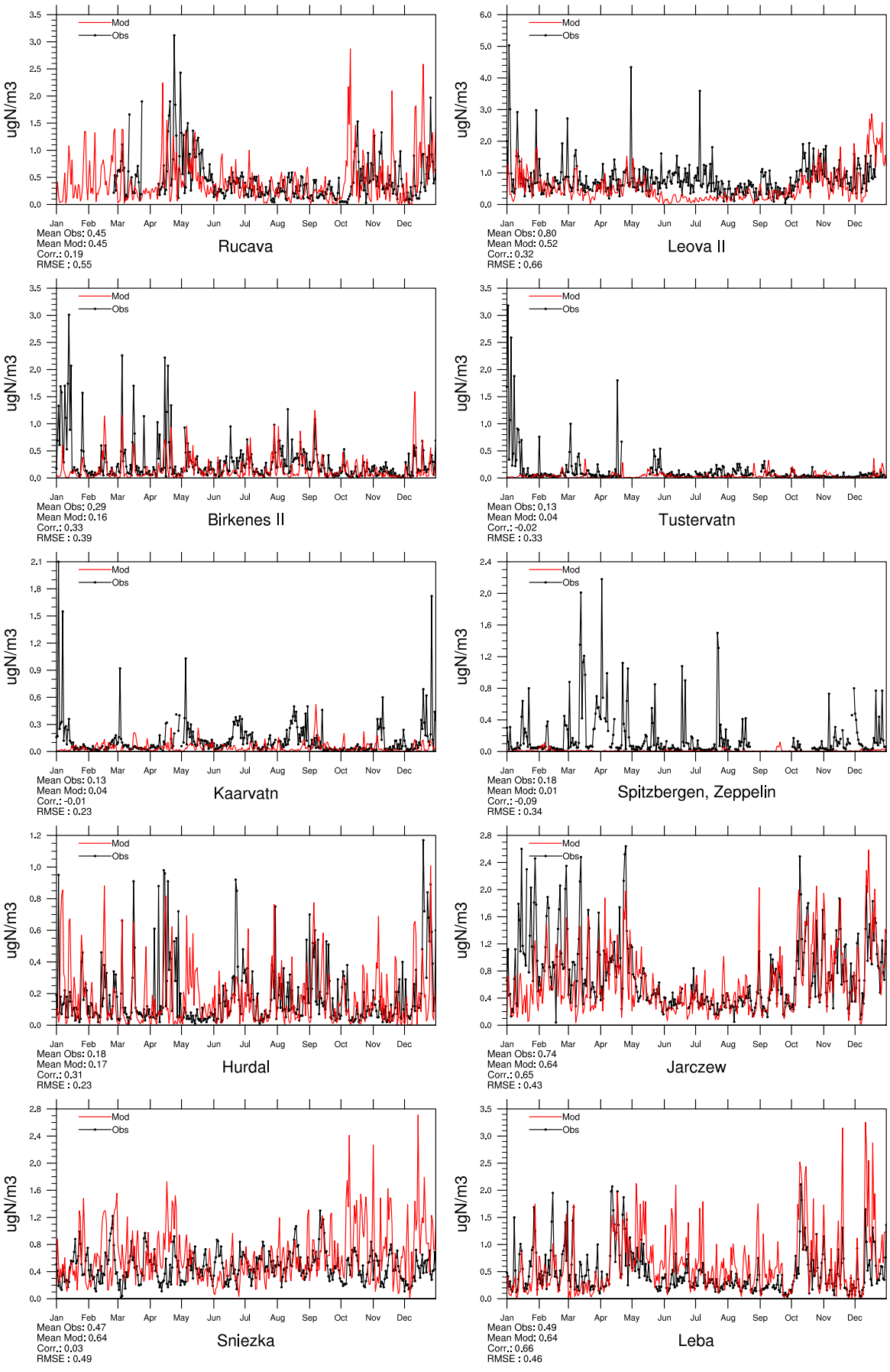

Figure 2.23: Comparison of model results and measurements (daily) total nitrate concentrations [μg(N) m^{-3}] for stations that have measured total nitrate in 2013.

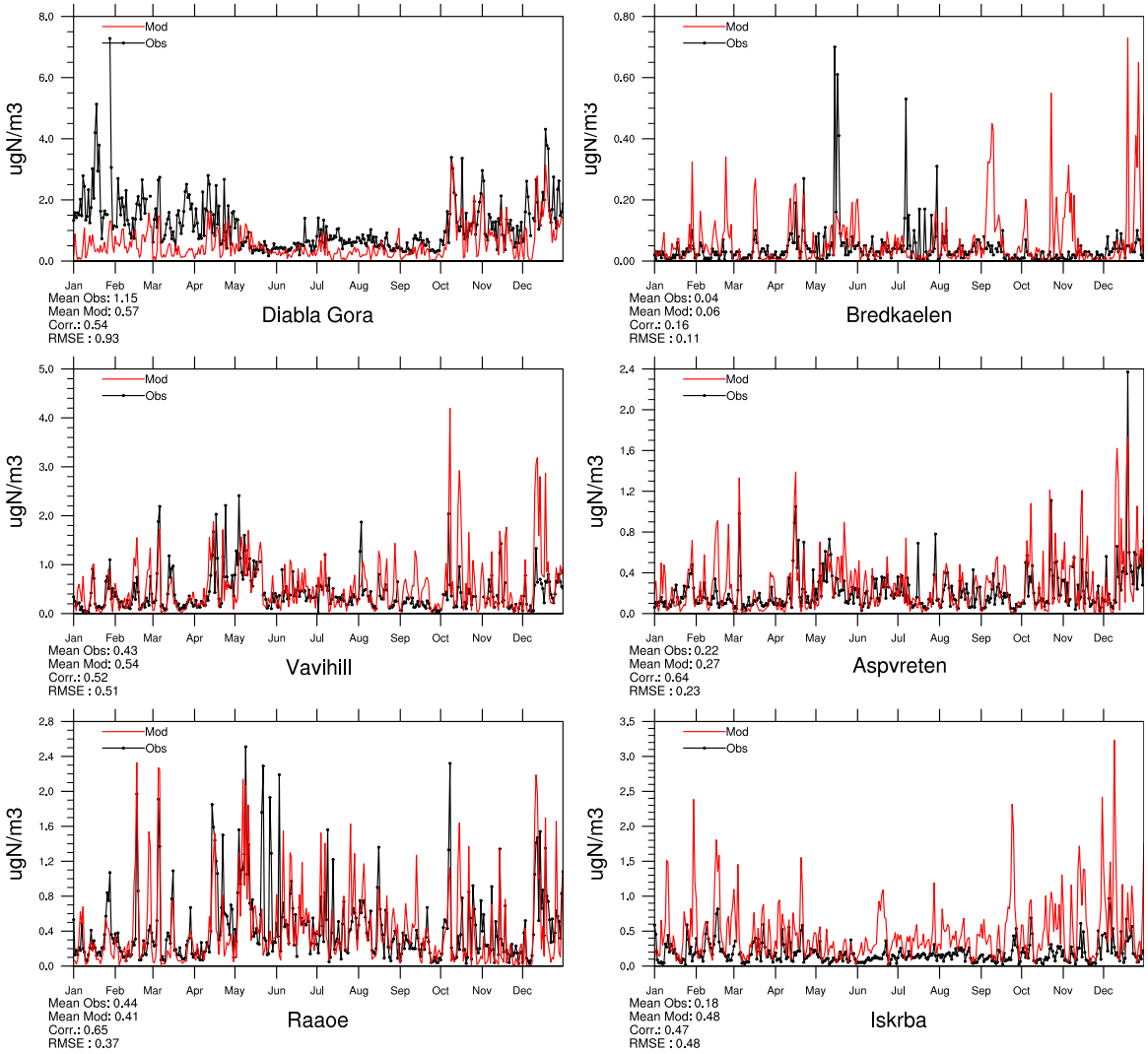

Figure 2.24: Comparison of model results and measurements (daily) total nitrate concentrations [μg(N) m^{-3}] for stations that have measured total nitrate in 2013.

Ammonia+ammonium in air

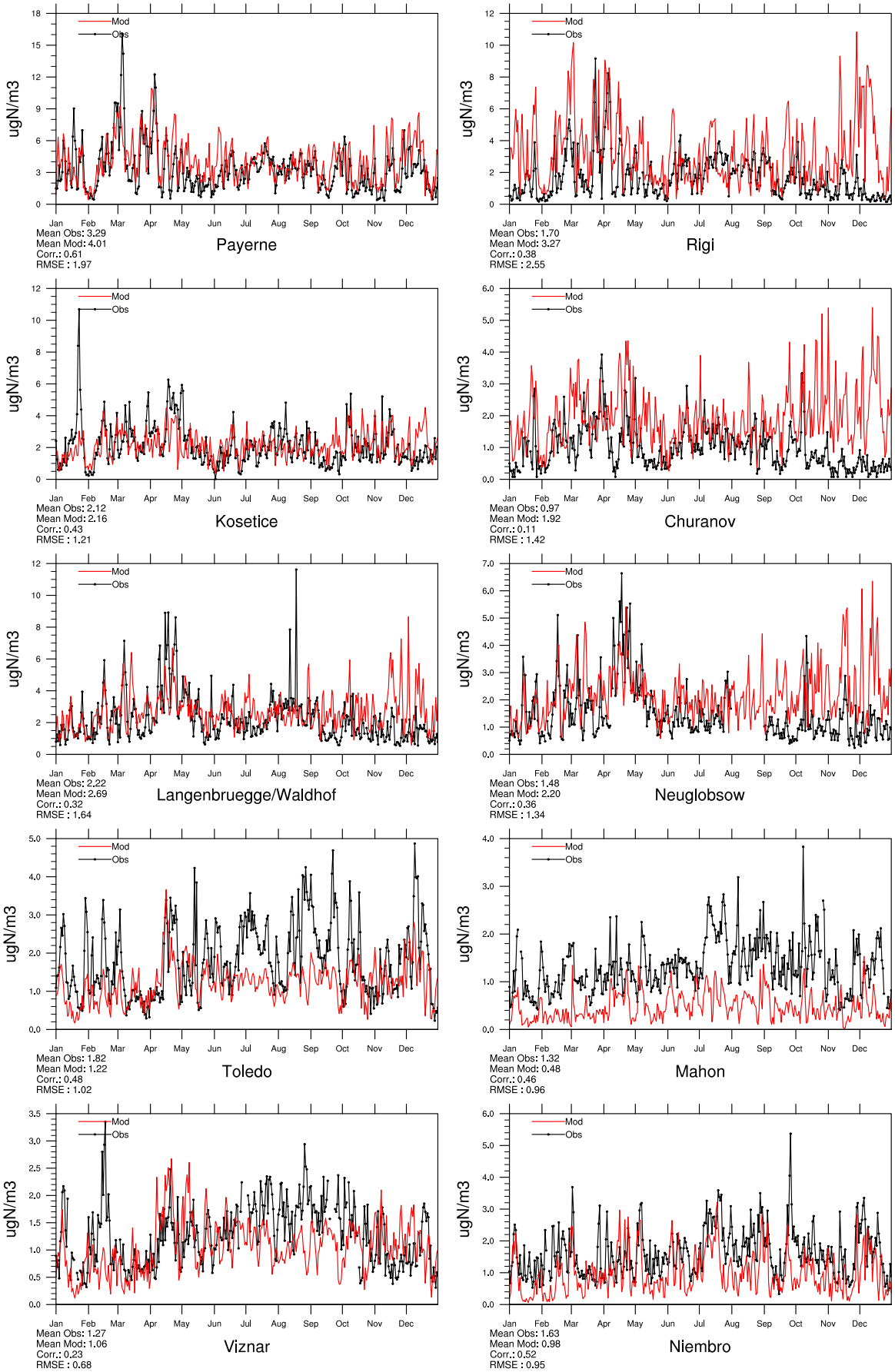

Figure 2.25: Comparison of model results and measurements (daily) total ammonium+ammonia concentrations [μg(N) m^{-3}] for stations that have measured total ammonium+ammonia in 2013.

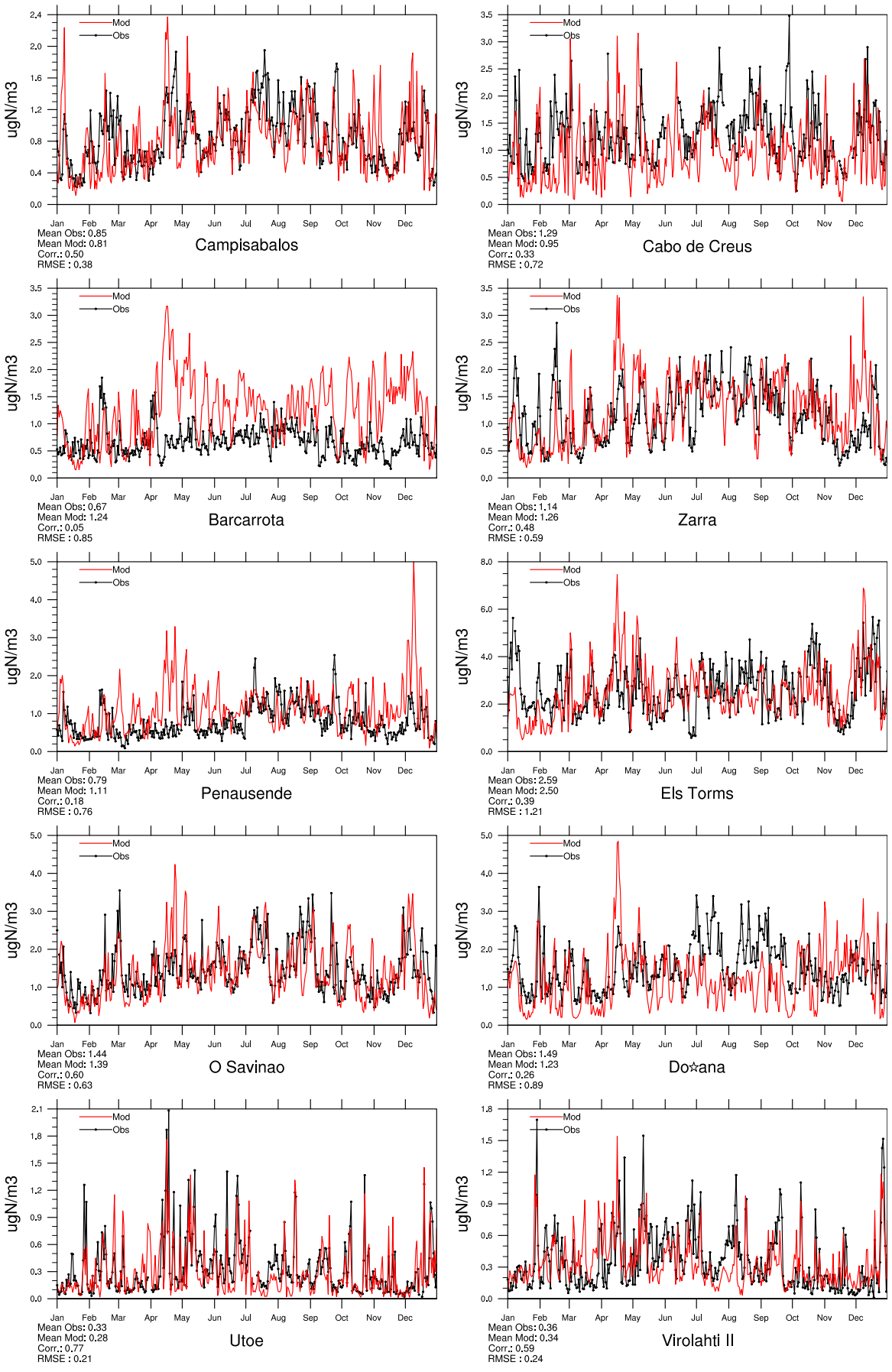

Figure 2.26: Comparison of model results and measurements (daily) total ammonium+ammonia concentrations [μg(N) m^{-3}] for stations that have measured total ammonium+ammonia in 2013.

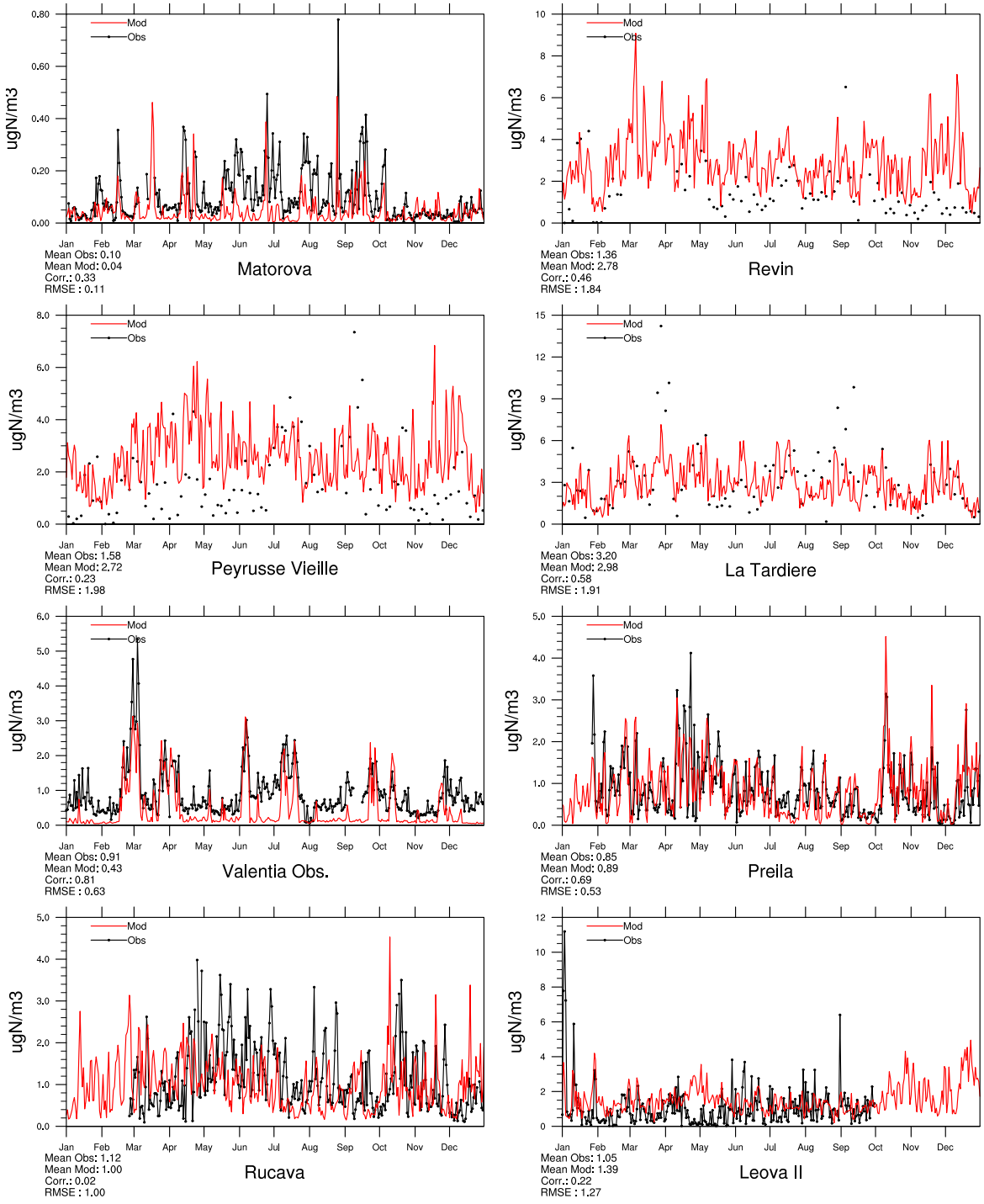

Figure 2.27: Comparison of model results and measurements (daily) total ammonium+ammonia concentrations [μg(N) m^{-3}] for stations that have measured total ammonium+ammonia in 2013.

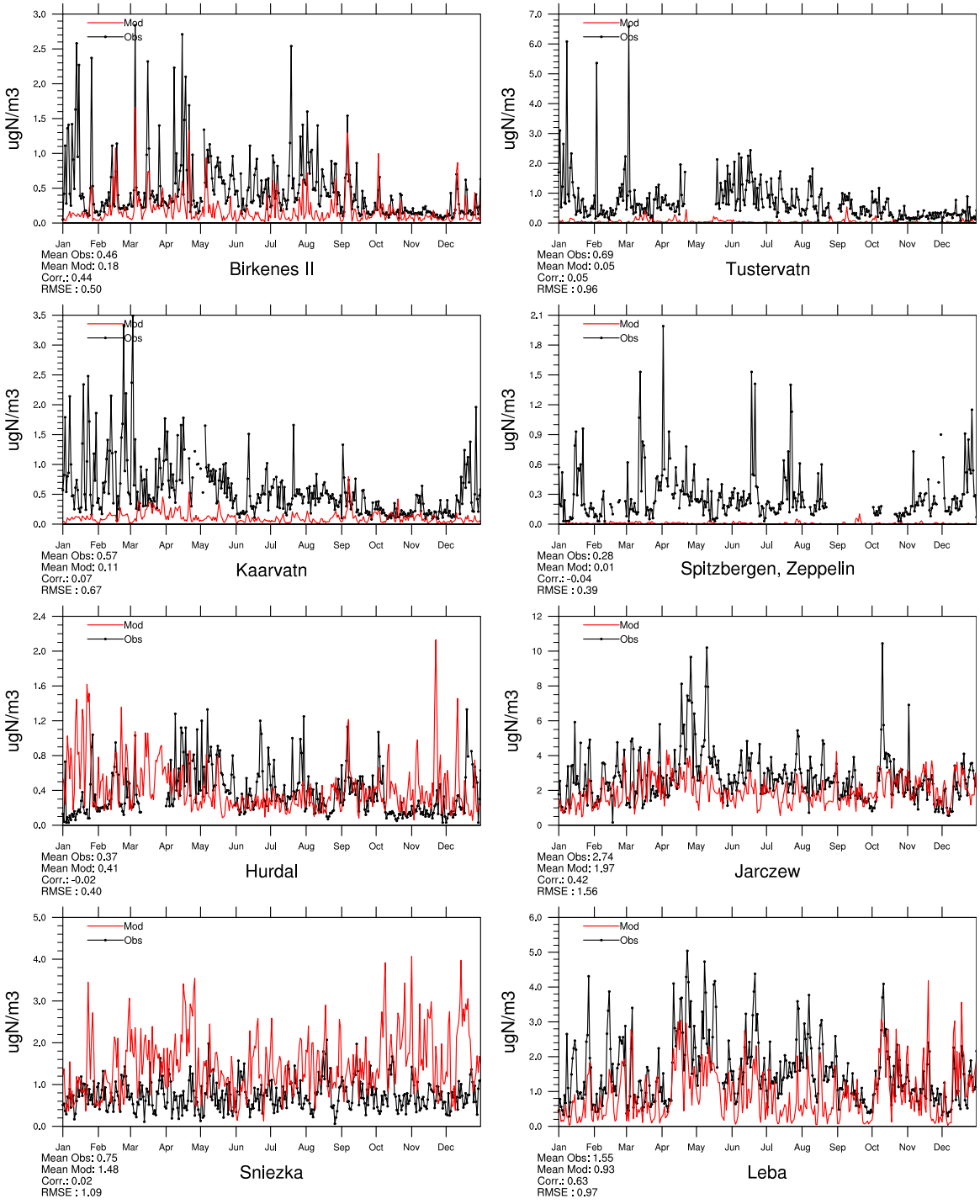

Figure 2.28: Comparison of model results and measurements (daily) total ammonium+ammonia concentrations [μg(N) m^{-3}] for stations that have measured total ammonium+ammonia in 2013.

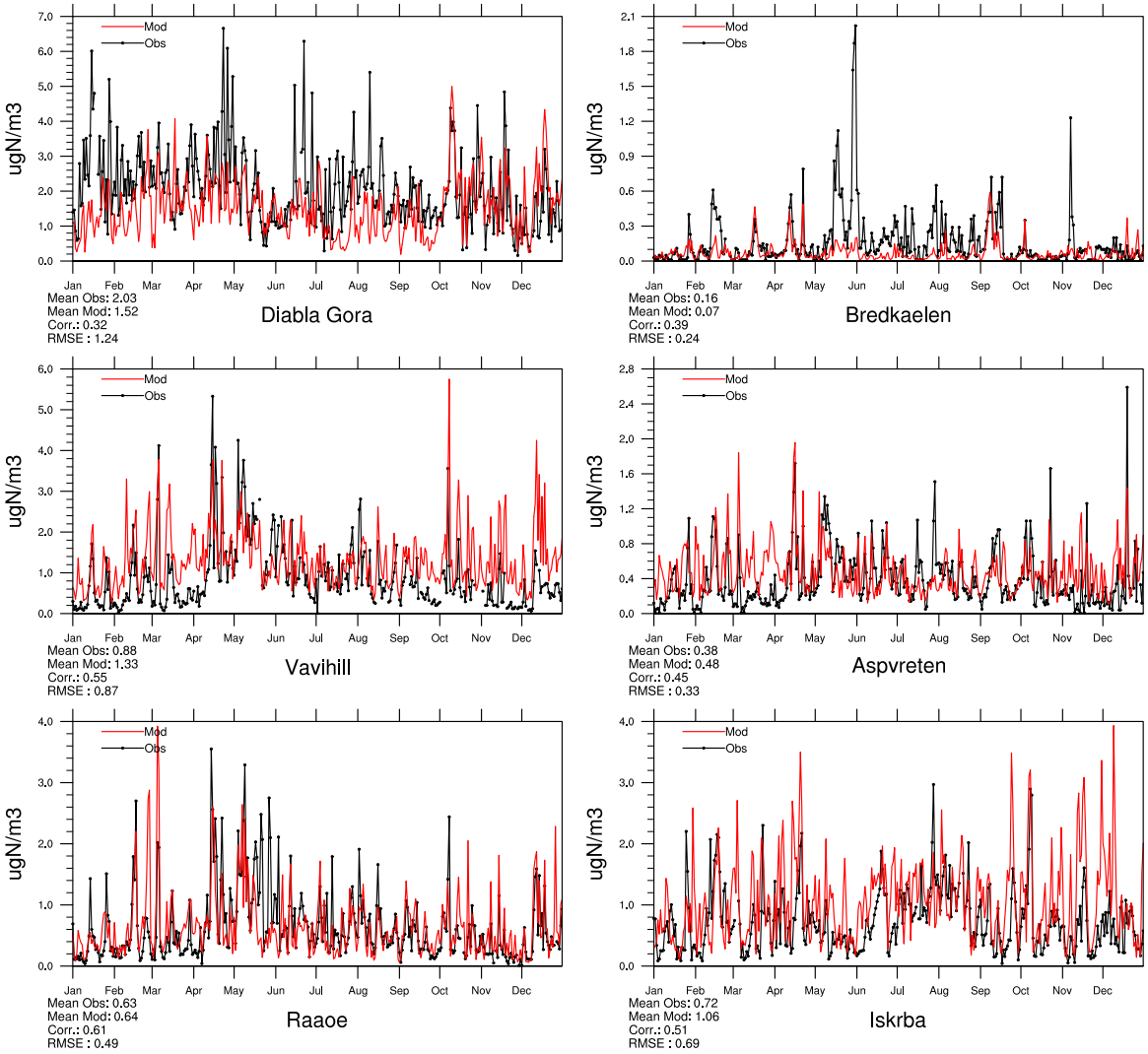

Figure 2.29: Comparison of model results and measurements (daily) total ammonium+ammonia concentrations [μg(N) m^{-3}] for stations that have measured total ammonium+ammonia in 2013.

Sulphur in precipitation

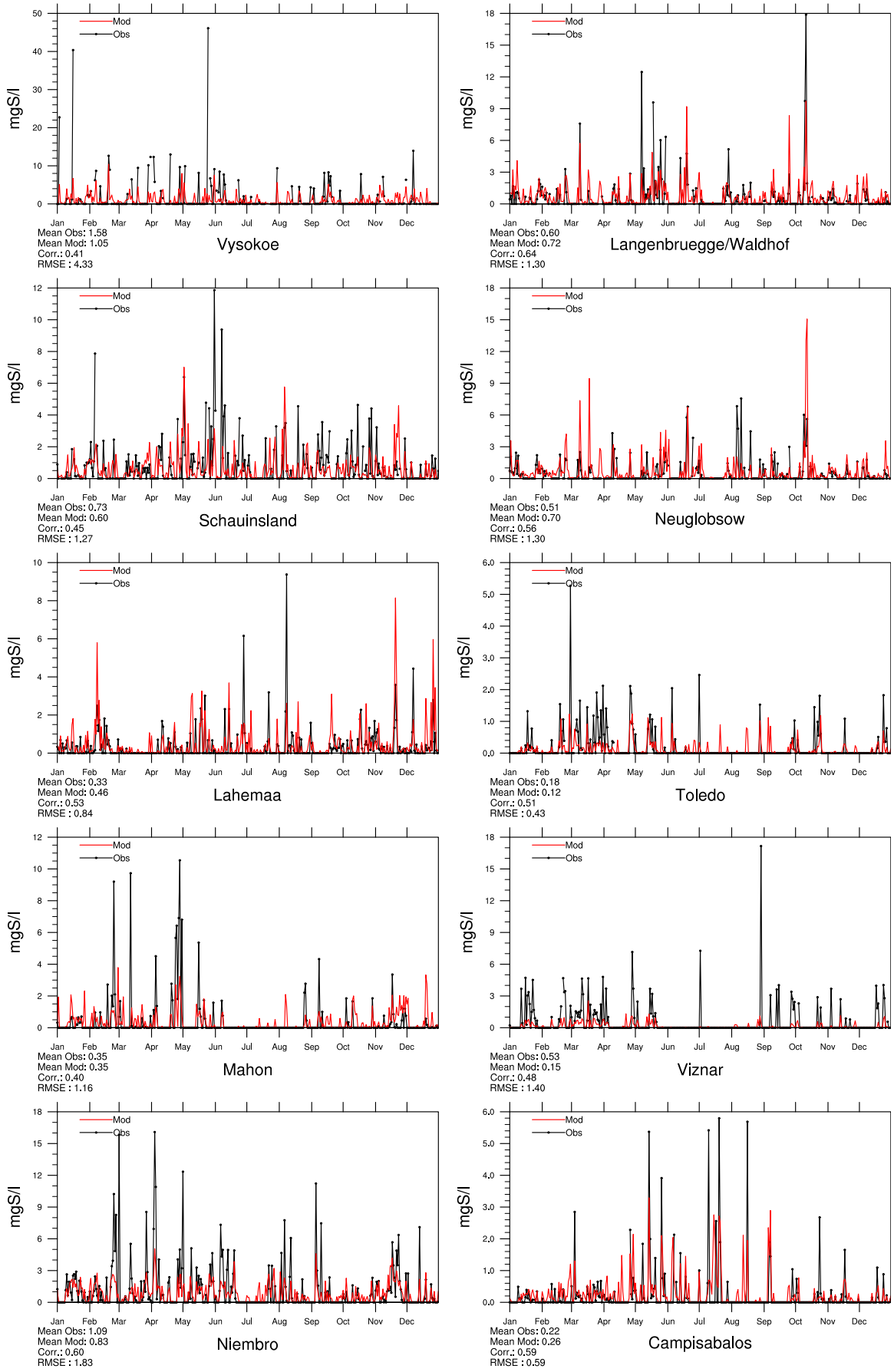

Figure 2.30: Comparison of model results and measurements (daily) for wet deposition of sulphur [mg(S)l^{-1}] in 2013.

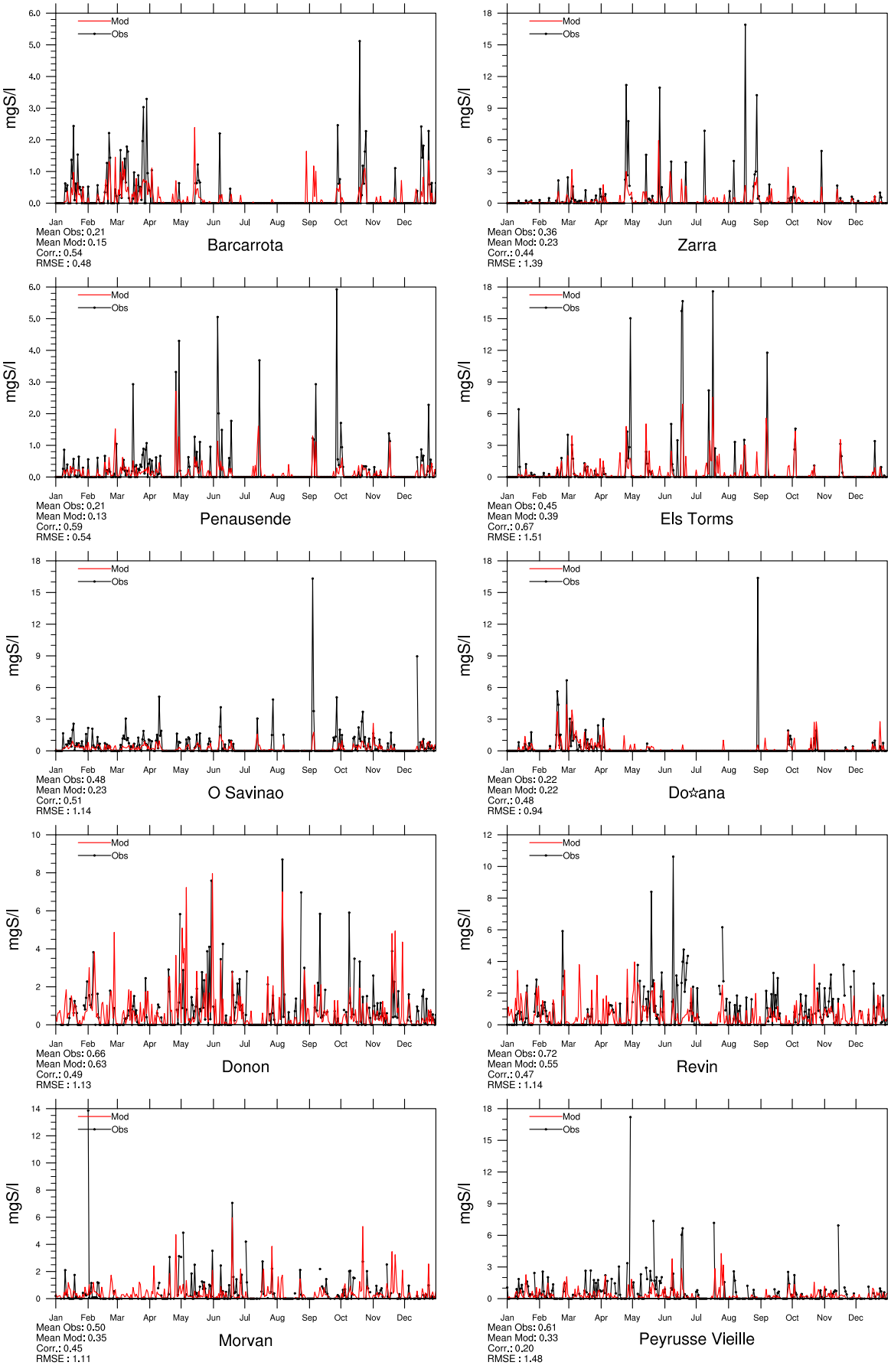

Figure 2.31: Comparison of model results and measurements (daily) for wet deposition of sulphur [mg(S)l^{-1}] in 2013.

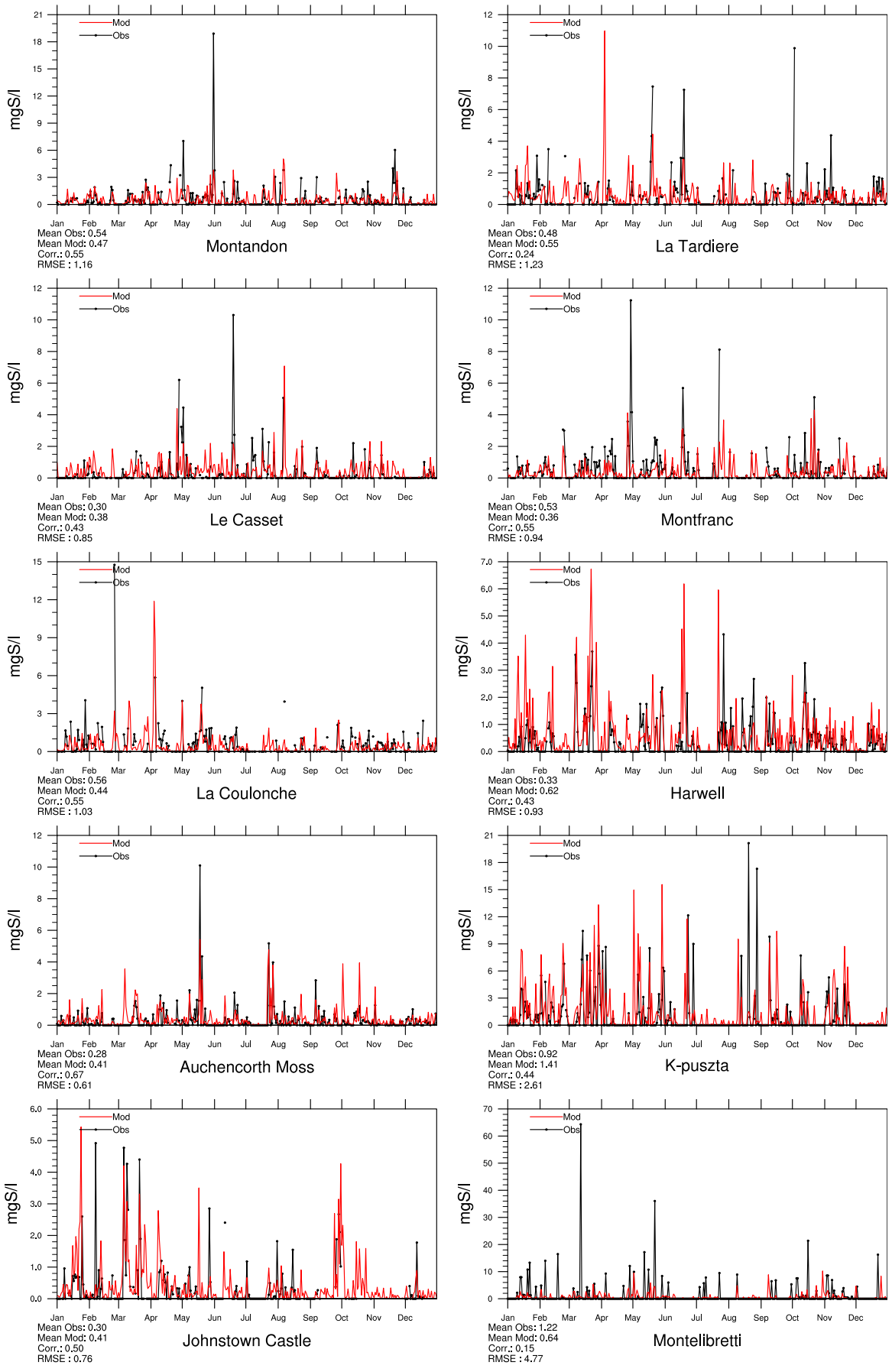

Figure 2.32: Comparison of model results and measurements (daily) for wet deposition of sulphur [mg(S)l^{-1}] in 2013.

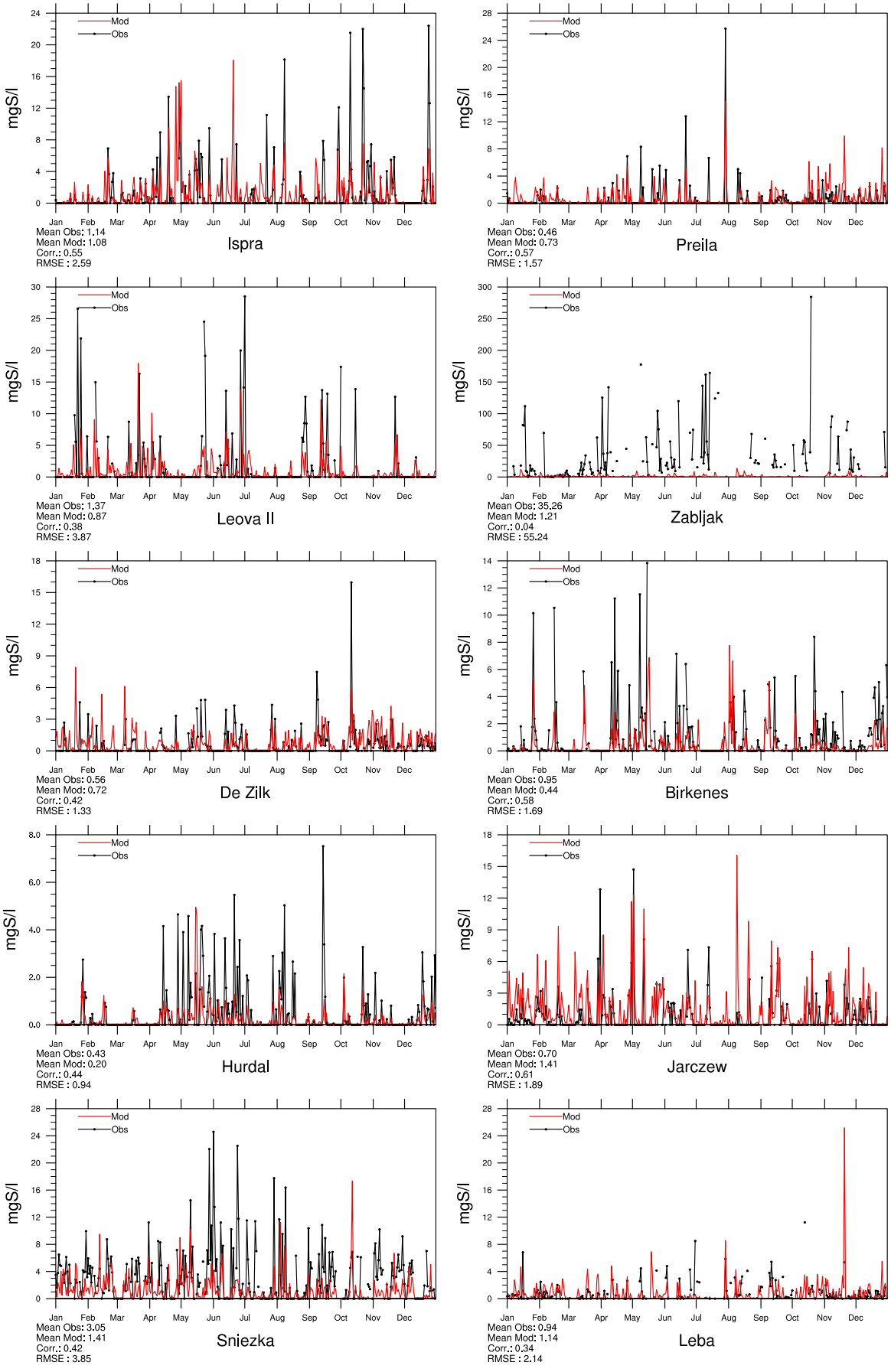

Figure 2.33: Comparison of model results and measurements (daily) for wet deposition of sulphur [mg(S)l^{-1}] in 2013.

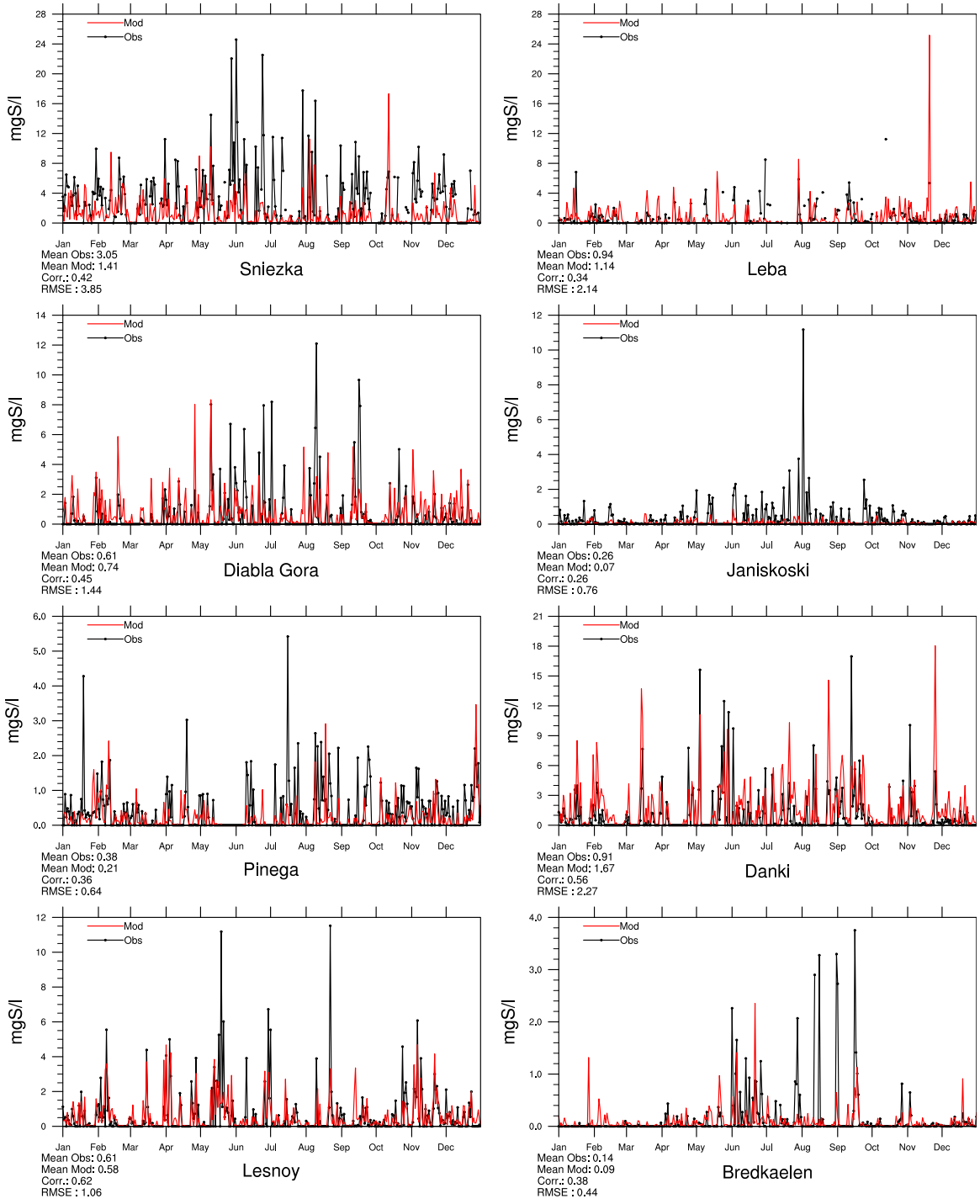

Figure 2.34: Comparison of model results and measurements (daily) for wet deposition of sulphur [mg(S)l^{-1}] in 2013.

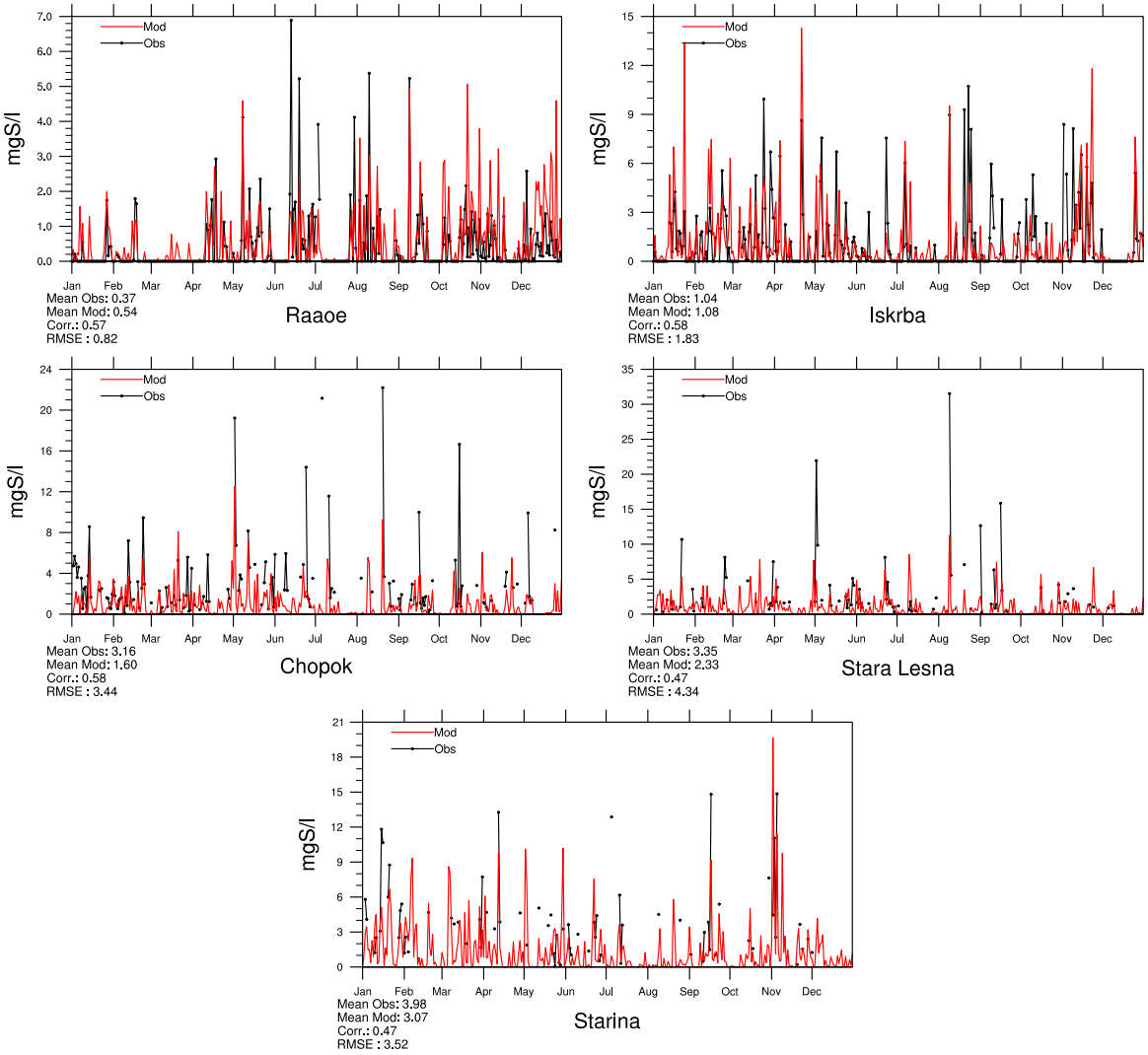

Figure 2.35: Comparison of model results and measurements (daily) for wet deposition of sulphur [mg(S)l^{-1}] in 2013.

Oxidized nitrogen in precipitation

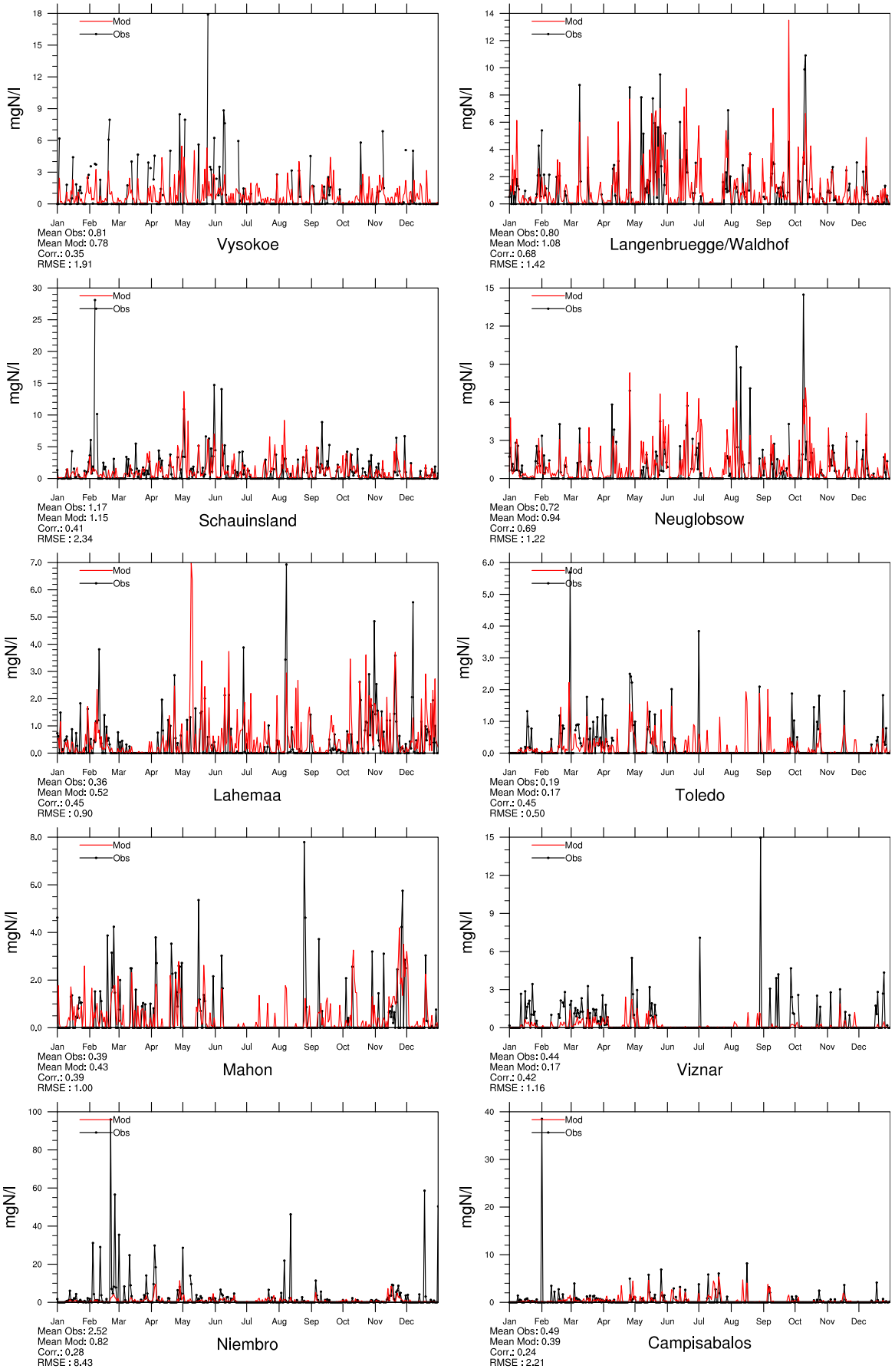

Figure 2.36: Comparison of model results and measurements (daily) for wet deposition of oxidized nitrogen [mg(N)l^{-1}] in 2013.

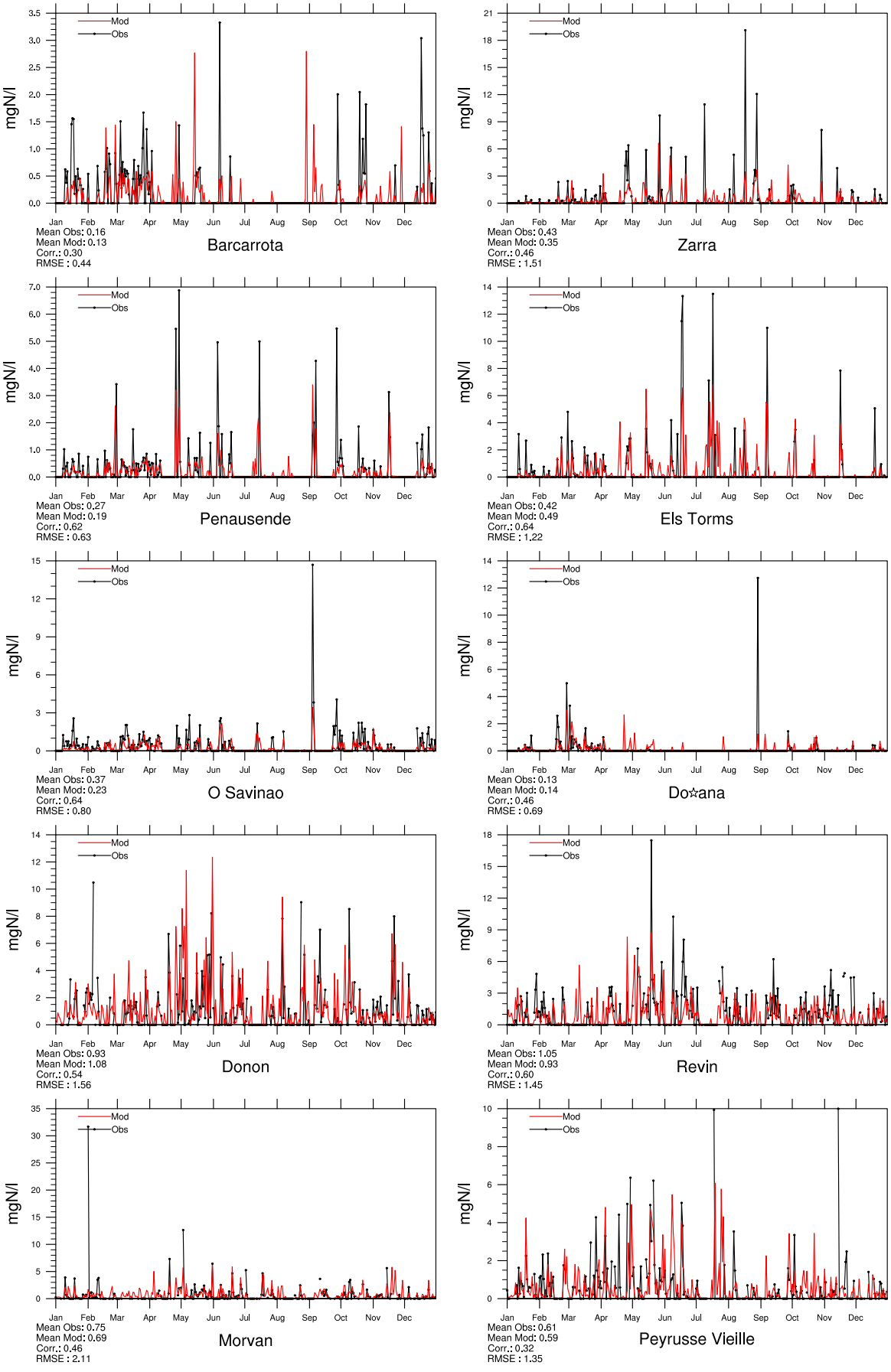

Figure 2.37: Comparison of model results and measurements (daily) for wet deposition of oxidized nitrogen [mg(N)l^{-1}] in 2013.

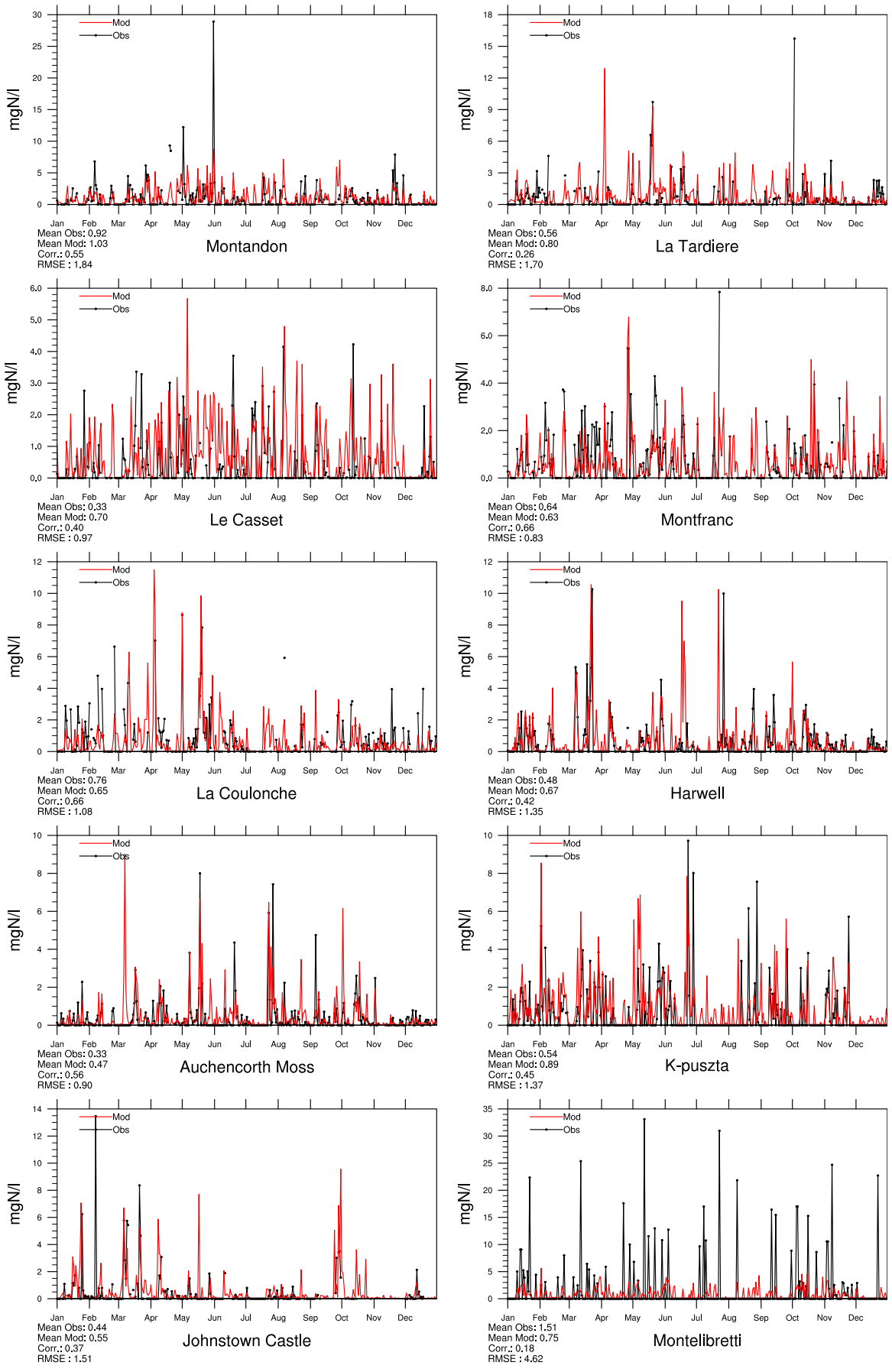

Figure 2.38: Comparison of model results and measurements (daily) for wet deposition of oxidized nitrogen [mg(N)l^{-1}] in 2013.

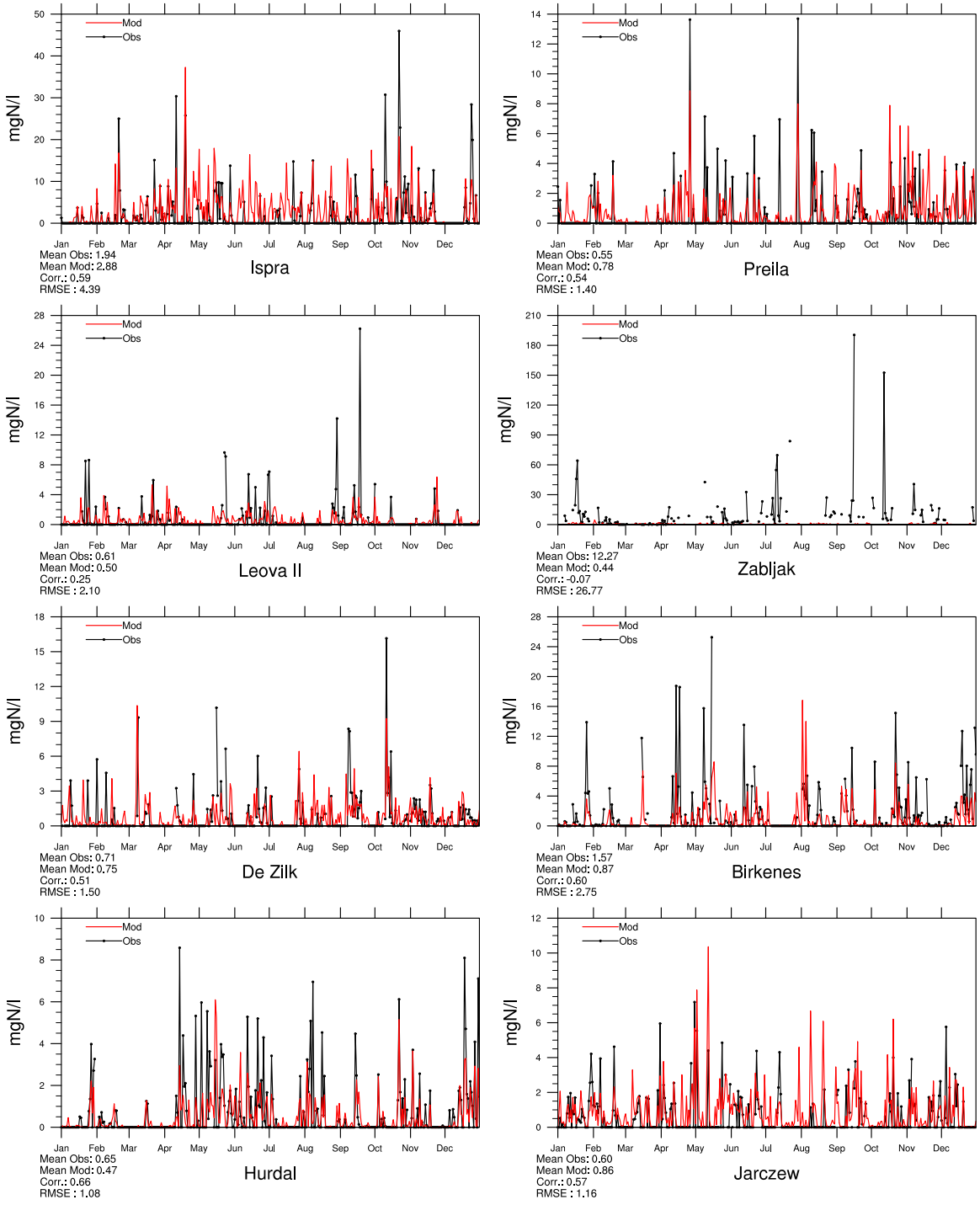

Figure 2.39: Comparison of model results and measurements (daily) for wet deposition of oxidized nitrogen [mg(N)l^{-1}] in 2013.

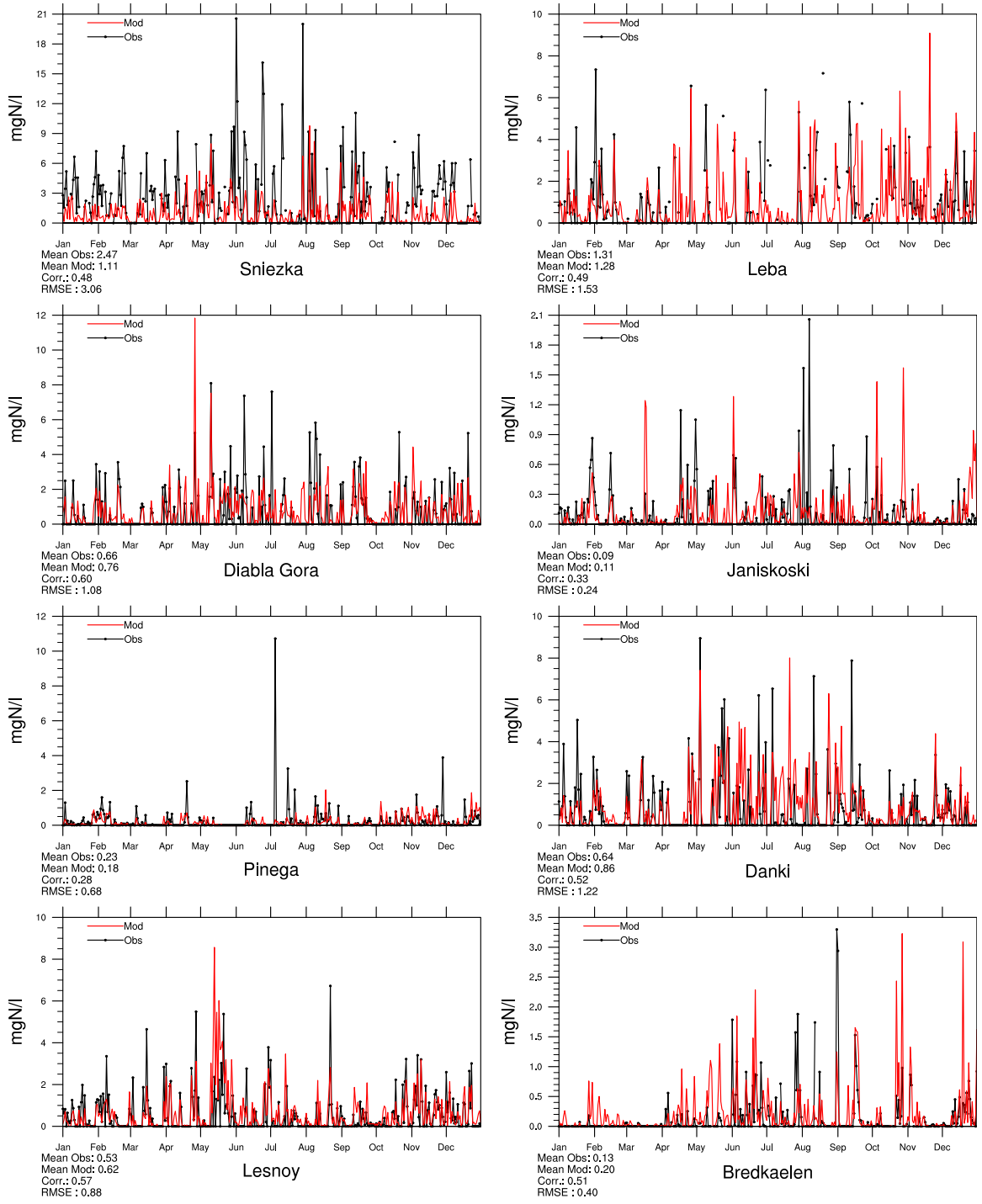

Figure 2.40: Comparison of model results and measurements (daily) for wet deposition of oxidized nitrogen [mg(N)l^{-1}] in 2013.

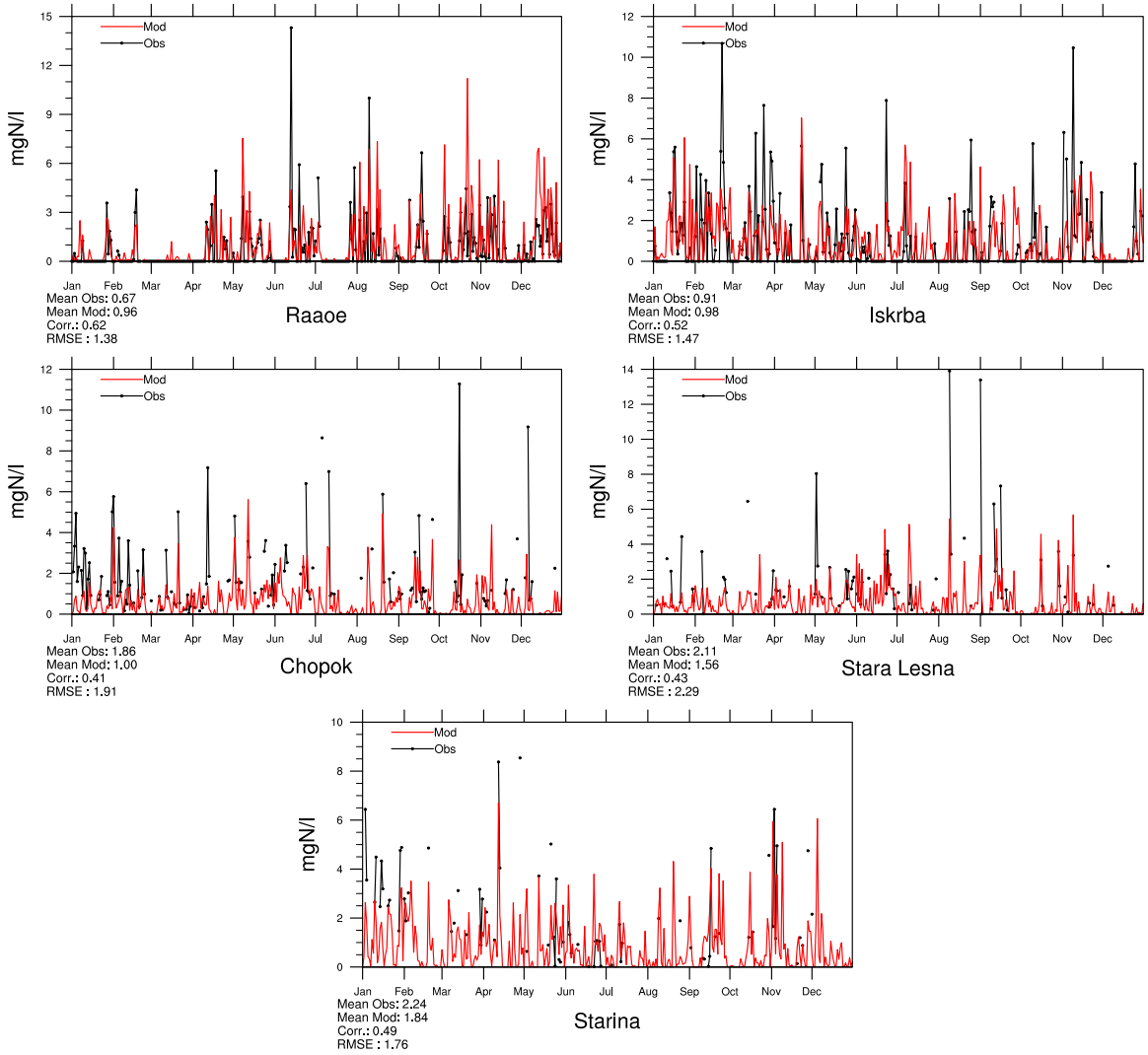

Figure 2.41: Comparison of model results and measurements (daily) for wet deposition of oxidized nitrogen [mg(N)l^{-1}] in 2013.

Reduced nitrogen in precipitation

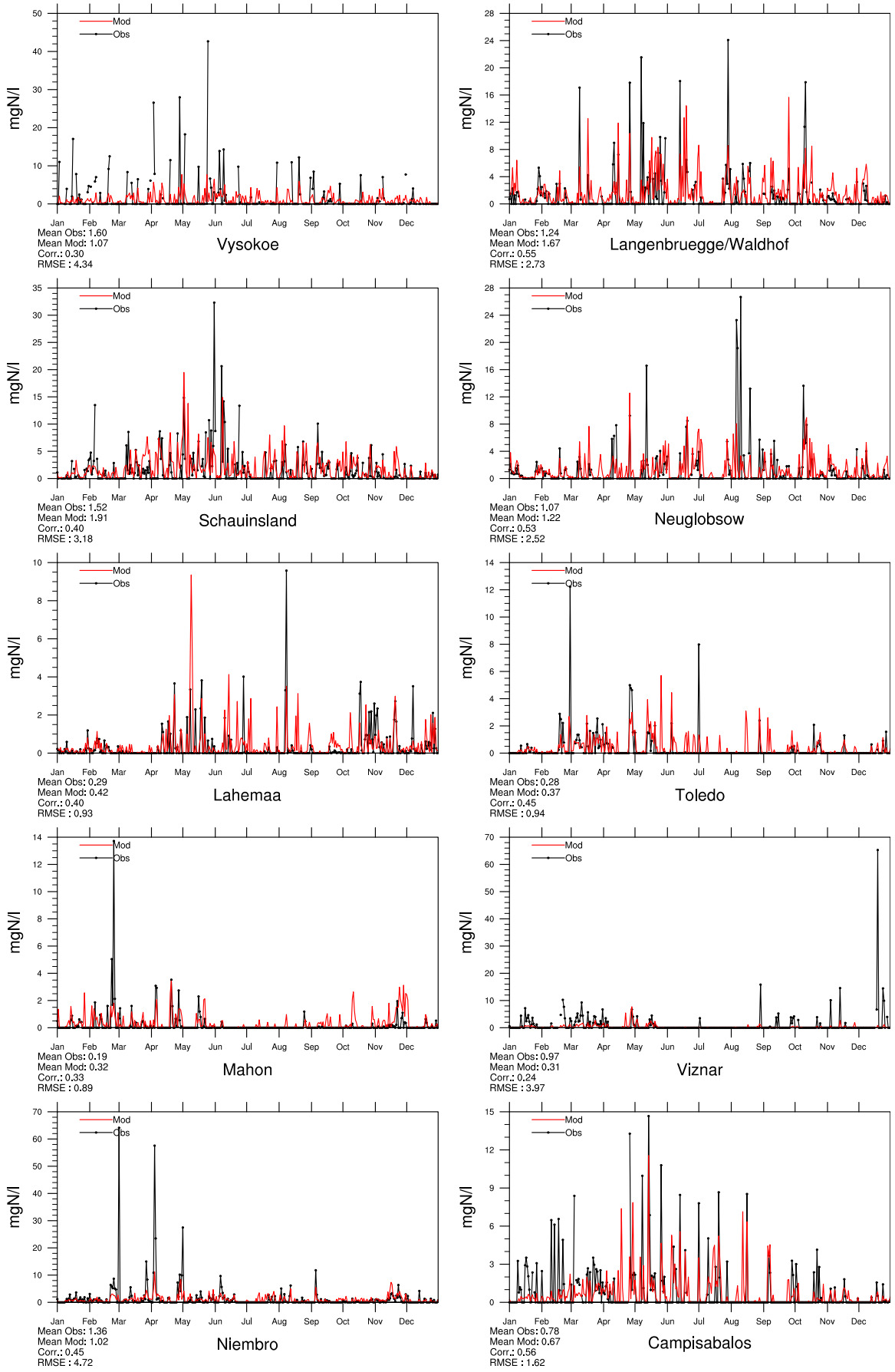

Figure 2.42: Comparison of model results and measurements (daily) for wet deposition of reduced nitrogen [mg(N)l^{-1}] in 2013.

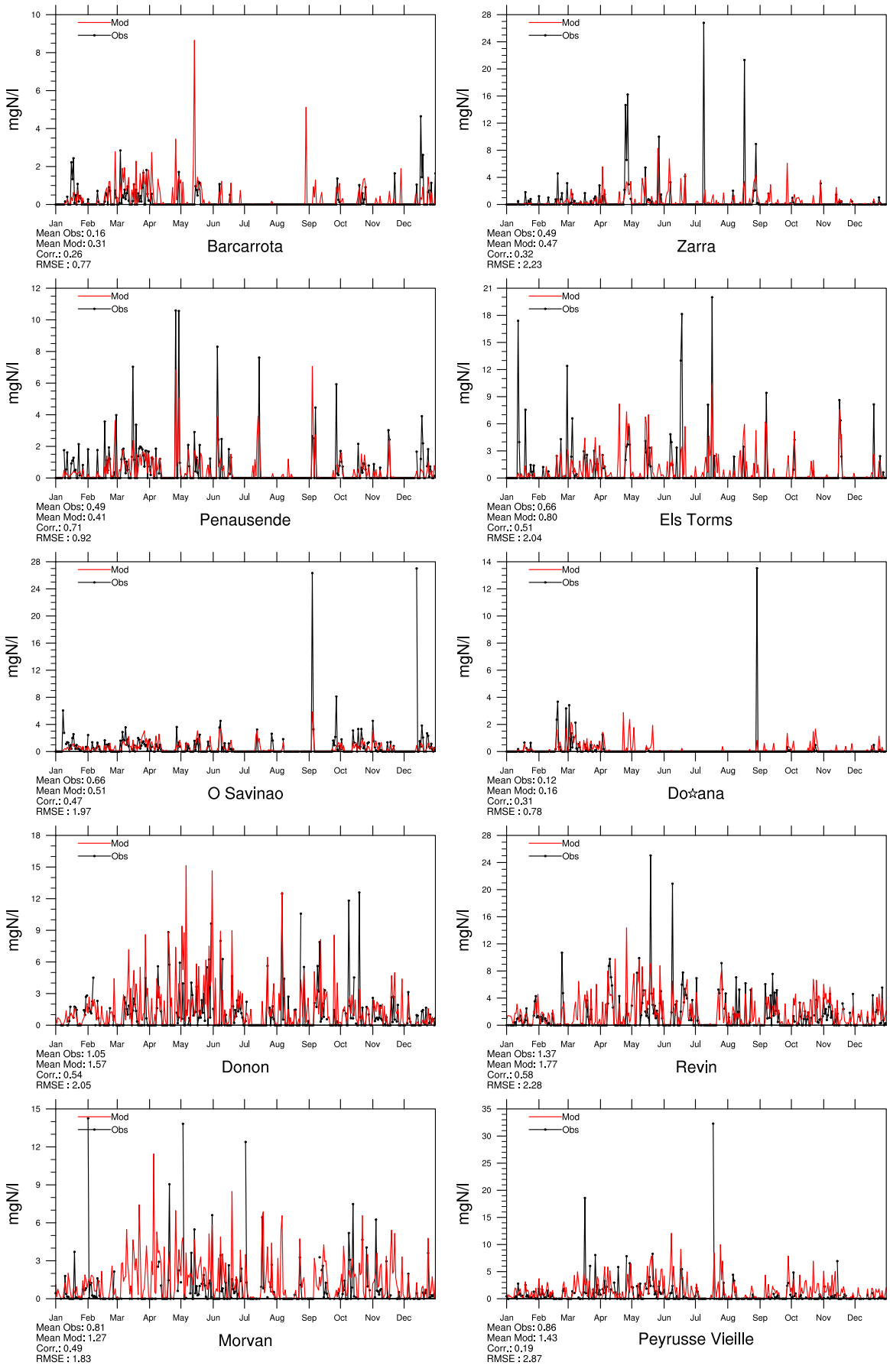

Figure 2.43: Comparison of model results and measurements (daily) for wet deposition of reduced nitrogen [mg(N)l^{-1}] in 2013.

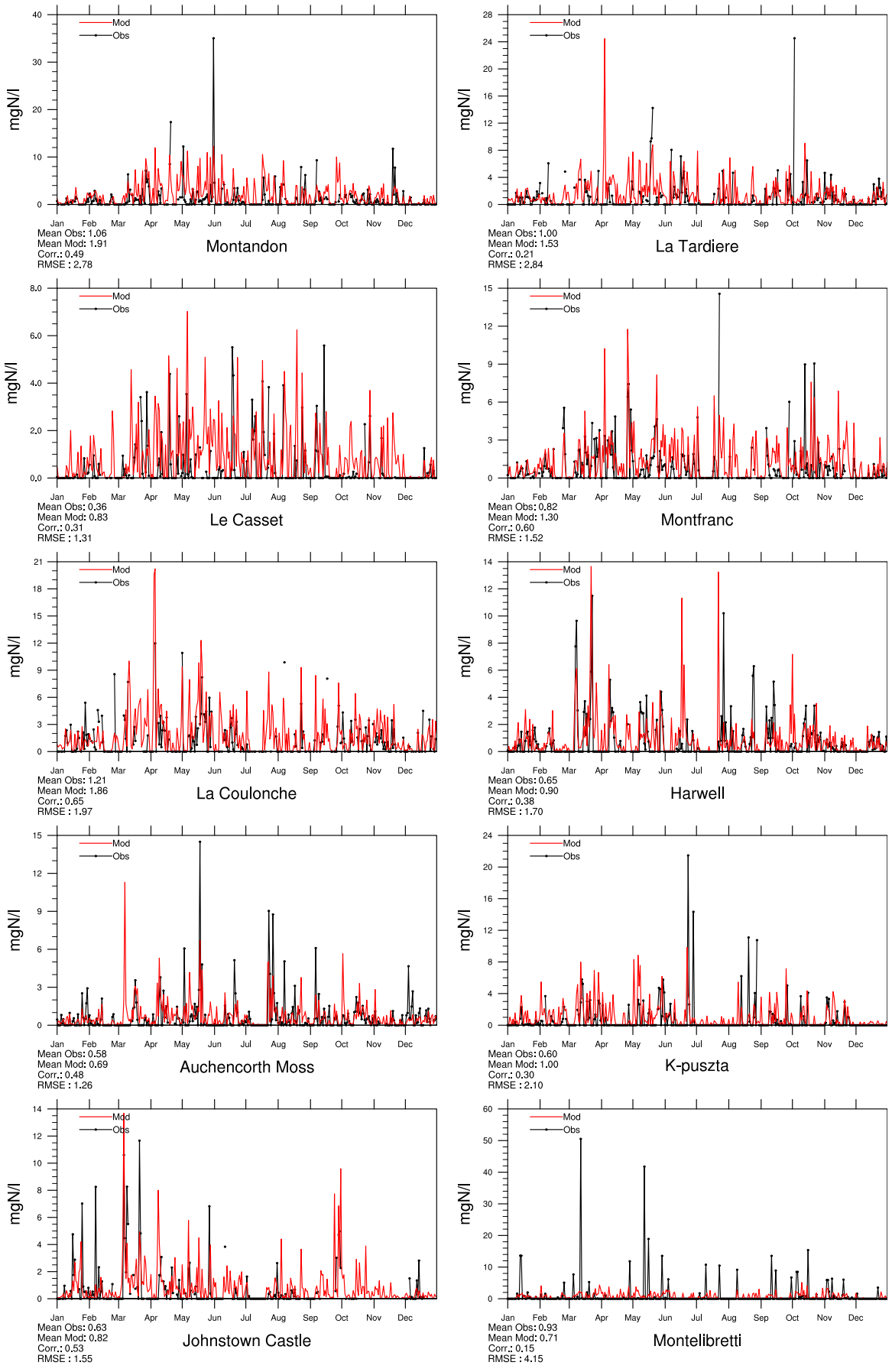

Figure 2.44: Comparison of model results and measurements (daily) for wet deposition of reduced nitrogen [mg(N)l^{-1}] in 2013.

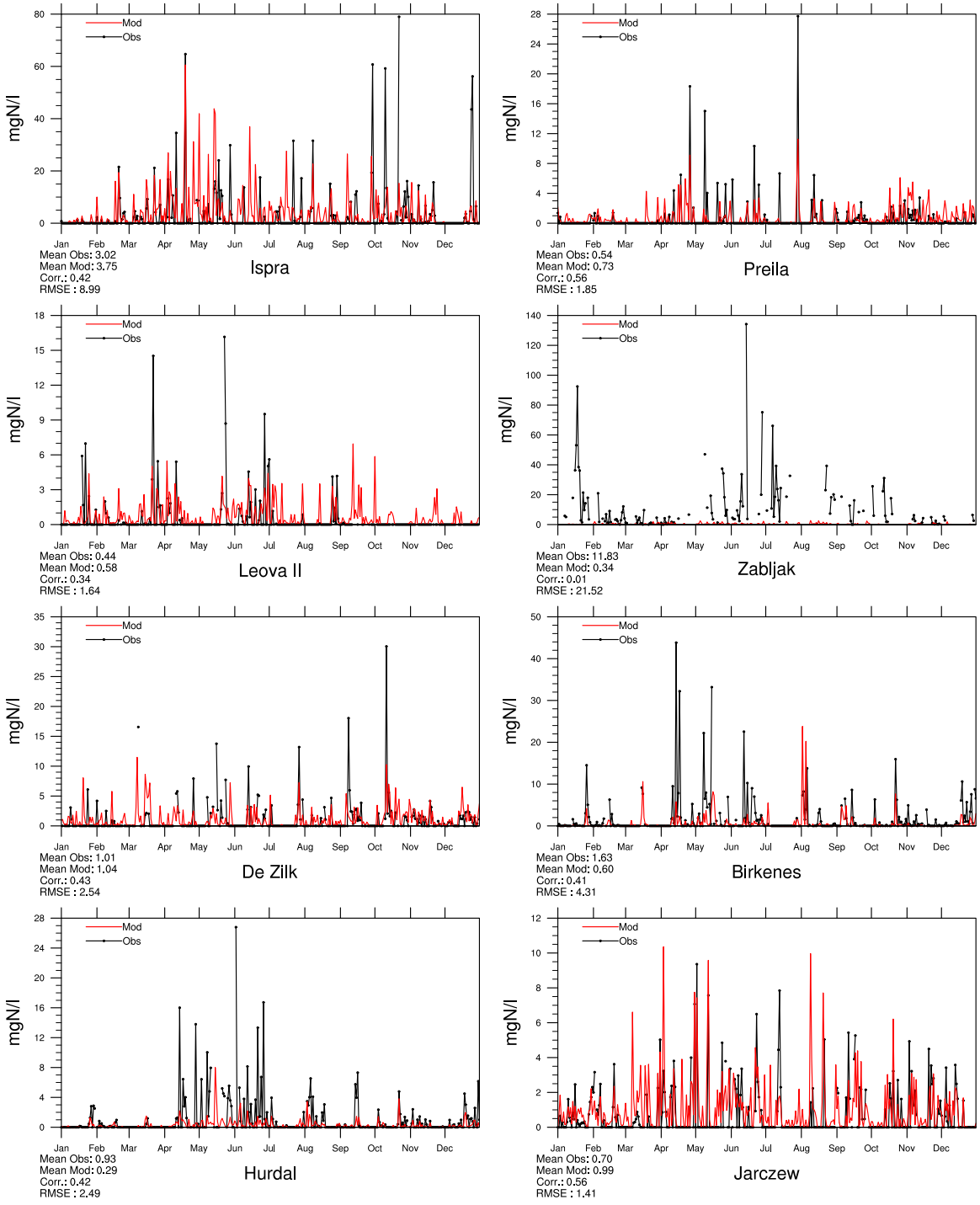

Figure 2.45: Comparison of model results and measurements (daily) for wet deposition of reduced nitrogen [mg(N)l^{-1}] in 2013.

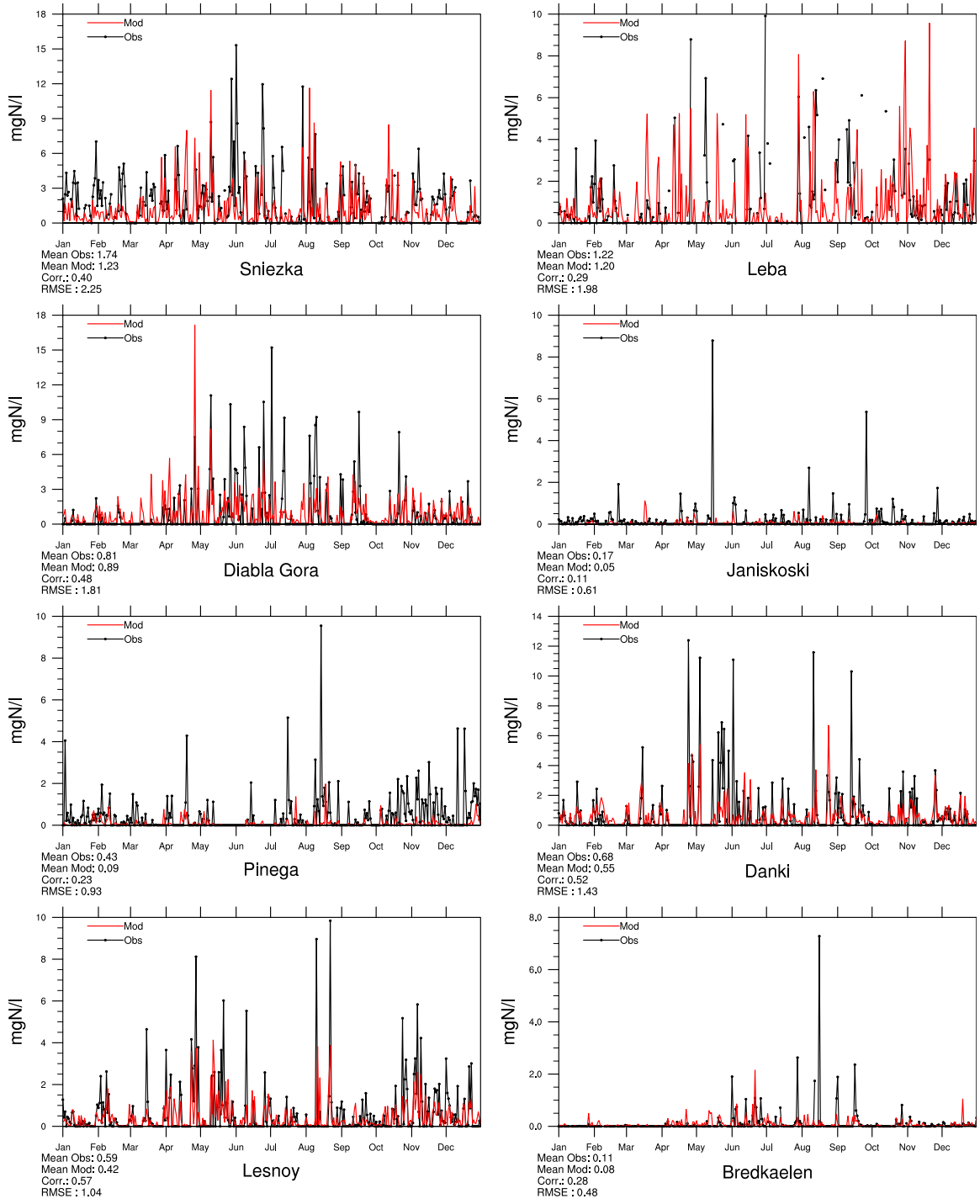

Figure 2.46: Comparison of model results and measurements (daily) for wet deposition of reduced nitrogen [mg(N)l^{-1}] in 2013.

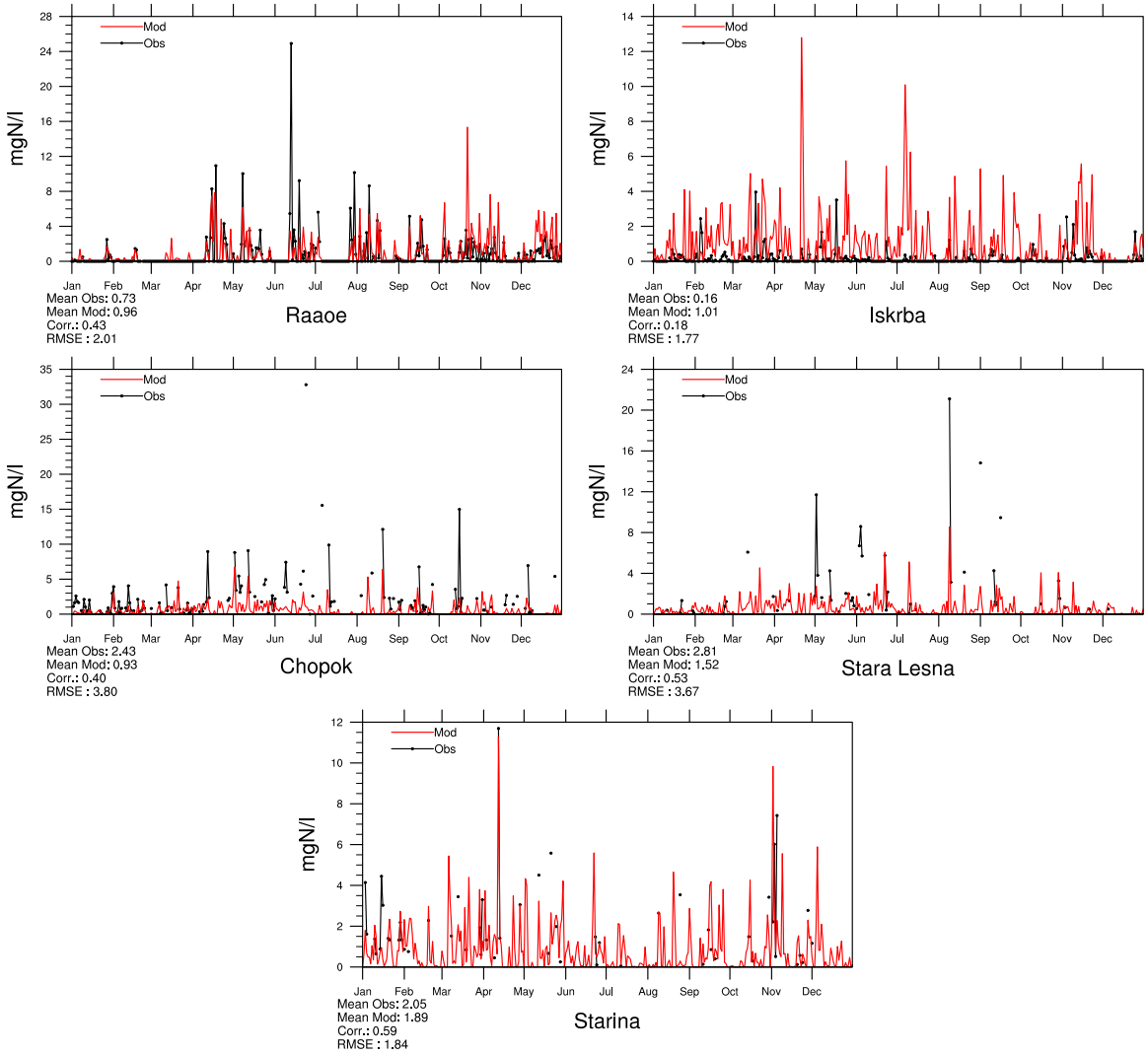

Figure 2.47: Comparison of model results and measurements (daily) for wet deposition of reduced nitrogen [mg(N)l^{-1}] in 2013.

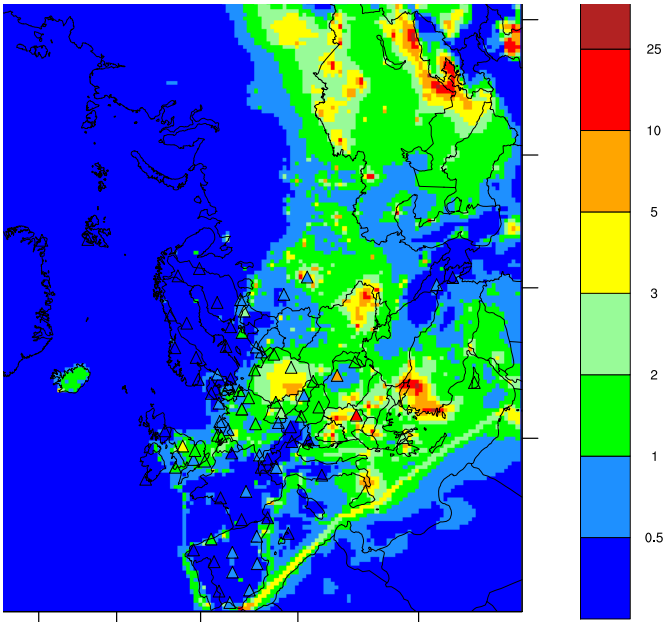

(a) SO_2

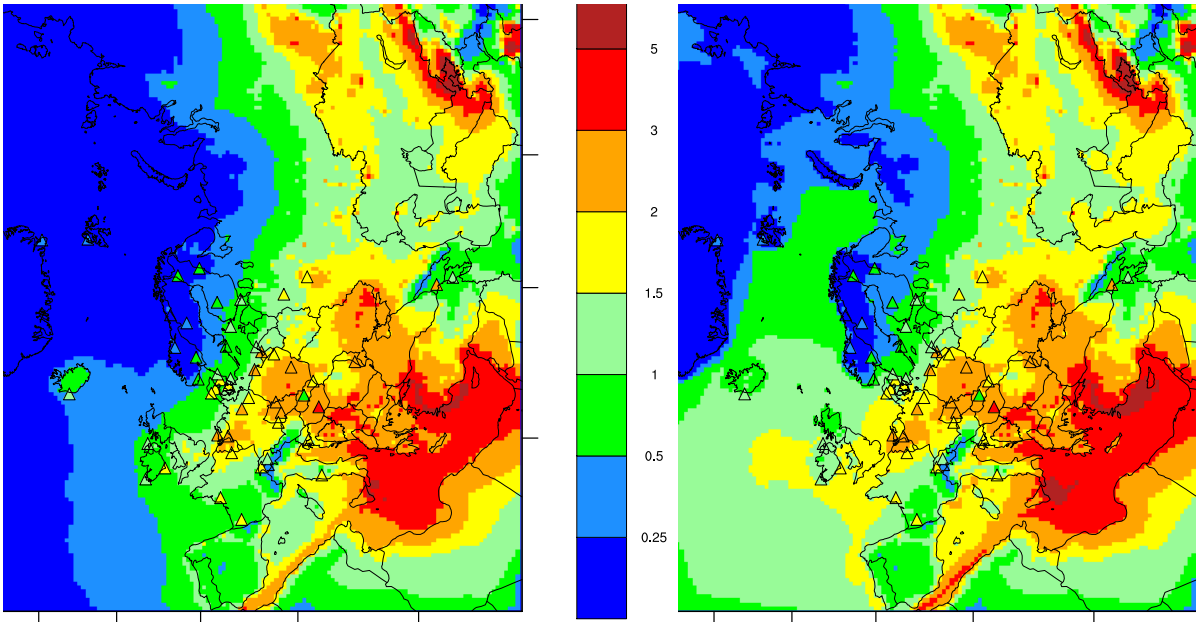

(b) SO_4^{2-} (c) SO_4^{2-}, sea salt corrected

Figure 2.48: Yearly averaged concentrations of SO_2, SO_4^{2-}, and SO_4^{2-} sea salt corrected, in air for 2013 [μg(S) m^{-3}]. The maps show model results, with observations superimposed by triangles.

2.3 Combined maps of model results and observations

In this section we present maps (Figures 2.48–2.50) showing both modelled and observed concentrations in air and concentrations in precipitation for selected sulphur and nitrogen species. In general, there is good agreement between model results and observations in 2013.

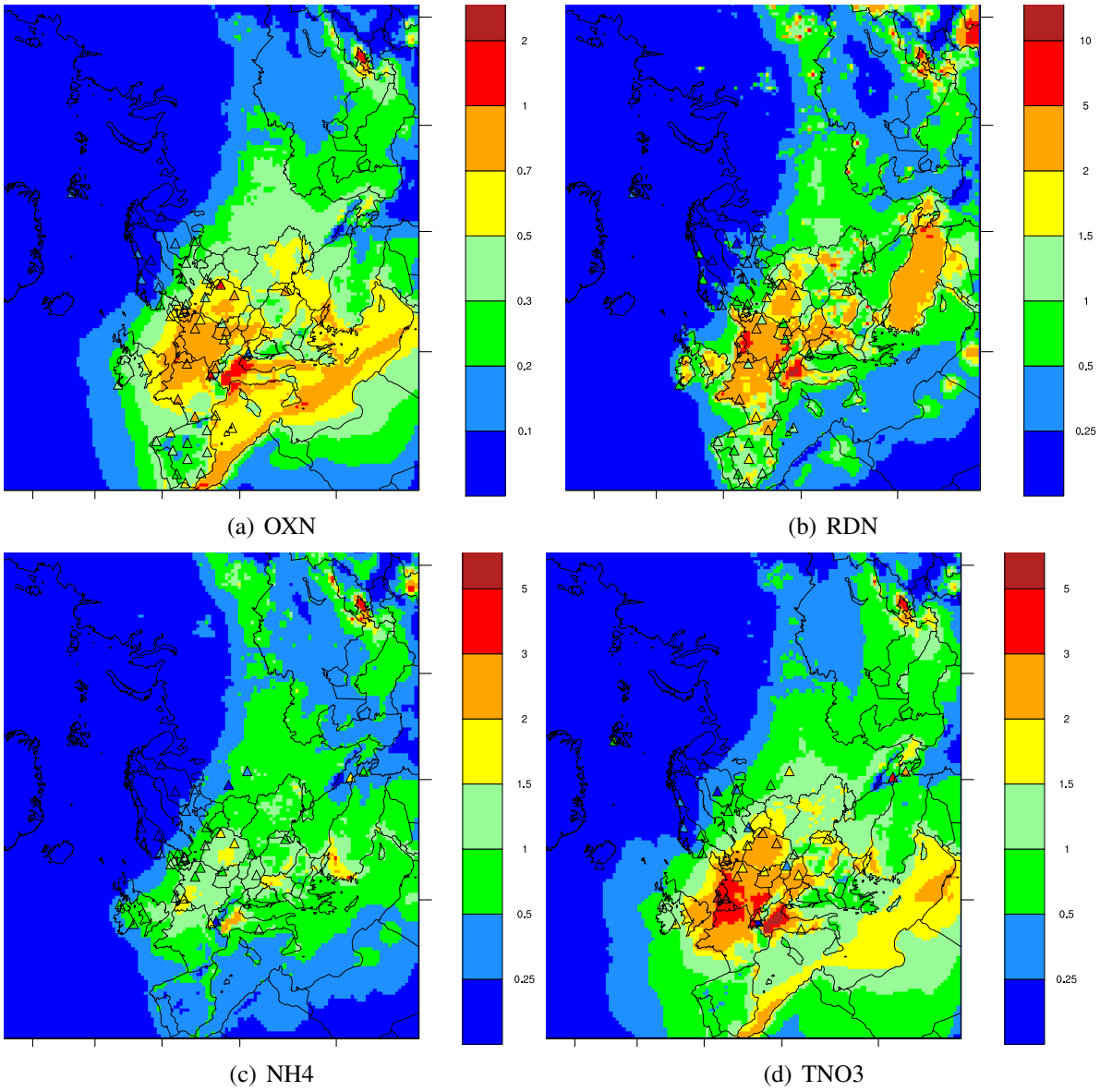

(a) OXN (b) RDN

(c) NH4 (d) TNO3

Figure 2.49: Yearly averaged concentrations of oxidized nitrogen (OXN), reduced nitrogen (RDN), ammonium (NH4), and total nitrate (TNO3), in air for 2013 [μg(N) m^{-3}]. The maps show model results, with observations superimposed by triangles.

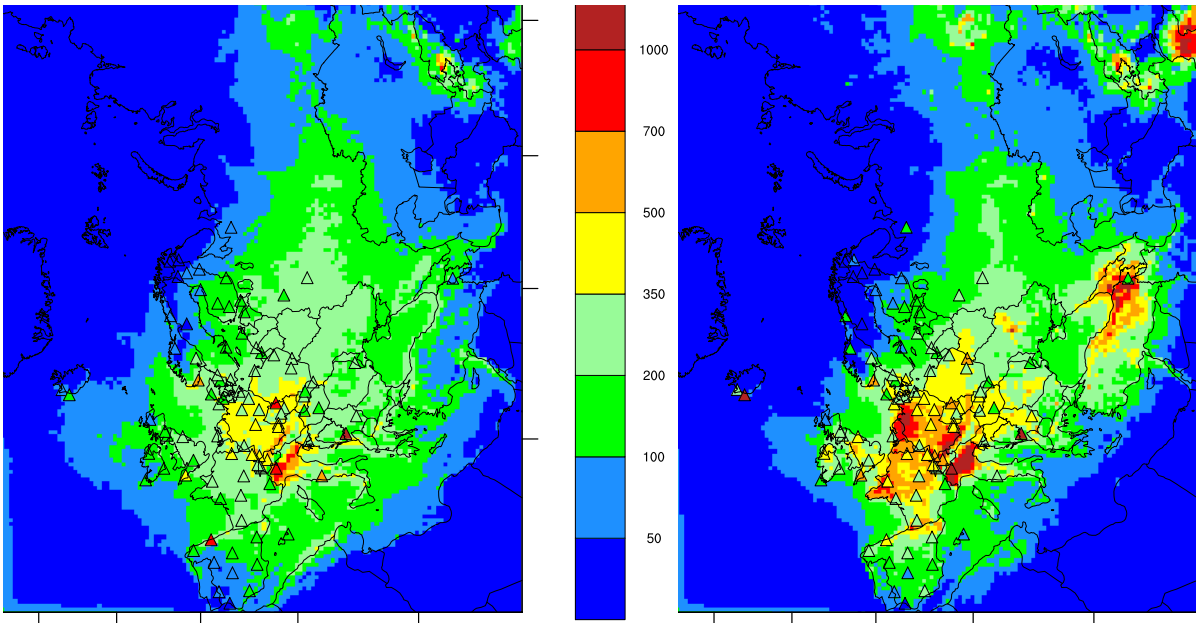

(a) WDEP OXN

(b) WDEP RDN

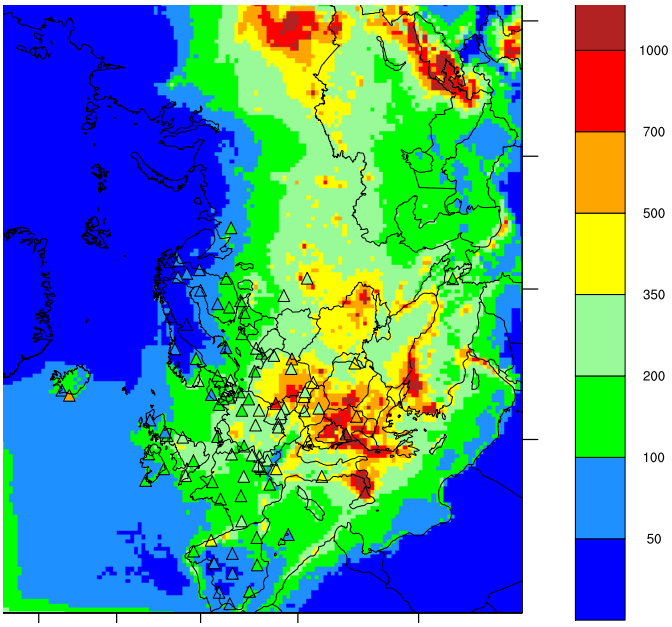

(c) WDEP SOX

Figure 2.50: Yearly wet deposition of oxidized nitrogen (OXN), reduced nitrogen (RDN), oxides of sulphur (SOX), in 2013 [μgN/m2 or μgS/m2]. The maps show model results, with observations superimposed by triangles.

References

H. Fagerli and W. Aas. Using the EMEP intensive measurement data to evaluate the performance of the EMEP model for nitrogen compounds. In *In Transboundary Acidification, Eutrophication and Ground Level Ozone in Europe in 2006. EMEP Status Report 1/2008*, pages 109–126. The Norwegian Meteorological Institute, Oslo, Norway, 2008.

H. Fagerli and A.G. Hjellbrekke. Acidification and eutrophication. In *Transboundary Acidification, Eutrophication and Ground Level Ozone in Europe in 2006. EMEP Status Report 1/2008*, pages 41–56. The Norwegian Meteorological Institute, Oslo, Norway, 2008.

H. Fagerli, B. M. Steensen, and A.-G. Hjellbrekke. Acidifying and eutrophying components: validation and combined maps. Supplementary material to EMEP Status Report 1/2012, available online at `www.emep.int`, The Norwegian Meteorological Institute, Oslo, Norway, 2012.

M. Gauss, S. Tsyro, B. M. Steensen, and A.-G. Hjellbrekke. Acidifying and eutrophying components. Supplementary material to EMEP Status Report 1/2014, available online at `www.emep.int`, The Norwegian Meteorological Institute, Oslo, Norway, 2014.

Á. Nyíri, M. Gauss, V. S. Semeena, and A.-G. Hjellbrekke. Acidifying and eutrophying components: validation and combined maps. Supplementary material to EMEP Status Report 1/2013, available online at `www.emep.int`, The Norwegian Meteorological Institute, Oslo, Norway, 2013.

D. Simpson, A. Benedictow, H. Berge, R. Bergström, L. D. Emberson, H. Fagerli, G. D. Hayman, M. Gauss, J. E. Jonson, M. E. Jenkin, A. Nyíri, C. Richter, V. S. Semeena, S. Tsyro, J.-P. Tuovinen, Á. Valdebenito, and P. Wind. The EMEP MSC-W chemical transport model – technical description. *Atmos. Chem. Physics*, 12(16):7825–7865, 2012. doi:10.5194/acp-12-7825-2012.

D. Simpson, S. Tsyro, P. Wind, and B. M. Steensen. Emep model development. In *Transboundary acidification, eutrophication and ground level ozone in Europe in 2011. EMEP Status Report 1/2013*. The Norwegian Meteorological Institute, Oslo, Norway, 2013.

D. Simpson, S. Tsyro, and P. Wind. Updates to the emep/msc-w model. In *Transboundary particulate matter, photo-oxidants, acidifying and eutrophying components. EMEP Status Report 1/2015*. The Norwegian Meteorological Institute, Oslo, Norway, 2015.

Cort J. Willmott. On the validation of models. *Physical Geography*, 2:184–194, 1981.

Cort J. Willmott. Some comments on the evaluation of model performance. *Bulletin American Meteorological Society*, 63(11):1309–1313, 1982. doi:10.1175/1520-0477(1982)063<1309:SCOTEO>2.0.CO;2.

CHAPTER 3

Ozone

M. Gauss, A.-G. Hjellbrekke, and S. Solberg

In this chapter the EMEP/MSC-W model is evaluated with respect to surface ozone concentrations in air. In the following section we present tables of mean values and model performance indicators, and in Section 3.2 time series are plotted for selected stations to illustrate the performance of the EMEP/MSC-W model for the year 2013 with respect to ozone. In Section 3.3 we present maps of ozone for 2013, created by combining measurements and model results.

3.1 Tables

Table 3.1 shows for daily maximum ozone and daily mean ozone the number of stations where measurements were available and data coverage criteria were satisfied (N_{stat}), measured yearly average over all stations (Obs), modelled yearly average over all stations (Mod), bias, correlation between observation and model for station yearly averages, root mean square error, and index of agreement (IOA, as defined in Section 2.1).

Model performance for daily maximum ozone is much better than for daily mean ozone, mainly due to the difficulty of reproducting night-time ozone correctly. While the bias in daily mean ozone amounts to +8% it is as low as +1% in the case of daily maximum ozone.

Statistics for individual stations are tabulated in the next section.

Modelled daily maximum ozone values have been evaluated against measurements from all stations that supply data to EMEP CCC. Table 3.2 summarises these comparisons, and Figures 3.1 to 3.18 show time series plots for selected stations representing the different regions of Europe. To judge model performance, Table 3.2 shows root mean square error (RMSE) and the *index of agreement* (IOA, defined in Section 2.1).

Similarly to last year (Gauss and Hjellbrekke 2013), the model performance is good for daily maximum ozone. At most of the stations, the index of agreement is between 0.8 and 0.9. In the Nordic countries, correlation and index of agreement have improved at most stations

Component	N_{stat}	Obs.	Mod.	Bias (%)	RMSE	Corr.	IOA
Ozone daily max (ppb)	111	41.12	41.40	1	2.80	0.79	0.87
Ozone daily mean (ppb)	111	31.84	34.40	8	4.57	0.71	0.75

Table 3.1: Comparison of model results and observations for 2013. Annual averages over all EMEP sites with measurements. N_{stat}= number of stations, wd=wet deposition, cp= concentration in precipitation, Corr. = spatial correlation coefficient, RMSE = root mean square error, IOA = index of agreement.

compared to last year, while in Central and Northwestern European countries it has decrease at most stations, although only slightly.

Some more detail is given in the next Section where different regions of the EMEP domain are addressed separately along with time series plots of model results and observations.

Table 3.2: Comparison of modelled versus observed ozone for year 2013. Concentrations are given as means of daily maximum ozone values [ppb]. Correlation coefficients (r), root mean square error (RMSE), and index of agreement (IOA) are included to judge the agreement between model and observations.

Code	Station	Obs. [ppb]	Mod. [ppb]	r	RMSE	IOA
		Nordic countries				
DK05	Keldsnor	38.78	38.29	0.68	7.60	0.81
DK12	Risoe	41.57	37.94	0.85	6.70	0.88
DK31	Ulborg	40.64	39.83	0.79	5.63	0.87
NO02	Birkenes II	39.53	40.81	0.74	5.10	0.85
NO15	Tustervatn	39.57	39.85	0.79	4.26	0.88
NO39	Kaarvatn	38.18	43.55	0.64	8.81	0.72
NO42	Spitzbergen, Zeppelin	35.75	38.73	0.58	6.56	0.72
NO43	Prestebakke	37.90	39.62	0.79	5.45	0.88
NO52	Sandve	39.98	40.59	0.74	4.82	0.85
NO56	Hurdal	35.10	37.07	0.75	6.47	0.85
NO89	Haukenes	39.16	39.14	0.72	6.01	0.84
SE05	Bredkaelen	37.80	36.90	0.75	5.58	0.85
SE11	Vavihill	40.63	38.64	0.83	6.08	0.89
SE12	Aspvreten	36.22	38.07	0.82	5.17	0.89
SE13	Esrange	39.43	36.80	0.72	5.82	0.81
SE14	Raaoe	41.61	38.83	0.82	5.73	0.88
SE32	Norra-Kvill	41.17	38.20	0.81	5.84	0.86
SE35	Vindeln	38.52	36.10	0.72	6.46	0.81
SE39	Grimsoe	39.01	37.60	0.80	5.38	0.88
		Eastern European Countries				
BG53	Rojen peak	44.34	46.51	0.63	6.83	0.77
CZ01	Svratouch	37.79	40.98	0.76	9.24	0.85
CZ03	Kosetice	39.88	41.59	0.79	8.42	0.87
CZ05	Churanov	46.69	41.81	0.49	13.64	0.67
CZ07	Kresin u Pacova	39.68	33.71	0.31	9.94	0.51
EE09	Lahemaa	38.21	37.74	0.80	5.53	0.88
EE11	Vilsandy	40.96	41.34	0.78	5.58	0.88
HU02	K-puszta	43.65	42.89	0.85	8.49	0.90
LT15	Preila	35.24	42.35	0.76	9.80	0.77
LV10	Rucava	41.31	39.11	0.82	6.56	0.88
LV16	Zoseni	40.27	37.04	0.69	7.87	0.81
PL02	Jarczew	39.29	39.97	0.84	7.35	0.91
PL03	Sniezka	48.38	40.61	0.70	11.50	0.74
PL04	Leba	40.07	41.13	0.81	6.01	0.89
PL05	Diabla Gora	40.89	38.36	0.74	8.48	0.84
RO03	Semenic	27.29	44.61	0.26	20.74	0.43
RO08	EM-3	47.09	44.53	0.61	7.69	0.77
SK02	Chopok	54.21	46.31	0.73	10.22	0.72
SK04	Stara Lesna	46.82	44.01	0.71	8.27	0.82
SK06	Starina	43.83	42.02	0.78	7.68	0.87

continued on next page

Code	Station	Obs.	Mod.	r	RMSE	IOA
SK07	Topolniky	46.64	45.28	0.86	8.68	0.91
	Central and NW European Countries					
AT02	Illmitz	44.62	43.77	0.82	8.80	0.89
AT05	Vorhegg	45.79	44.87	0.65	10.74	0.77
AT30	Pillersdorf	40.67	41.53	0.83	8.71	0.90
AT32	Sulzberg	46.27	43.75	0.67	10.25	0.79
AT34	Sonnblick	55.25	49.34	0.62	9.57	0.71
AT38	Gerlitzen	51.54	46.48	0.71	9.01	0.78
AT40	Masenberg	47.66	43.21	0.78	8.78	0.84
AT41	Haunsberg	41.04	41.69	0.78	9.18	0.88
AT42	Heidenreichstein	41.36	42.14	0.84	7.83	0.90
AT43	Forsthof	43.19	42.52	0.85	8.23	0.91
AT45	Dunkelsteinerwald	41.93	41.76	0.84	9.85	0.89
AT46	Gaenserndorf	41.09	41.75	0.87	8.04	0.92
AT47	Stixneusiedl	41.58	41.75	0.84	8.64	0.91
AT48	Zoebelboden	43.37	41.98	0.73	9.36	0.85
AT49	Grebenzen	49.46	43.64	0.66	10.13	0.73
BE01	Offagne	37.52	40.37	0.83	7.88	0.88
BE32	Eupen	36.49	38.63	0.87	7.44	0.91
BE35	Vezin	37.52	38.92	0.83	7.56	0.90
CH01	Jungfraujoch	42.20	53.84	0.39	15.46	0.45
CH02	Payerne	40.31	44.44	0.69	12.37	0.77
CH03	Taenikon	40.20	42.96	0.75	11.91	0.81
CH04	Chaumont	46.90	44.50	0.69	9.20	0.81
CH05	Rigi	47.19	44.08	0.65	10.91	0.77
DE01	Westerland/Wenningsted	42.03	39.69	0.77	6.45	0.85
DE02	Langenbruegge/Waldhof	38.88	38.30	0.86	7.07	0.91
DE03	Schauinsland	45.70	44.19	0.69	8.44	0.82
DE07	Neuglobsow	38.10	38.40	0.83	7.60	0.90
DE08	Schmuecke	42.65	39.61	0.81	8.04	0.88
DE09	Zingst	38.98	38.52	0.80	6.41	0.88
FR08	Donon	40.11	42.15	0.74	8.82	0.84
FR09	Revin	37.77	40.73	0.80	8.22	0.86
FR10	Morvan	41.28	42.01	0.75	7.42	0.85
FR13	Peyrusse Vieille	41.70	41.14	0.70	7.72	0.83
FR14	Montandon	36.03	43.37	0.67	11.92	0.72
FR15	La Tardiere	41.85	40.44	0.64	9.52	0.78
FR16	Le Casset	51.63	44.70	0.61	10.22	0.66
FR17	Montfranc	43.58	42.51	0.64	7.27	0.79
FR18	La Coulonche	41.76	40.75	0.76	7.65	0.83
FR19	Pic du Midi	57.30	49.75	0.40	12.21	0.57
FR30	Puy de Dme	48.97	43.25	0.61	9.70	0.69
GB02	Eskdalemuir	37.88	39.39	0.77	5.29	0.86
GB06	Lough Navar	35.35	39.45	0.73	6.68	0.78
GB13	Yarner Wood	36.95	40.67	0.77	6.97	0.81
GB14	High Muffles	37.95	39.91	0.73	6.24	0.83
GB15	Strath Vaich Dam	40.84	39.02	0.82	4.46	0.89

continued on next page

Code	Station	Obs.	Mod.	r	RMSE	IOA
GB31	Aston Hill	38.98	39.68	0.68	6.36	0.80
GB33	Bush	38.99	38.75	0.72	5.11	0.85
GB35	Great Dun Fell	38.55	39.62	0.55	6.66	0.73
GB36	Harwell	34.94	38.53	0.74	7.80	0.82
GB37	Ladybower	33.11	38.03	0.72	7.88	0.77
GB38	Lullington Heath	33.29	40.55	0.72	9.99	0.72
GB39	Sibton	36.42	39.01	0.76	7.18	0.84
GB43	Narberth	38.73	40.41	0.71	6.09	0.82
GB45	Wicken Fen	33.76	38.15	0.85	7.20	0.87
GB48	Auchencorth Moss	36.27	38.75	0.72	5.58	0.82
GB49	Weybourne	39.75	38.78	0.76	6.19	0.86
GB50	St. Osyth	36.26	36.91	0.73	7.30	0.83
GB52	Lerwick	39.27	42.10	0.76	5.49	0.83
GB53	Charlton Mackrell	39.36	39.02	0.77	6.09	0.86
IE01	Valentia Obs.	43.50	43.02	0.74	4.86	0.85
IE31	Mace Head	42.93	41.82	0.70	5.22	0.82
NL07	Eibergen	34.35	37.80	0.79	9.60	0.85
NL09	Kollumerwaard	36.56	38.81	0.80	6.36	0.87
NL10	Vreedepeel	33.98	37.20	0.85	8.19	0.89
NL44	Cabauw Wielsekade	33.73	35.70	0.83	7.65	0.89
NL91	De Zilk	38.00	38.54	0.74	8.03	0.83
		Mediterranean Countries				
CY02	Ayia Marina	55.84	50.34	0.68	8.66	0.74
ES01	Toledo	47.26	46.75	0.80	6.37	0.86
ES06	Mahon	49.41	48.48	0.59	7.26	0.75
ES07	Viznar	51.91	47.26	0.61	10.07	0.66
ES08	Niembro	42.47	45.00	0.80	5.65	0.86
ES09	Campisabalos	47.11	46.40	0.72	6.44	0.82
ES10	Cabo de Creus	43.84	47.07	0.71	8.39	0.79
ES11	Barcarrota	46.26	46.41	0.67	9.20	0.74
ES12	Zarra	50.29	45.53	0.73	8.43	0.75
ES13	Penausende	46.48	45.59	0.79	6.24	0.86
ES14	Els Torms	46.20	44.58	0.73	7.34	0.82
ES16	O Savinao	34.40	44.09	0.71	12.75	0.69
ES17	Doana	51.59	47.72	0.75	9.97	0.77
GR01	Aliartos	34.97	47.09	0.70	14.00	0.60
GR02	Finokalia	54.90	51.05	0.71	7.68	0.78
IT01	Montelibretti	45.24	48.10	0.75	11.48	0.80
IT04	Ispra	45.99	51.91	0.88	12.85	0.92
MT01	Giordan lighthouse	48.38	49.46	0.52	7.64	0.72
SI08	Iskrba	45.06	44.56	0.79	8.76	0.86
SI31	Zarodnje	46.36	44.67	0.79	8.71	0.86
SI32	Krvavec	56.03	45.26	0.69	14.05	0.68
SI33	Kovk	42.11	43.96	0.77	8.86	0.87

3.2 Time series

In this section we present time series plots for a selection of stations that have supplied data on acidifying and eutrophying components to EMEP CCC for 2013. The plots show daily model results and measurements of ozone, where available.

Nordic sites

In addition to the statistics for the Nordic sites listed in Table 3.2, measured and modelled ozone levels are compared for Nordic sites in Figures 3.1–3.3. As seen in the plots the model performs well for ozone, both in terms of levels and seasonality. At the majority of Nordic sites the IOA is between 0.80 and 0.9, which is a clearly better result than we had for 2010 (Gauss et al. 2012), but slightly worse than for 2012 (Gauss et al. 2014). Out of the 17 sites, for which data were analized both in (Gauss et al. 2014) and this year, the model performance has decreased at 15 sites, remained constant at 16 sites, but the magnitude of this decrease is very small.

The biases are sometimes positive and sometimes negative with no clear tendency of over or underestimation. Stations with relatively large ($>$ 3ppb) biases are Risoe (DK12), Kaarvatn (NO39).

Eastern European sites

Measured and modelled maximum ozone levels for sites in the Eastern European region are shown in Figures 3.4 to 3.6. These sites are mostly typical continental sites with a clear summer maximum, reflecting local/regional ozone production in summer, and a winter minimum. In general the model performance is rather good, and largely in line with the performance in earlier years (Gauss et al. 2014, Gauss and Hjellbrekke 2013). It is clearly better than the performance for 2010 (Gauss et al. 2012).

Out of the 19 sites, for which data were analized both in (Gauss and Hjellbrekke 2013) and this year, the model performance, in terms of the index of agreement, has decreased at 12 sites, but only slighly. CZ07 and RO03, which were not included in this analysis last year, did not deliver data throughout they year, which explains the relatively low index of agreement. Especially at CZ07, the agreement is rather good for the period September to December for which measurement data are available. The index of agreement is larger than 0.8 at most stations.

Relatively large biases ($>$ 3ppb) are seen at CZ01, CZ05, CZ07, LT15, LV16, PL03, RO03, and SK02.

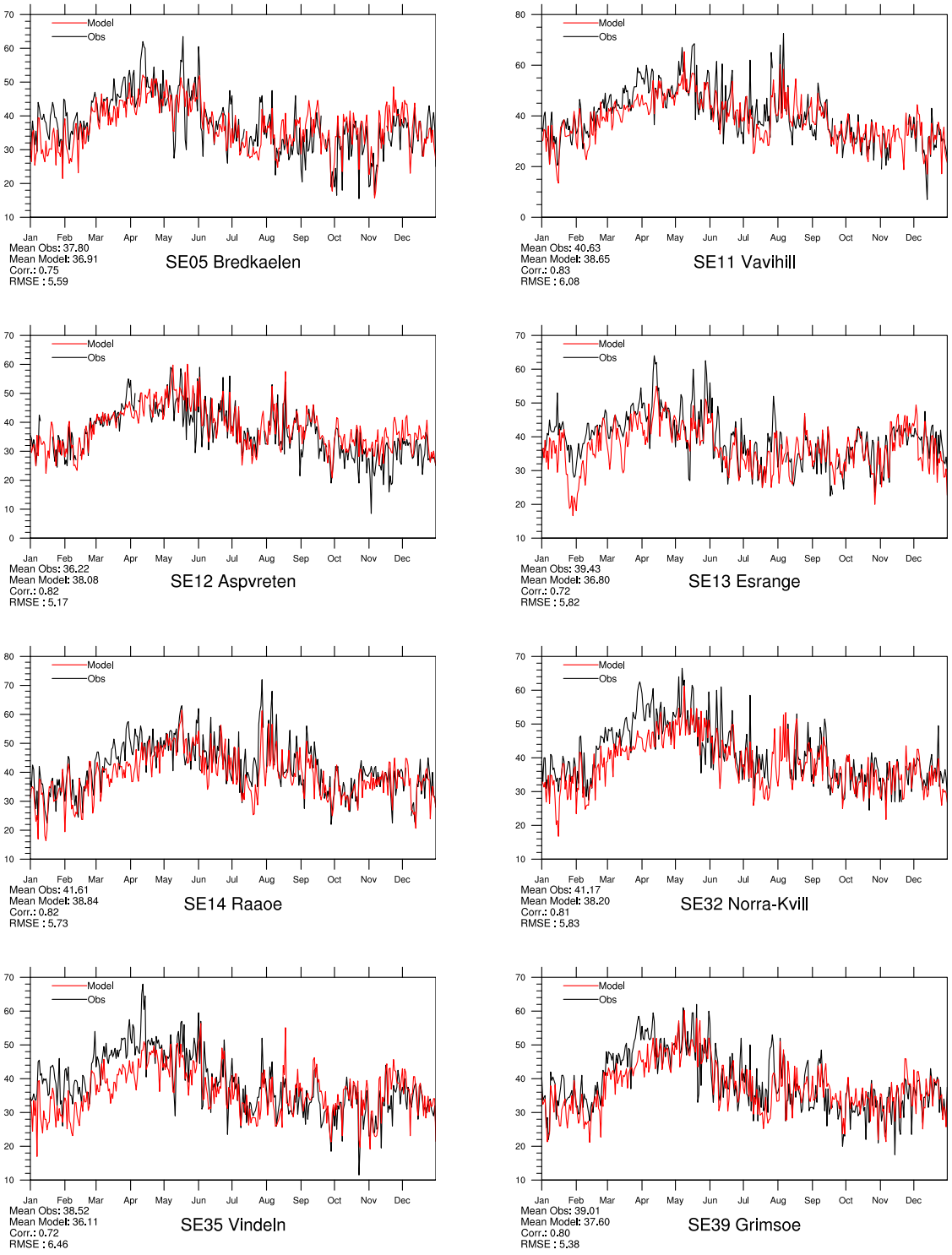

Figure 3.1: Modelled versus Observed Daily Maximum Ozone [ppb] at Swedish sites for 2013. *Note that in some plots the vertical axis does not start at zero.*

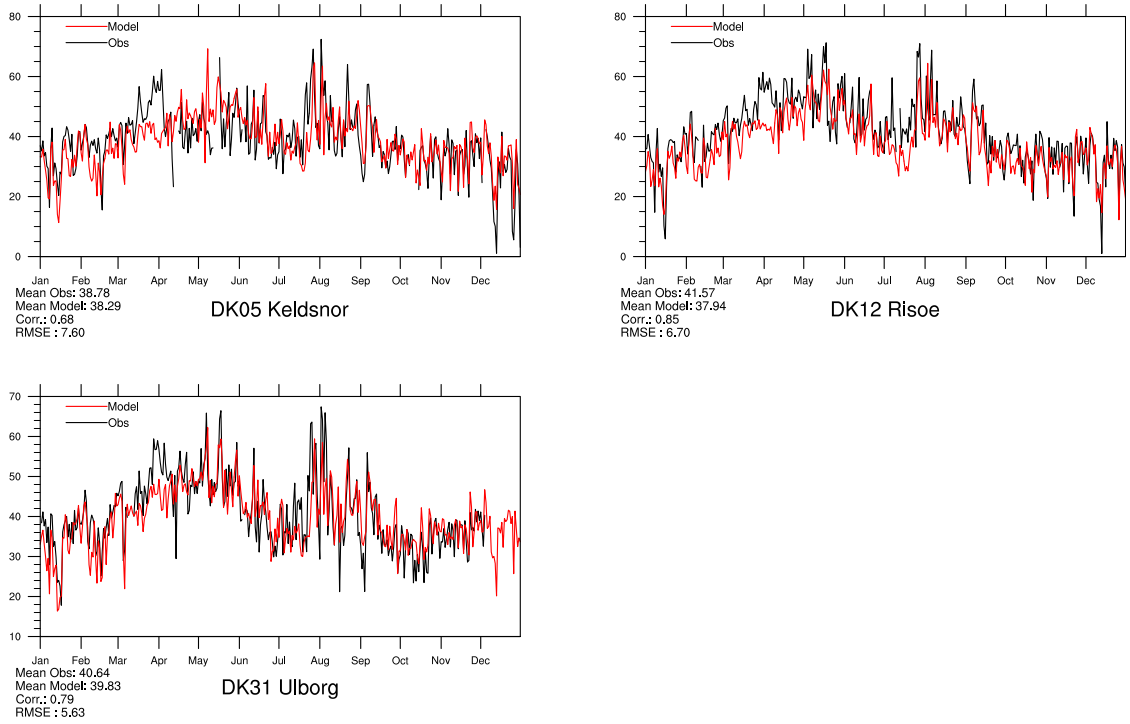

Figure 3.2: Modelled versus Observed Daily Maximum Ozone [ppb] at Danish sites for 2013. *Note that in some plots the vertical axis does not start at zero.*

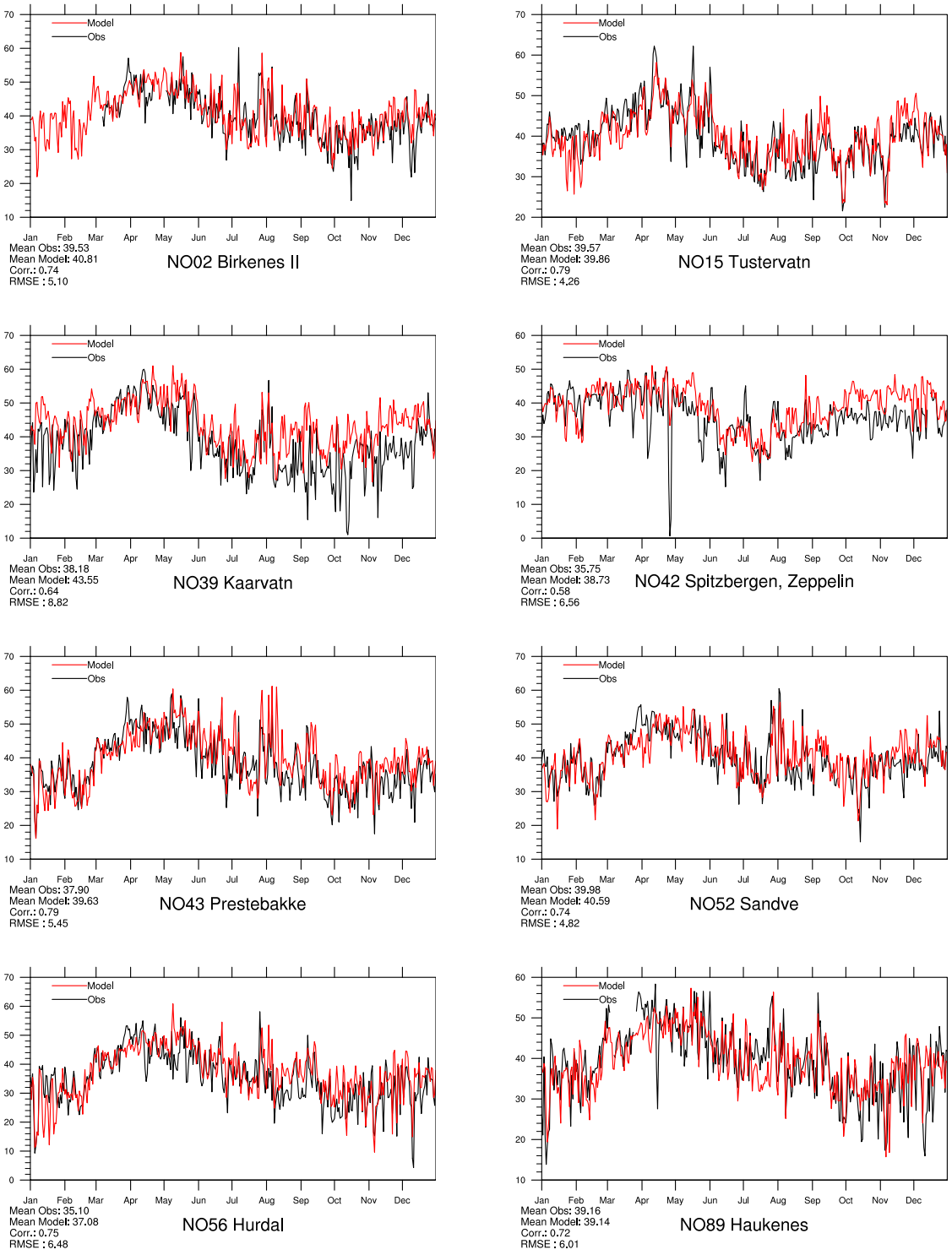

Figure 3.3: Modelled versus Observed Daily Maximum Ozone [ppb] at Norwegian sites for 2013. *Note that in some plots the vertical axis does not start at zero.*

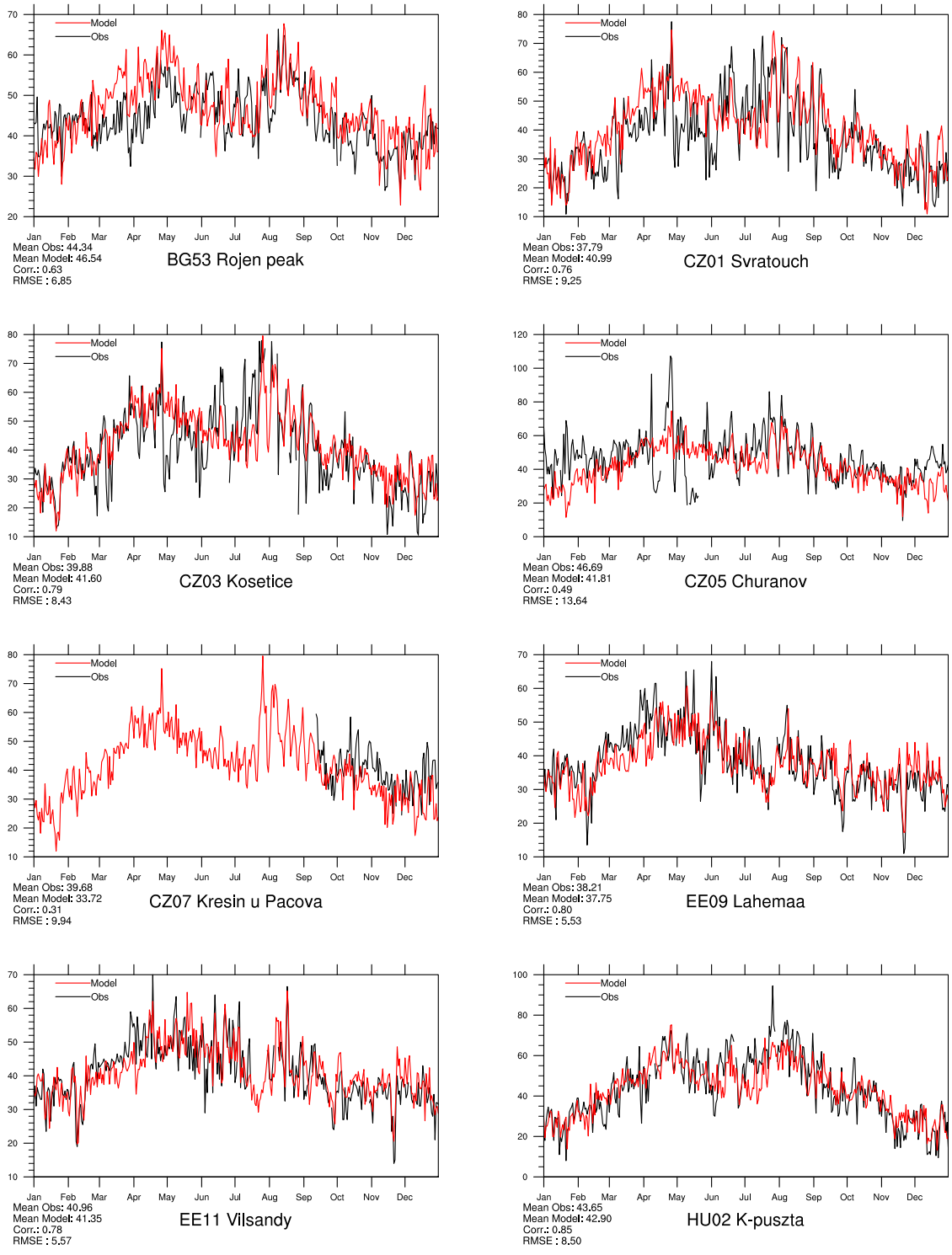

Figure 3.4: Modelled versus Observed Daily Maximum Ozone [ppb] at Eastern European sites for 2013. *Note that in some plots the vertical axis does not start at zero.*

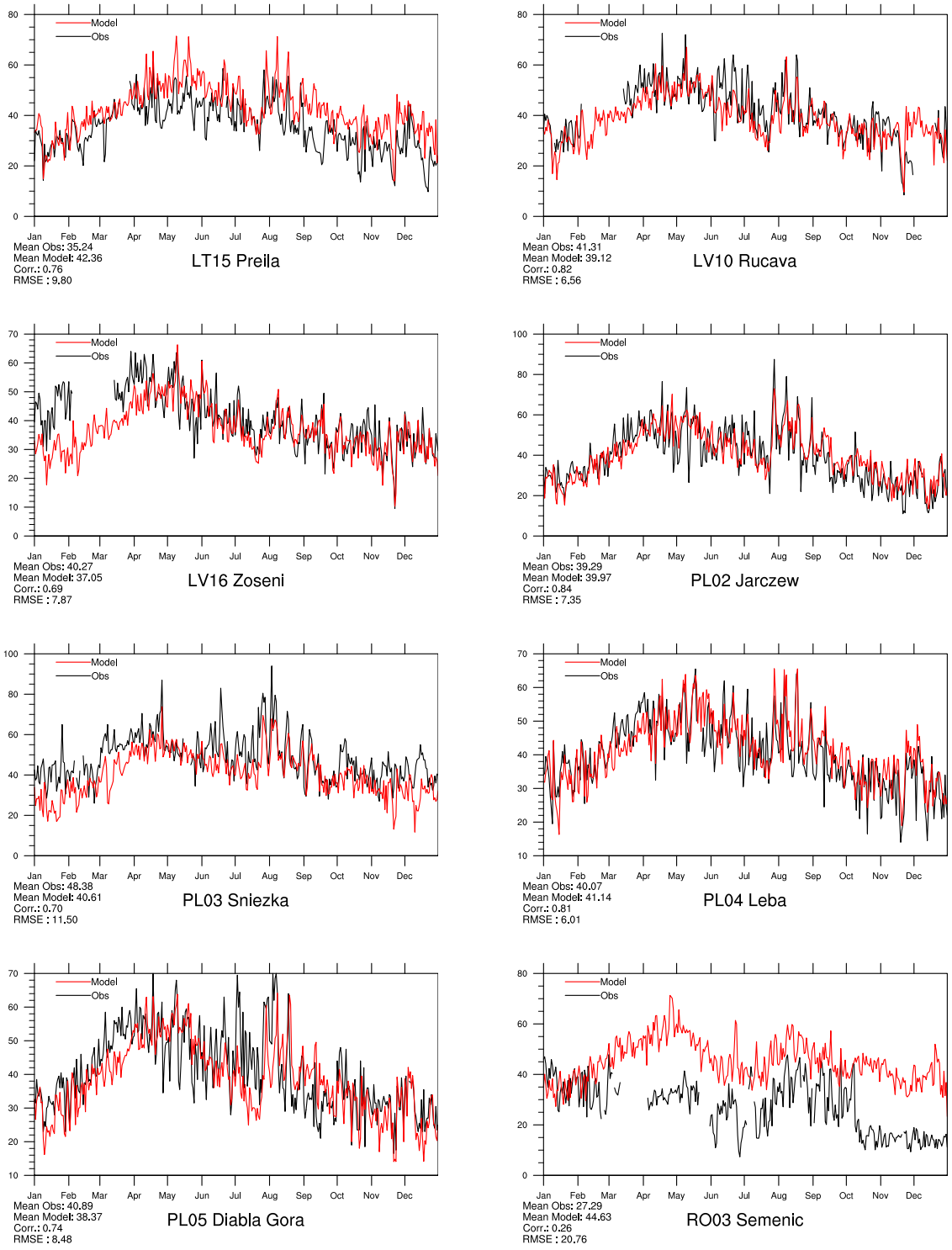

Figure 3.5: Modelled versus Observed Daily Maximum Ozone [ppb] at Eastern European sites for 2013. *Note that in some plots the vertical axis does not start at zero.*

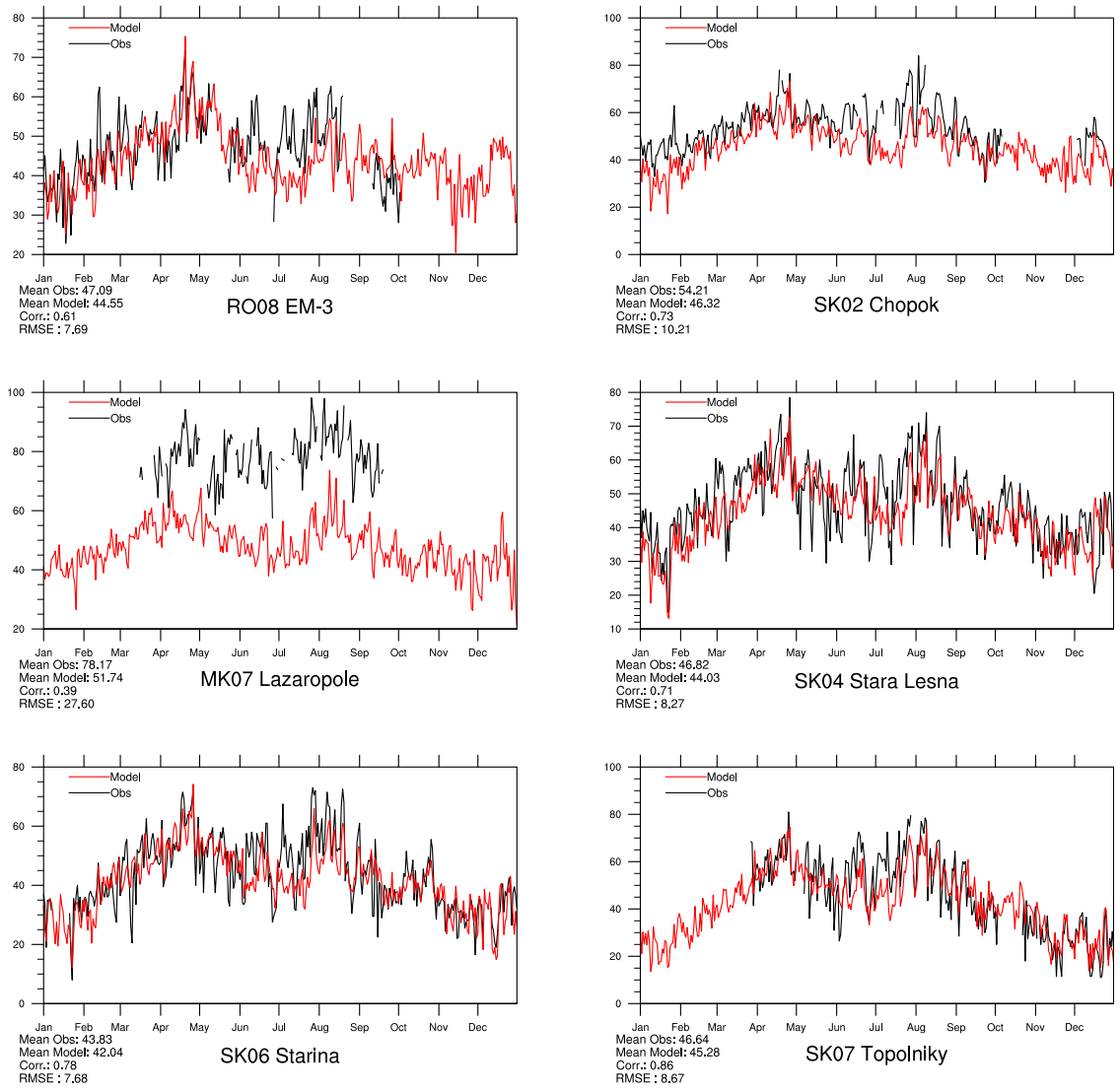

Figure 3.6: Modelled versus Observed Daily Maximum Ozone [ppb] at Eastern European sites for 2013. *Note that in some plots the vertical axis does not start at zero.*

Central and Northwestern European sites

Measured and modelled maximum ozone levels for selected sites in Central and Northwestern Europe are shown in Figures 3.7–3.15. These sites are mainly typical continental sites with a clear summer maximum, reflecting local/regional ozone production in summer, and a winter minimum. Concentrations at the site Mace Head in Ireland (IE31) are partly used to specify background conditions for the EMEP model, so that good performance, at least for the seasonal cycle, is guaranteed.

The overall model performance is very good in this area with many correlations better than 0.8 and small biases, although the performance is slightly lower than last year (Gauss et al. 2014) at many stations.

As usual, the comparison between model and observation has problems in mountainous areas, most notably at Jungfraujoch (CH01), Le Casset (FR16), Pic du Midi (FR19), and Puy de Dome (FR30).

Mediterranean sites

Measured and modelled ozone levels for selected sites in the Mediterranean region are shown in Figures 3.16–3.18. The meteorological situation in and around the Mediterranean basin differs considerably from the rest of Europe. This region also receives more solar radiation resulting in conditions favourable for ozone production. Hence these sites have some of the highest ozone levels in Europe.

In general the model performance is good for most sites in this region, with IOA values between 0.74 and 0.92.

Exception with lower IOA are MT01 (where there are gaps in measurement data), ES07 (relatively high altitude), and SI32 (which has also a large negative bias), and GR01.

In general, the biases in this region tend to be higher than in other regions (e.g. O Savinao, Aliartos, and Krvavek), although the correlation is still satisfactory (0.7).

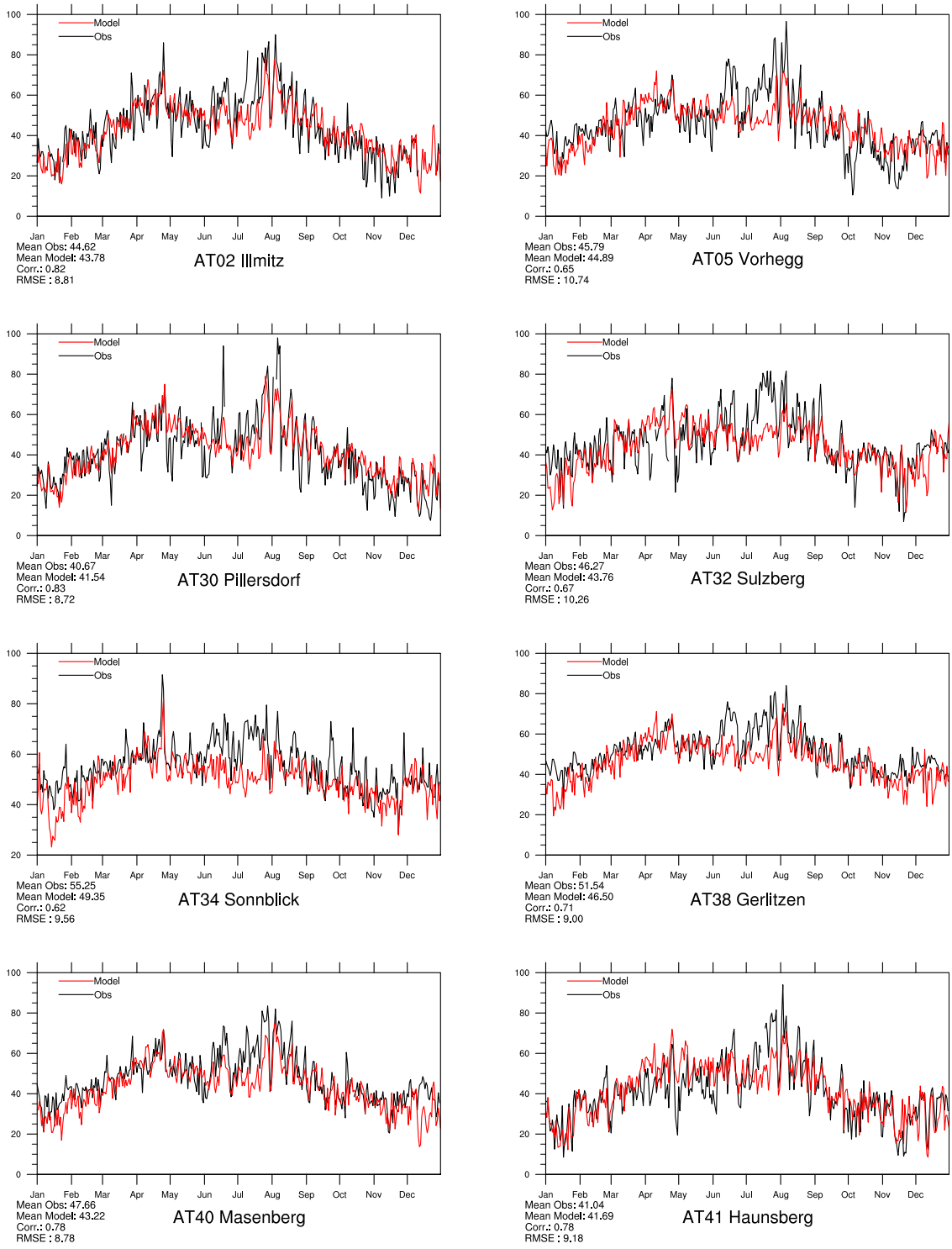

Figure 3.7: Modelled versus Observed Daily Maximum Ozone [ppb] at Austrian sites for 2013. *Note that in some plots the vertical axis does not start at zero.*

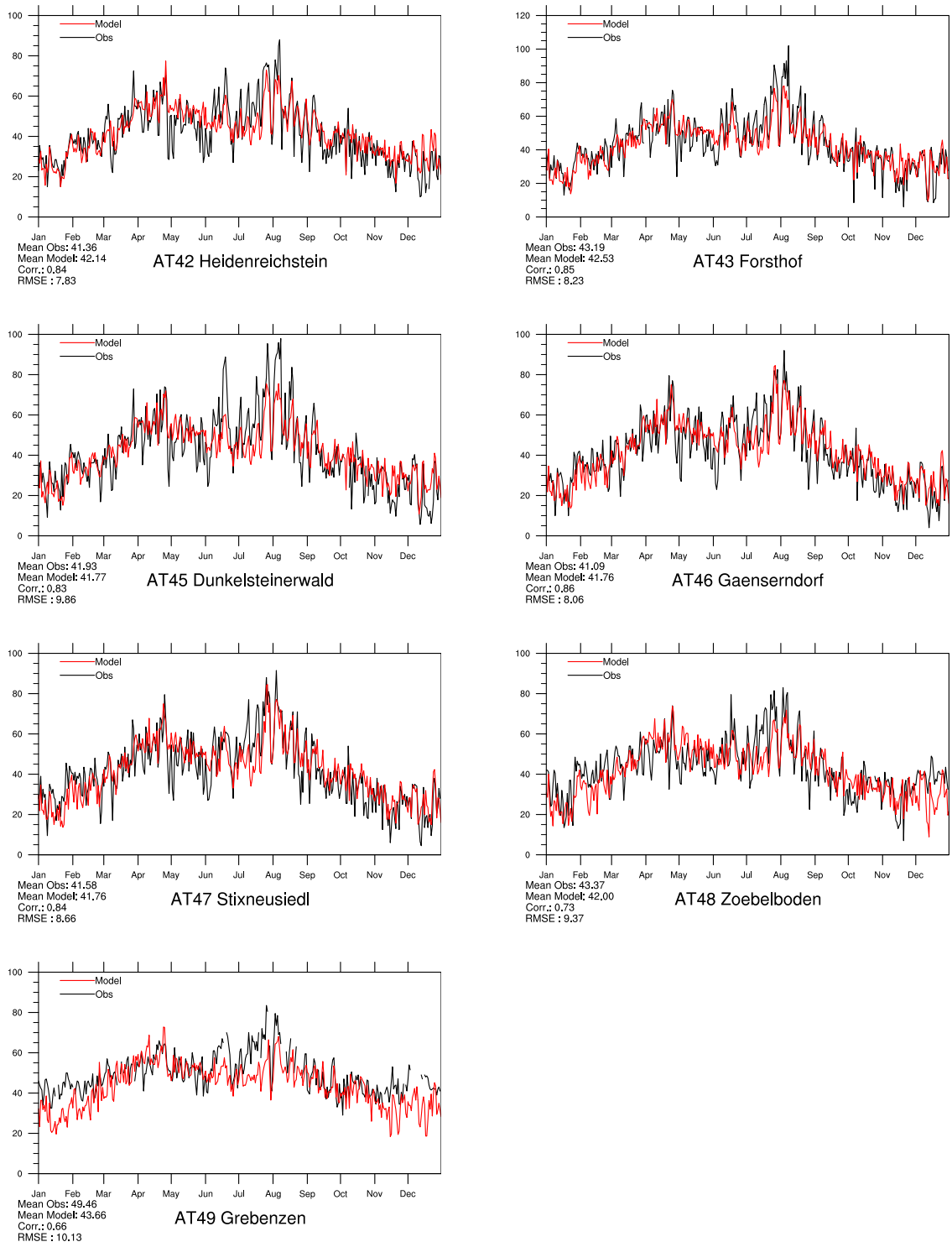

Figure 3.8: Modelled versus Observed Daily Maximum Ozone [ppb] at Austrian sites for 2013.

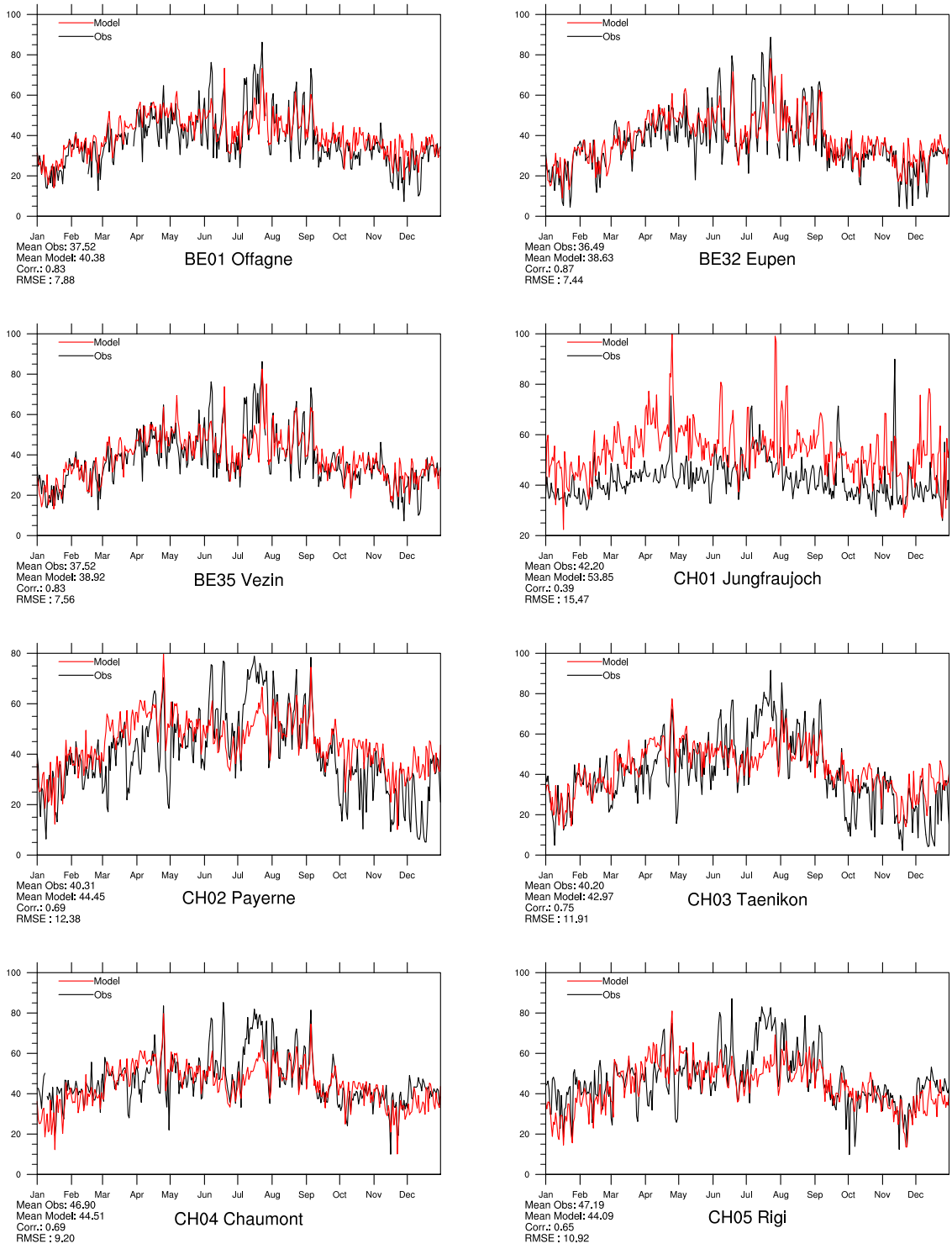

Figure 3.9: Modelled versus Observed Daily Maximum Ozone [ppb] at sites in Belgium and Switzerland for 2013. *Note that in some plots the vertical axis does not start at zero.*

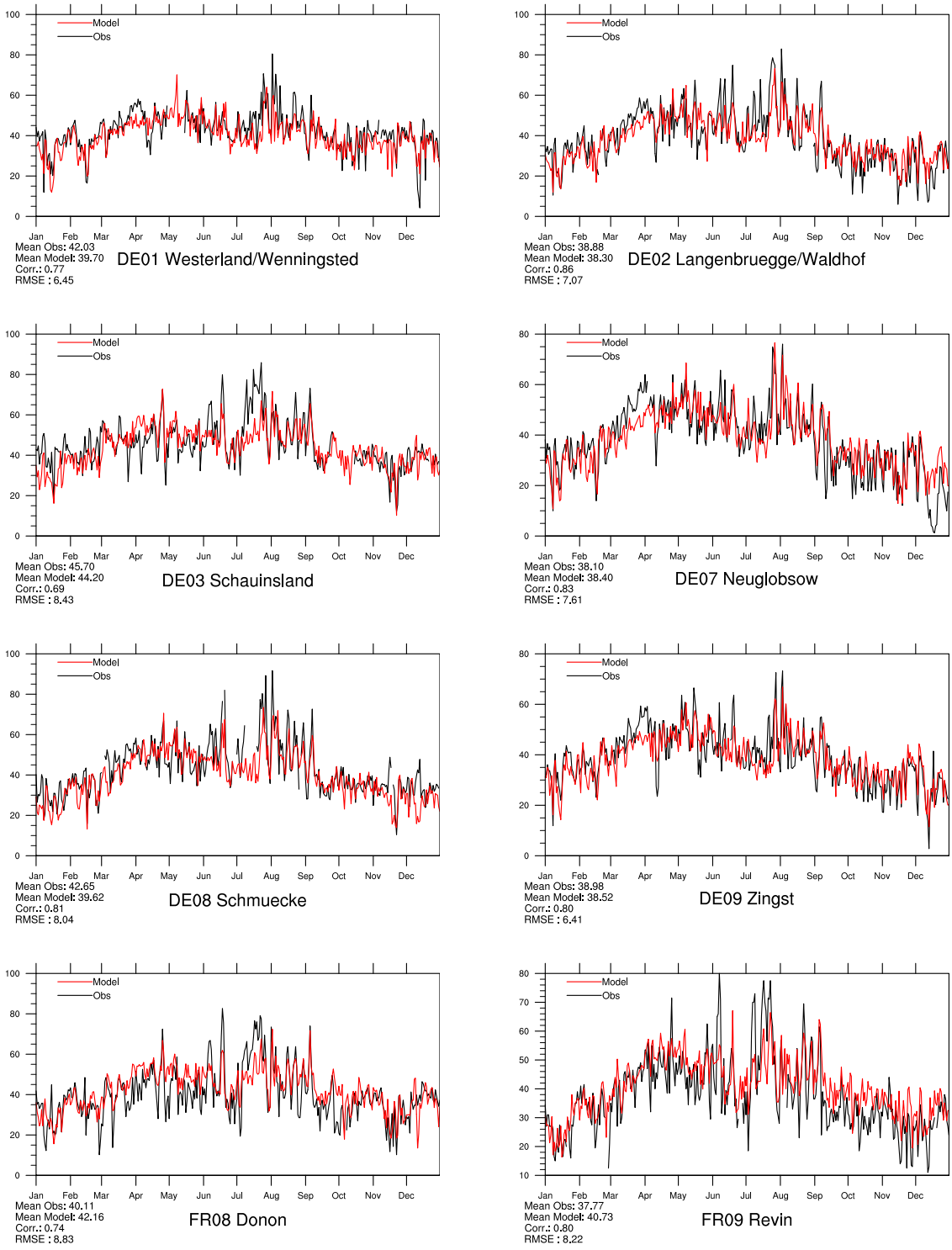

Figure 3.10: Modelled versus Observed Daily Maximum Ozone [ppb] at sites in Germany and France for 2013. *Note that in some plots the vertical axis does not start at zero.*

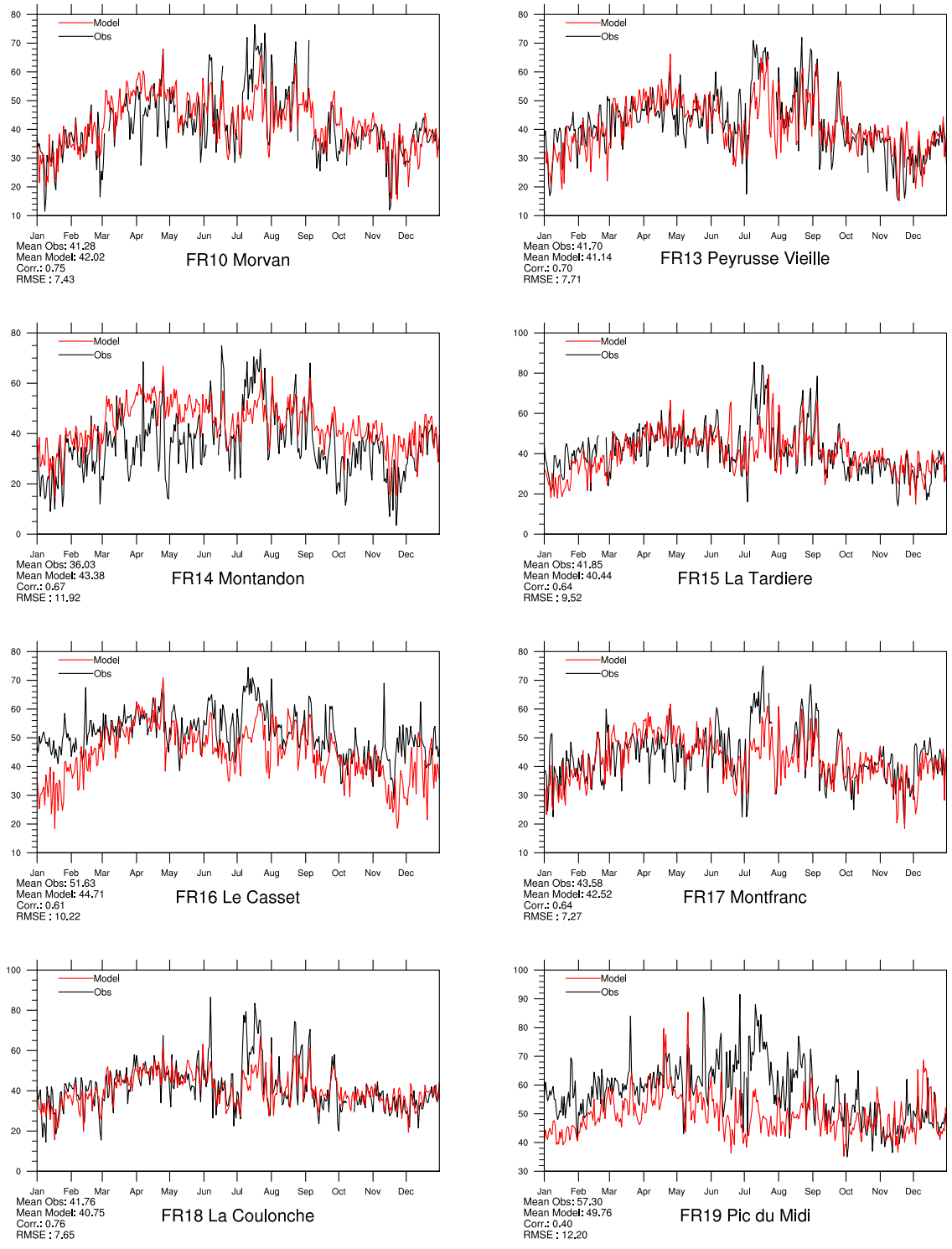

Figure 3.11: Modelled versus Observed Daily Maximum Ozone [ppb] at French sites for 2013. *Note that in some plots the vertical axis does not start at zero.*

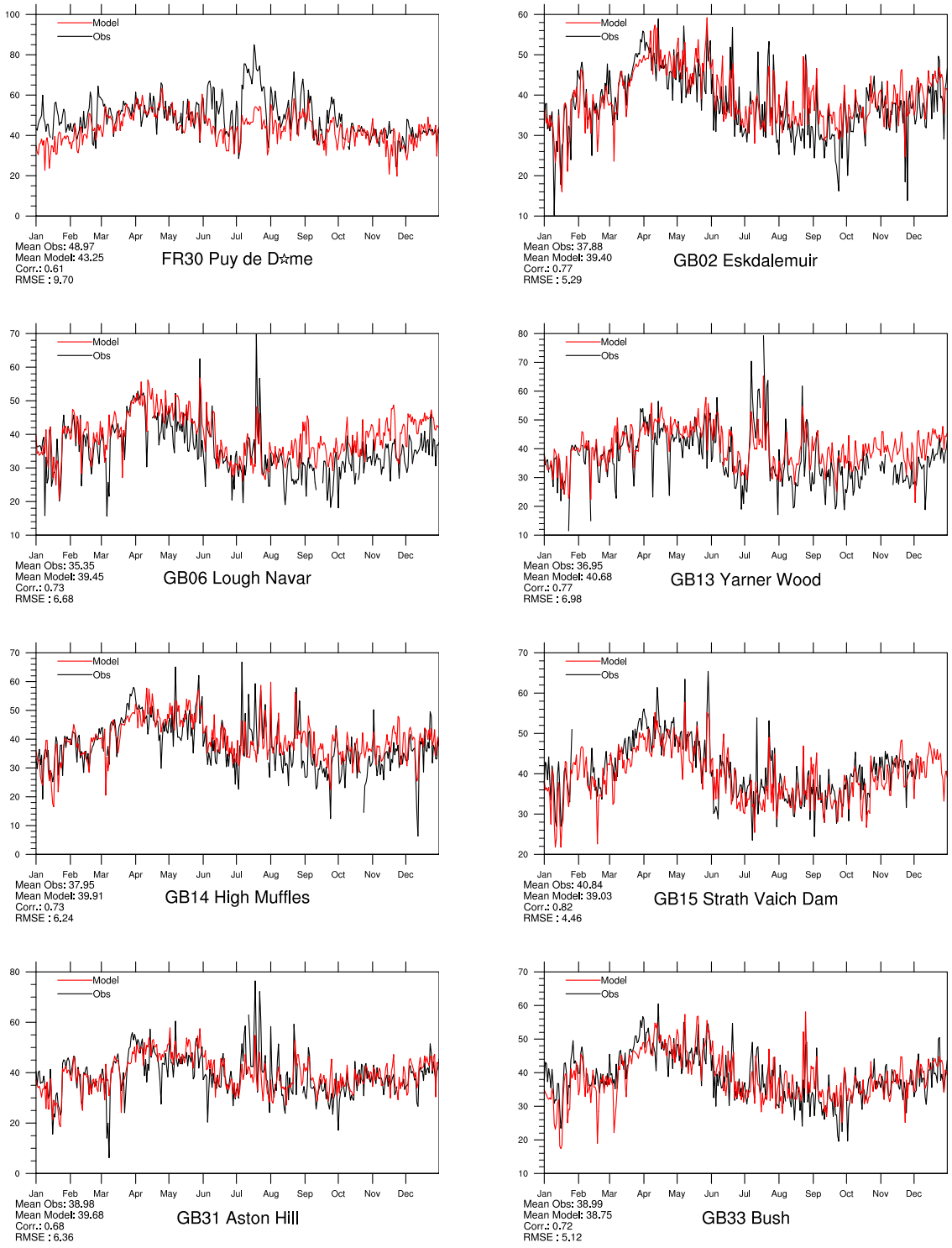

Figure 3.12: Modelled versus Observed Daily Maximum Ozone [ppb] at French and British sites for 2013. *Note that in some plots the vertical axis does not start at zero.*

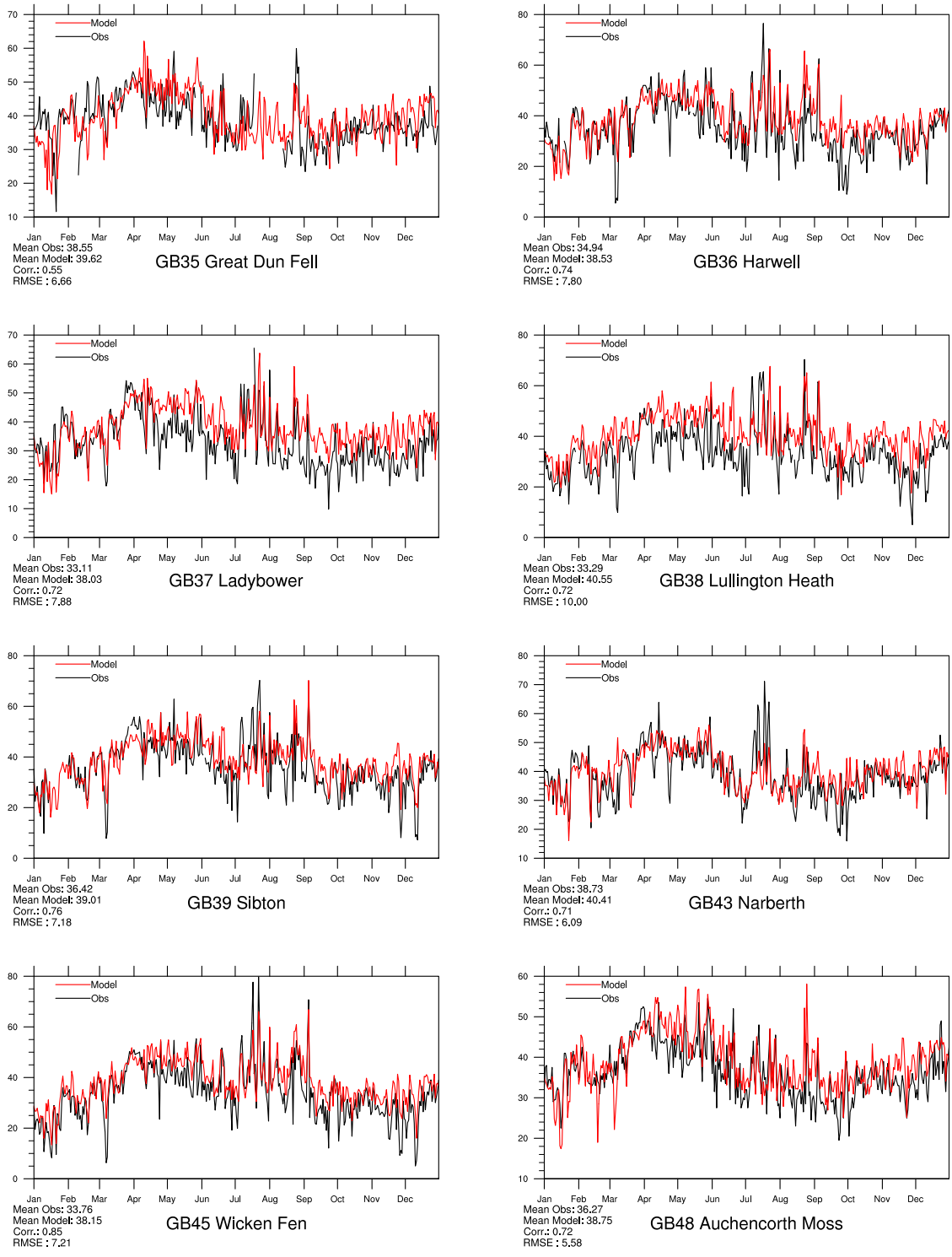

Figure 3.13: Modelled versus Observed Daily Maximum Ozone [ppb] at British sites for 2013. *Note that in some plots the vertical axis does not start at zero.*

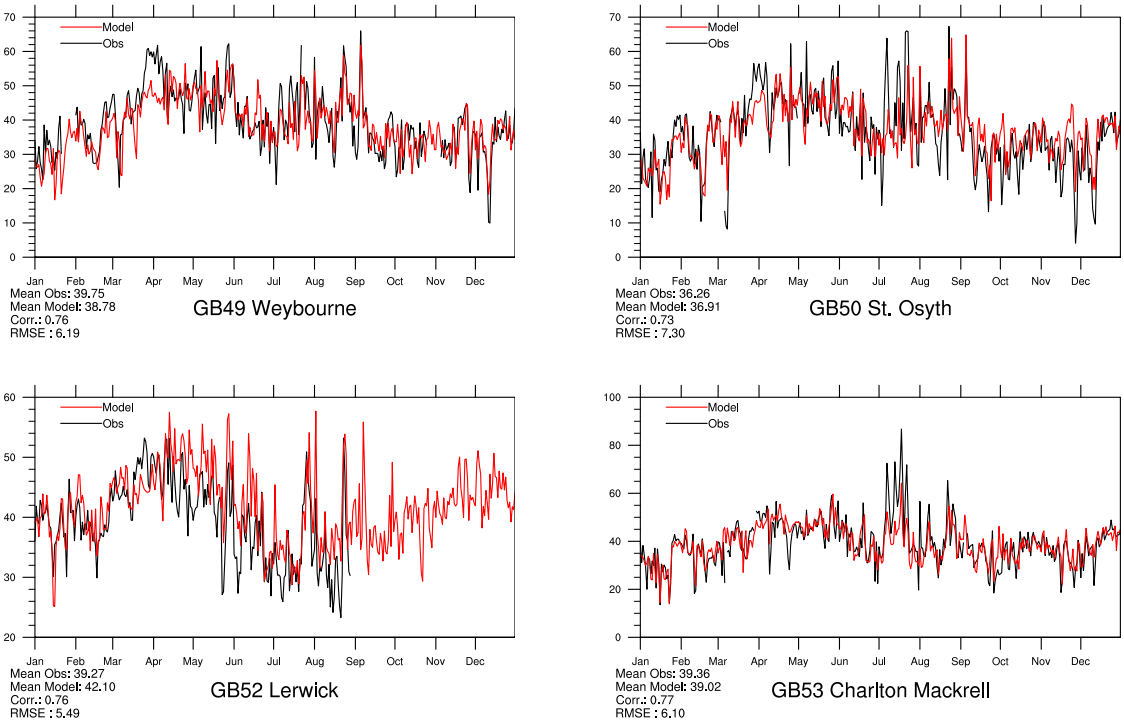

Figure 3.14: Modelled versus Observed Daily Maximum Ozone [ppb] at British sites for 2013. *Note that in some plots the vertical axis does not start at zero.*

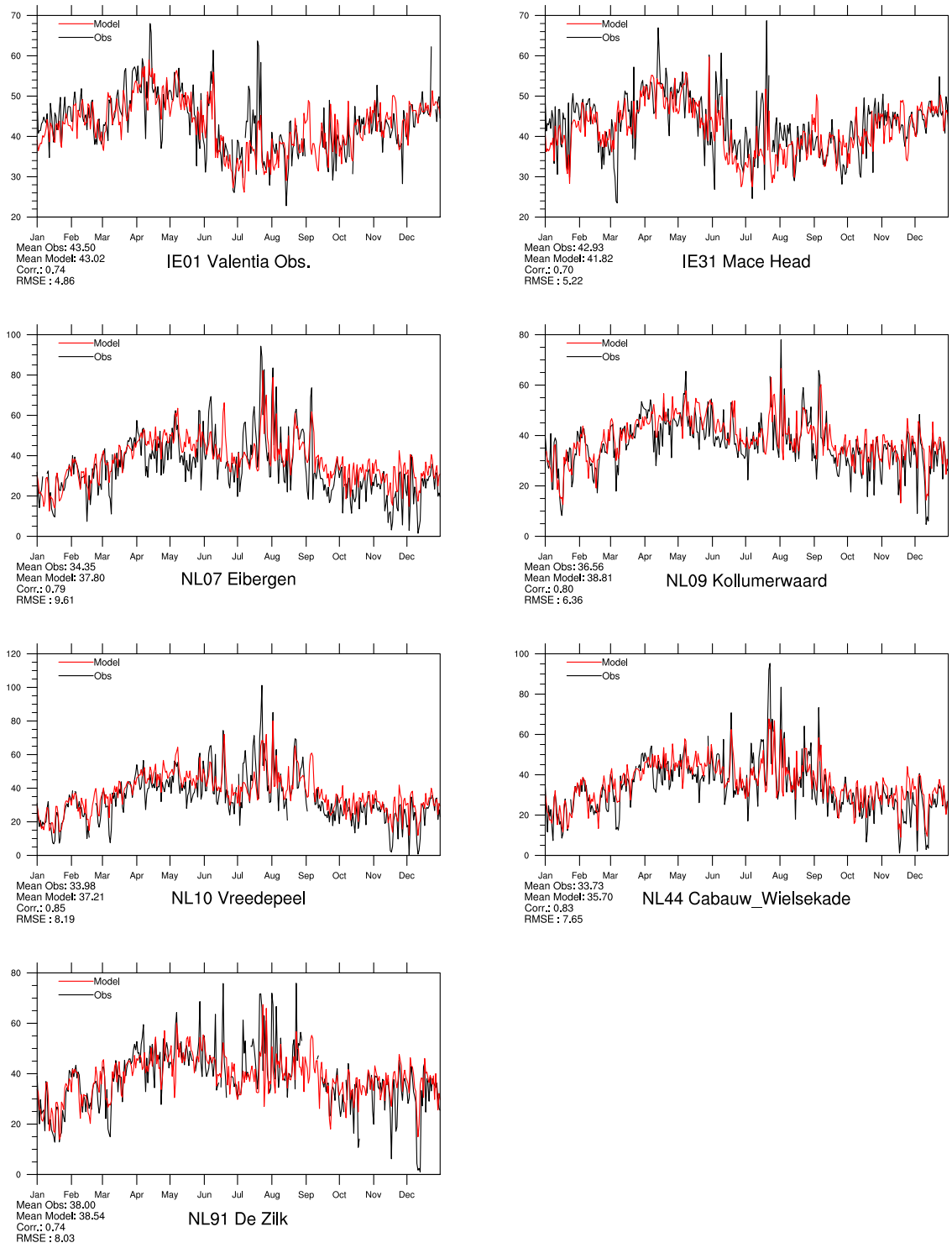

Figure 3.15: Modelled versus Observed Daily Maximum Ozone [ppb] at Irish and Dutch sites for 2013. *Note that in some plots the vertical axis does not start at zero.*

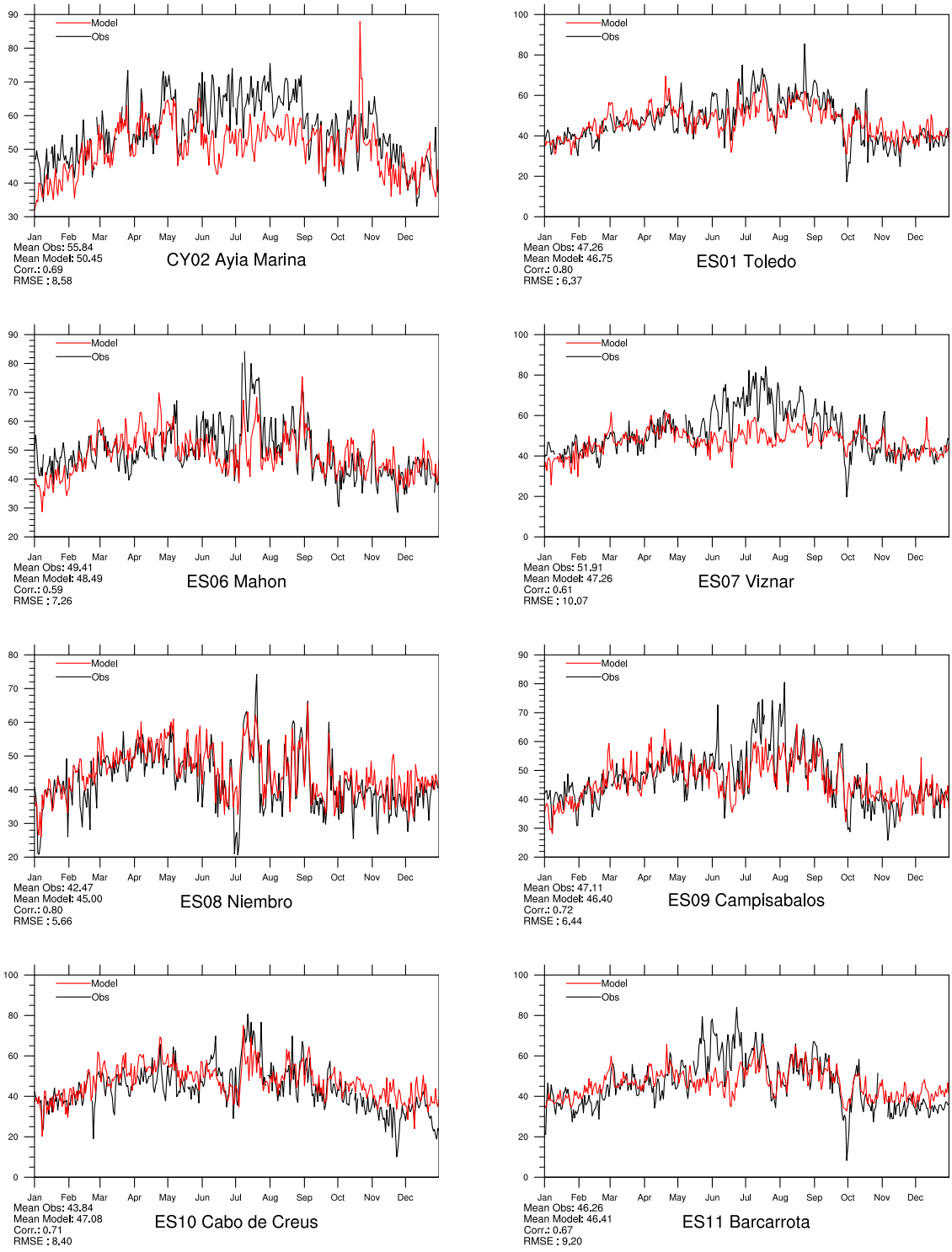

Figure 3.16: Modelled versus Observed Daily Maximum Ozone [ppb] at Mediterranean sites (Cyprus and Spain) for 2013. *Note that in some plots the vertical axis does not start at zero.*

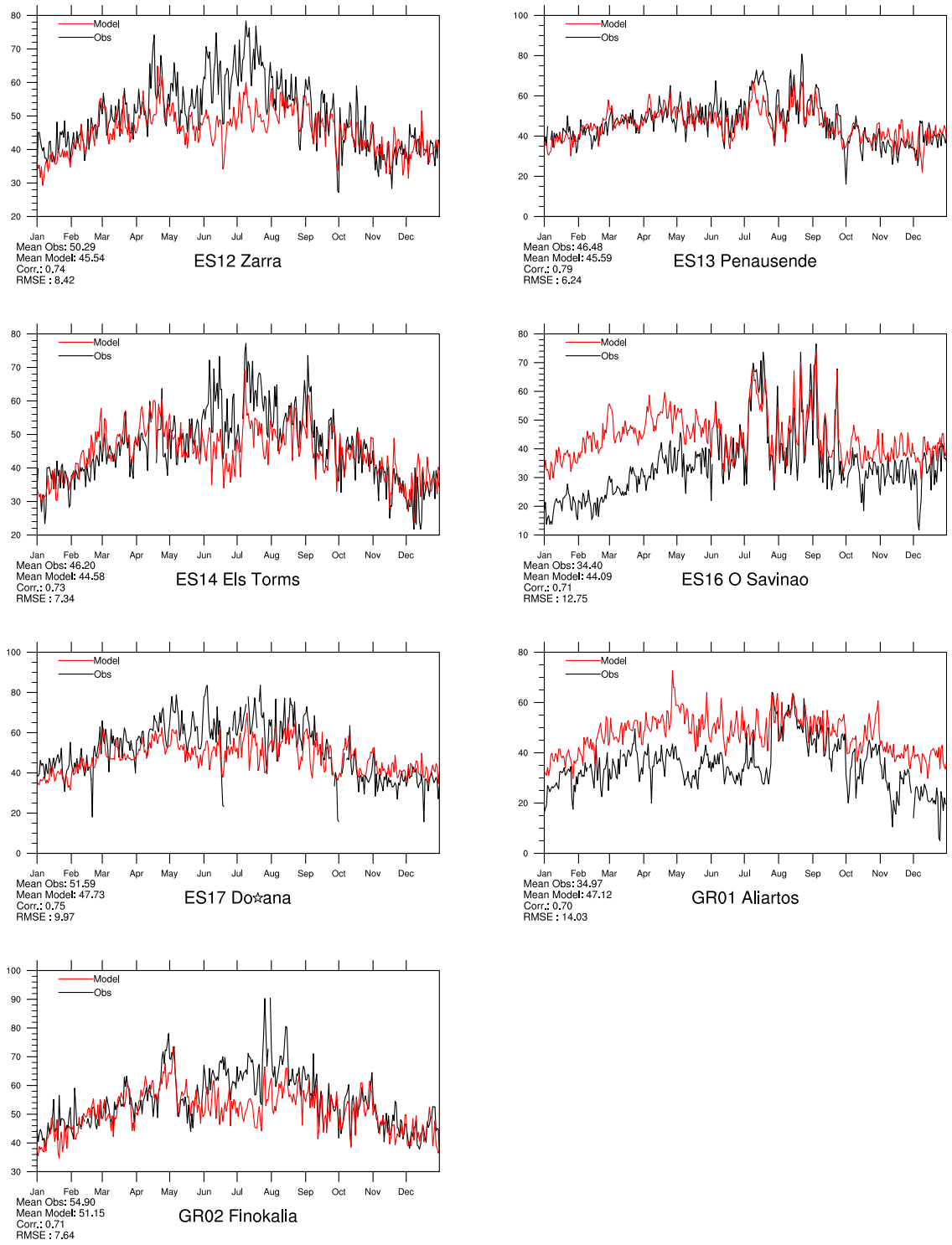

Figure 3.17: Modelled versus Observed Daily Maximum Ozone [ppb] at Mediterranean Sites (Spain and Greece) for 2013. *Note that in some plots the vertical axis does not start at zero.*

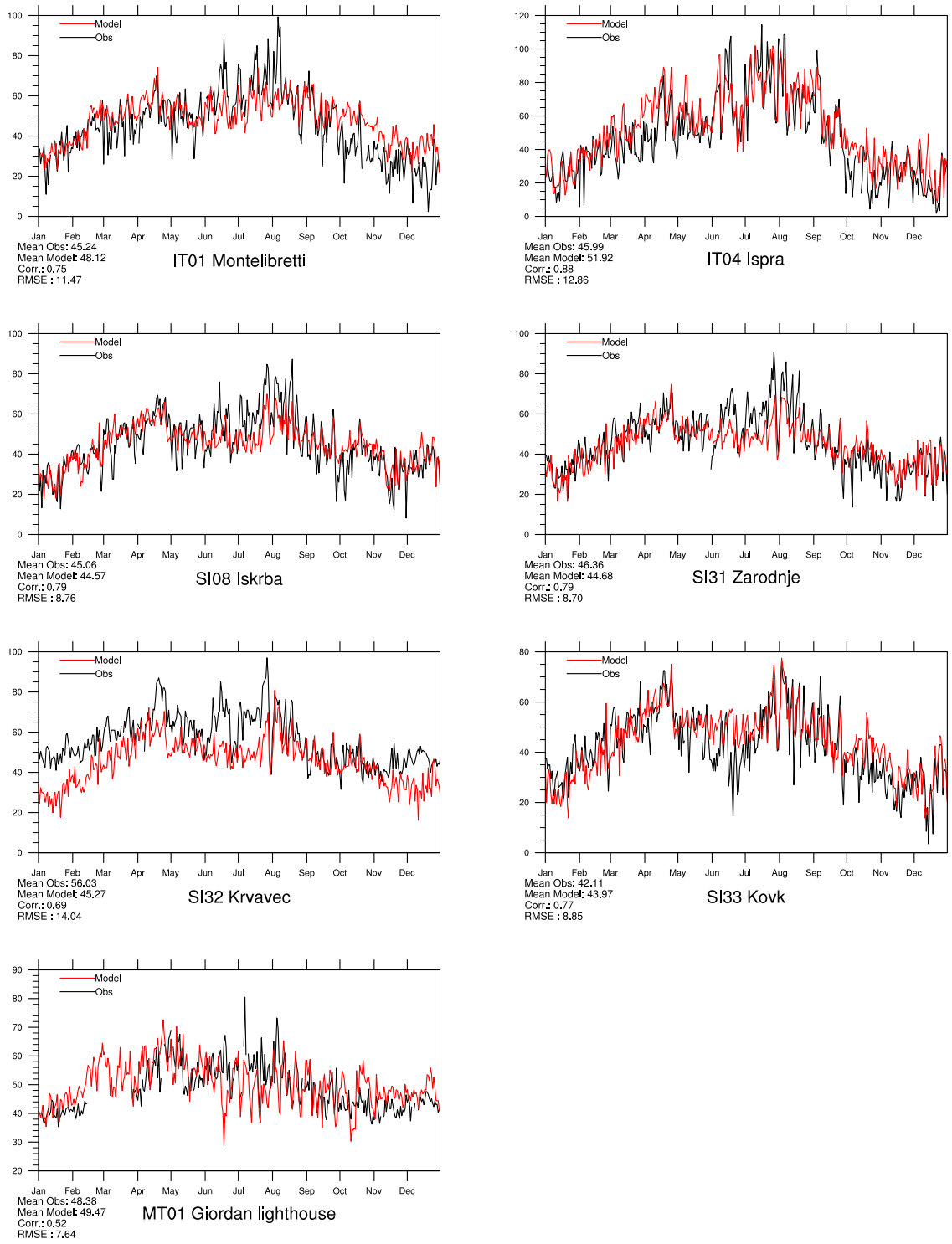

Figure 3.18: Modelled versus Observed Daily Maximum Ozone [ppb] at Mediterranean Sites for 2013.

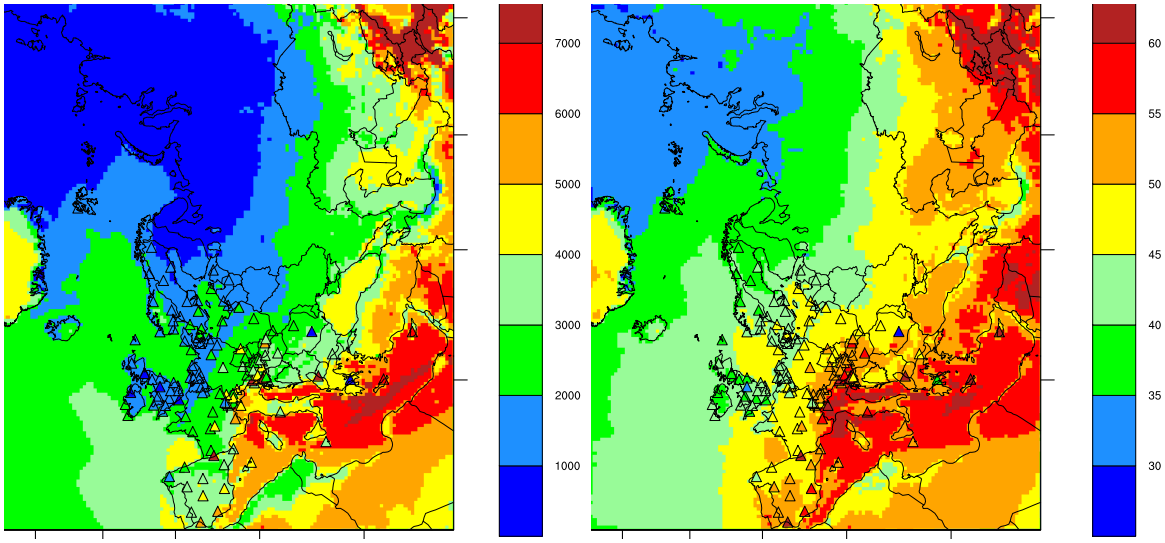

(a) SOMO35 (b) Max ozone

Figure 3.19: SOMO35 (ppb.days) and yearly averaged daily maximum ozone (ppb). The maps show model results, with observations superimposed by triangles.

3.3 Combined maps of model results and observations

In Figure 3.19, maps of modeled SOMO35 and maximum daily ozone are shown. Observations, taken from the EMEP network for 2013, are super-imposed with triangles. By and large, the plots show good agreement between model and observations also for this year.

References

M. Gauss and A.-G. Hjellbrekke. Photo-oxidants: validation and combined maps. Supplementary material to EMEP Status Report 1/2013, available online at www.emep.int, The Norwegian Meteorological Institute, Oslo, Norway, 2013.

M. Gauss, A. C. Benedictow, and A.-G. Hjellbrekke. Photo-oxidants: validation and combined maps. Supplementary material to emep status report 1/2012, available online at www.emep.int, The Norwegian Meteorological Institute, Oslo, Norway, 2012.

M. Gauss, B. M. Steensen, and A.-G. Hjellbrekke. Ozone. Supplementary material to EMEP Status Report 1/2014, available online at www.emep.int, The Norwegian Meteorological Institute, Oslo, Norway, 2014.

CHAPTER 4

PM_{10}, $PM_{2.5}$ and individual aerosol components

S. Tsyro, M. Gauss, and A.-G. Hjellbrekke

This chapter presents an evaluation of the EMEP/MSC-W model performance in terms of particulate matter. Tables of model skill are presented for the entire EMEP domain and for a large number of individual EMEP measurement stations.

4.1 Tables

Table 4.1 shows for PM and individual components the number of stations where measurements were available and data coverage criteria were satisfied (N_{stat}), measured yearly average over all stations (Obs), modelled yearly average over all stations (Mod), bias, correlation between observation and model for station yearly averages, root mean square error, and index of agreement (IOA, as defined in Section 2.1).

Tables 4.2 to 4.9 show model performance at individual stations for different components.

On average, the model underestimates annual mean measured PM_{10} by 28% and $PM_{2.5}$ by 19% for 2013. The annual spatial correlations between model results and measurements are 0.70 for PM_{10} and 0.84 for $PM_{2.5}$. The slightly worse model performance for PM_{10} than for $PM_{2.5}$ is likely due to existing uncertainties in modelling natural PM components, e.g. windblown mineral dust, causing also inaccuracy in coarse NO_3. In addition, there are yet unaccounted components to PM_{10} (biogenic organic aerosol, agricultural dust).

On an annual basis, the model shows quite variable performance for the individual aerosol components, and also when compared with measurements obtained with different sampling methods (e.g. filter-packs/denuders and high/low volume samples). Calculated SO_4 is mostly lower by around 20% compared to observations. The model underestimates total NO_3 by 11% and overestimates NO_3 in $PM_{2.5}$ by 34%, whereas calculated NO_3 in PM_{10} is quite close to measurements (only 3% bias). The overestimation of NO_3 in $PM_{2.5}$ is mainly due to too high modelled concentrations in summer and probably related to the current model's attribution of 27% of coarse NO_3 to the $PM_{2.5}$ fraction). On the other hand, NO_3 measurements are

Component	N_{stat}	Obs.	Mod.	Bias (%)	RMSE	Corr.	IOA
PM_{10} ($\mu g\ m^{-3}$)	42	13.43	9.69	-28	5.41	0.70	0.68
$PM_{2.5}$ ($\mu g\ m^{-3}$)	35	9.48	7.64	-19	2.90	0.84	0.84
SO_4^{2-}, including sea salt ($\mu g\ m^{-3}$)	37	1.59	1.28	-19	0.54	0.80	0.85
SO_4^{2-}, sea salt corrected ($\mu g\ m^{-3}$)	23	1.21	0.89	-27	0.39	0.95	0.90
SO_4^{2-} in PM_{10} ($\mu g\ m^{-3}$)	14	1.54	0.99	-35	0.67	0.60	0.62
SO_4^{2-} in $PM_{2.5}$ ($\mu g\ m^{-3}$)	15	1.78	1.40	-21	1.17	0.44	0.60
NO_3^- ($\mu g\ m^{-3}$)	18	1.85	1.65	-11	0.97	0.86	0.86
NO_3^- in PM_{10} ($\mu g\ m^{-3}$)	14	1.14	1.17	3	0.44	0.77	0.88
NO_3^- in $PM_{2.5}$ ($\mu g\ m^{-3}$)	14	1.18	1.58	34	0.69	0.90	0.90
NH_4^+ ($\mu g\ m^{-3}$)	22	0.95	0.77	-19	0.37	0.78	0.84
NH_4^+ in PM_{10} ($\mu g\ m^{-3}$)	7	0.78	0.60	-23	0.38	0.64	0.77
NH_4^+ in $PM_{2.5}$ ($\mu g\ m^{-3}$)	14	0.84	0.90	7	0.25	0.87	0.93
EC in $PM_{2.5}$ (μg(C) m^{-3})	15	0.33	0.35	5	0.18	0.82	0.88
OC in $PM_{2.5}$ (μg(C) m^{-3})	15	2.48	1.05	-58	1.68	0.81	0.52
Na+ ($\mu g\ m^{-3}$)	24	0.82	0.89	9	0.53	0.82	0.89
Na+ in PM_{10} ($\mu g\ m^{-3}$)	7	0.48	0.22	-53	0.47	0.93	0.49
Na+ in $PM_{2.5}$ ($\mu g\ m^{-3}$)	13	0.10	0.08	-18	0.05	0.70	0.81

Table 4.1: Comparison of model results and observations for 2013. Annual averages over all EMEP sites with measurements. N_{stat}= number of stations, wd=wet deposition, cp= concentration in precipitation, Corr. = spatial correlation coefficient, RMSE = root mean square error, IOA = index of agreement.

known to be prone to negative artefact due to NO_3 evaporation, especially in summer. NH_4 is quite reasonably reproduced by the model, being biased by -19% against total ammonium data (e.g. sampling without size cut-off) and only 7% bias for NH_4 in $PM_{2.5}$). NH_4 in PM_{10}) is underestimated as the model calculates only fine NH_4.

Modelled elemental carbon (EC) in $PM_{2.5}$ has a relatively small (5%) bias on the annual basis. The model performs well for all seasons, showing somewhat larger overestimation by 22% for the summer. Averaged over 4 sites with data, calculated EC in PM_{10} is 33% higher than observed, but this overestimation is mainly due to overestimation for only one site (Spanish Montseny) with less than 30% days data coverage.

Organic carbon (OC) is in general underestimated by the model, and most pronouncedly so in winter. And finally, Na from sea salt is calculated quite well by the model, with small bias and good spatial correlation compared to total Na and Na in $PM_{2.5}$ observations. Na in PM_{10} is underestimated mainly because of a larger underestimation at one Spanish site Niembro (only 6 Spanish and one German site with data available).

For evaluation of modeled mineral dust see Chapter *Mineral Dust* in the EMEP Status Report 1/2015.

Table 4.2: Statistical analysis of model calculated PM_{10} against daily observations in 2013. Obs: measured mean, Mod: calculated mean, Bias: calculated as (Mod-Obs)/Obs x100%, R: temporal correlation coefficient, and RMSE: Root mean Square Error.

Site	Name	Obs	Mod	Bias	R	RMSE	IOA
Daily							
AT02	Illmitz	20.64	11.45	-45.0	0.51	14.79	0.59
AT05	Vorhegg	7.30	8.58	18.0	0.39	8.33	0.59
AT48	Zoebelboden	9.40	10.90	16.0	0.49	7.83	0.66
CH01	Jungfraujoch	2.14	4.03	88.0	0.38	4.90	0.53
CH02	Payerne	15.47	9.57	-38.0	0.64	11.12	0.69
CH03	Taenikon	15.30	11.13	-27.0	0.59	10.34	0.70
CH04	Chaumont	7.94	9.57	21.0	0.61	6.59	0.77
CH05	Rigi	7.68	8.74	14.0	0.52	6.89	0.71
CY02	Ayia Marina	26.40	21.82	-17.0	0.70	25.58	0.74
CZ01	Svratouch	13.92	12.00	-14.0	0.33	9.23	0.59
CZ03	Kosetice	14.43	11.55	-20.0	0.39	11.42	0.55
CZ05	Churanov	8.15	9.69	19.0	0.28	8.32	0.53
DE01	Westerland/Wenningsted	17.97	12.77	-29.0	0.73	8.28	0.77
DE02	Langenbruegge/Waldhof	15.64	11.22	-28.0	0.45	10.19	0.59
DE03	Schauinsland	8.51	9.39	10.0	0.41	7.01	0.63
DE07	Neuglobsow	13.80	10.01	-27.0	0.52	8.30	0.66
DE08	Schmuecke	10.48	10.70	2.0	0.26	8.55	0.54
DE09	Zingst	13.94	10.51	-25.0	0.60	7.81	0.72
DE44	Melpitz	22.04	11.80	-46.0	0.49	13.81	0.55
ES01	Toledo	10.02	5.99	-40.0	0.61	6.60	0.70
ES06	Mahon	17.39	14.59	-16.0	0.71	6.58	0.81
ES07	Viznar	14.02	12.79	-9.0	0.71	9.20	0.80
ES08	Niembro	15.63	8.19	-48.0	0.30	10.92	0.52
ES09	Campisabalos	6.51	5.06	-22.0	0.73	3.96	0.83
ES10	Cabo de Creus	16.93	11.77	-30.0	0.46	8.99	0.60
ES11	Barcarrota	12.85	6.87	-47.0	0.59	8.72	0.64
ES12	Zarra	9.38	8.64	-8.0	0.74	5.42	0.83
ES13	Penausende	8.08	4.81	-40.0	0.67	5.27	0.71
ES14	Els Torms	11.41	8.32	-27.0	0.51	7.36	0.66
ES16	O Savinao	9.52	6.36	-33.0	0.62	5.14	0.71
ES17	Doana	14.77	9.38	-36.0	0.47	9.02	0.60
ES78	Montseny	14.18	10.53	-26.0	0.63	6.67	0.73
GB36	Harwell	13.26	11.13	-16.0	0.68	6.42	0.77
GB48	Auchencorth Moss	6.53	8.14	25.0	0.58	4.26	0.72
IT01	Montelibretti	25.02	11.68	-53.0	0.50	17.57	0.54
LV10	Rucava	14.24	7.60	-47.0	0.27	10.59	0.50
MD13	Leova II	28.09	11.37	-60.0	-0.01	30.18	0.41
PL05	Diabla Gora	15.67	9.71	-38.0	0.43	11.24	0.59
RO08	EM-3	15.31	6.63	-57.0	0.46	11.60	0.50
SE05	Bredkaelen	3.42	2.14	-37.0	0.59	2.30	0.68
SE12	Aspvreten	7.08	4.86	-31.0	0.57	4.38	0.69
SE14	Raaoe	13.35	9.42	-29.0	0.73	6.44	0.78
SI08	Iskrba	12.60	9.41	-25.0	0.58	7.55	0.72

Table 4.3: Same as Table 4.2, but against hourly and weekly observations.

Site	Name	Obs	Mod	Bias	R	RMSE	IOA
Hourly							
CZ03	Kosetice	19.28	11.37	-41.0	0.54	12.20	0.60
ES09	Campisabalos	8.95	4.82	-46.0	0.78	5.47	0.76
ES12	Zarra	11.68	8.59	-26.0	0.74	6.19	0.80
ES13	Penausende	8.85	4.78	-46.0	0.71	5.54	0.69
ES16	O Savinao	9.69	6.04	-38.0	0.71	4.66	0.70
FR09	Revin	17.87	12.32	-31.0	0.59	9.36	0.68
FR10	Morvan	12.86	8.96	-30.0	0.49	9.79	0.62
FR13	Peyrusse Vieille	14.90	10.06	-32.0	0.44	8.60	0.60
FR14	Montandon	16.42	8.96	-45.0	0.65	10.19	0.65
FR15	La Tardiere	15.83	12.64	-20.0	0.57	8.44	0.71
GB06	Lough Navar	11.39	8.86	-22.0	0.60	5.87	0.72
GB36	Harwell	16.58	12.52	-24.0	0.69	8.42	0.74
GB43	Narberth	15.59	11.16	-28.0	0.56	9.42	0.66
GB48	Auchencorth Moss	7.98	8.80	10.0	0.70	4.48	0.83
HU02	K-puszta	20.33	12.34	-39.0	0.59	11.56	0.66
MK07	Lazaropole	20.50	13.21	-36.0	0.34	16.32	0.56
NL07	Eibergen	15.39	14.49	-6.0	0.47	8.68	0.66
NL09	Kollumerwaard	17.62	13.09	-26.0	0.57	8.87	0.68
NL10	Vreedepeel	21.90	15.28	-30.0	0.46	14.86	0.60
NL44	Cabauw Wielsekade	19.75	14.95	-24.0	0.55	10.28	0.68
NL91	De Zilk	18.85	16.89	-10.0	0.52	8.80	0.69
SE11	Vavihill	13.02	8.48	-35.0	0.55	7.38	0.66
Weekly							
NO02	Birkenes II	4.90	3.79	-23.0	0.56	2.38	0.71
NO39	Kaarvatn	3.15	1.41	-55.0	0.18	2.77	0.46
NO56	Hurdal	4.55	4.30	-5.0	-0.37	3.35	0.14

Table 4.4: Statistical analysis of model calculated $PM_{2.5}$ against daily observations in 2013. Obs: measured mean, Mod: calculated mean, Bias: calculated as (Mod-Obs)/Obs x100%, R: temporal correlation coefficient, and RMSE: Root mean Square Error.

Site	Name	Obs	Mod	Bias	R	RMSE	IOA
AT02	Illmitz	15.92	9.88	-38.0	0.48	12.19	0.59
CH02	Payerne	12.92	8.68	-33.0	0.70	9.31	0.76
CH05	Rigi	6.55	7.58	16.0	0.50	6.69	0.70
CY02	Ayia Marina	12.78	14.48	13.0	0.58	8.95	0.74
CZ03	Kosetice	14.10	9.90	-30.0	0.48	9.82	0.60
DE02	Langenbruegge/Waldhof	11.79	8.54	-28.0	0.56	8.14	0.67
DE03	Schauinsland	6.79	7.89	16.0	0.41	6.03	0.63
DE07	Neuglobsow	10.05	7.76	-23.0	0.58	6.89	0.71
DE08	Schmuecke	7.97	8.78	10.0	0.36	7.27	0.60
DE44	Melpitz	18.03	9.70	-46.0	0.54	11.94	0.58
ES01	Toledo	5.34	3.92	-27.0	0.69	2.80	0.78
ES06	Mahon	5.80	7.09	22.0	0.57	4.65	0.61
ES07	Viznar	9.35	7.60	-19.0	0.65	5.22	0.76
ES08	Niembro	6.54	5.09	-22.0	0.71	3.30	0.81
ES09	Campisabalos	4.80	3.75	-22.0	0.77	2.81	0.85
ES10	Cabo de Creus	7.40	6.47	-13.0	0.52	4.41	0.70
ES11	Barcarrota	7.22	4.26	-41.0	0.59	5.33	0.64
ES12	Zarra	4.82	6.14	27.0	0.60	4.30	0.70
ES13	Penausende	4.53	3.43	-24.0	0.74	2.99	0.80
ES14	Els Torms	6.19	5.65	-9.0	0.71	3.45	0.81
ES16	O Savinao	6.69	4.31	-36.0	0.80	3.48	0.81
ES78	Montseny	11.16	8.54	-23.0	0.62	4.95	0.71
GB36	Harwell	8.98	7.57	-16.0	0.75	5.29	0.83
GB48	Auchencorth Moss	4.25	4.26	0.0	0.76	2.82	0.87
HU02	K-puszta	16.99	11.16	-34.0	0.69	9.04	0.75
IT04	Ispra	17.30	16.89	-2.0	0.37	16.57	0.61
LV10	Rucava	9.21	6.01	-35.0	0.33	6.58	0.56
NL09	Kollumerwaard	10.00	8.53	-15.0	0.69	6.52	0.81
NL10	Vreedepeel	15.07	11.58	-23.0	0.56	10.55	0.70
NL44	Cabauw Wielsekade	12.54	10.52	-16.0	0.65	7.63	0.78
NL91	De Zilk	10.01	9.70	-3.0	0.61	7.74	0.76
PL05	Diabla Gora	12.83	8.10	-37.0	0.44	9.55	0.61
SE05	Bredkaelen	1.86	1.36	-27.0	0.69	1.08	0.78
SE14	Raaoe	5.47	4.49	-18.0	0.35	4.55	0.58
SI08	Iskrba	10.56	7.89	-25.0	0.52	6.45	0.69

Table 4.5: Same as Table 4.4, but against hourly and weekly observations.

Site	Name	Obs	Mod	Bias	R	RMSE	IOA
Hourly							
CZ03	Kosetice	15.28	9.94	-35.0	0.54	10.84	0.59
FR09	Revin	12.74	9.84	-23.0	0.61	7.80	0.74
FR15	La Tardiere	11.01	9.92	-10.0	0.63	7.64	0.77
GB36	Harwell	12.66	8.41	-34.0	0.73	8.56	0.75
GB48	Auchencorth Moss	4.59	4.27	-7.0	0.80	2.87	0.89
SE11	Vavihill	6.28	5.32	-15.0	0.71	3.60	0.82
SE12	Aspvreten	5.11	3.30	-35.0	0.66	3.25	0.71
Weekly							
NO02	Birkenes II	2.92	2.14	-27.0	0.48	1.62	0.64
NO39	Kaarvatn	2.25	1.00	-56.0	0.21	2.24	0.44
NO56	Hurdal	3.14	3.22	3.0	-0.26	2.62	0.17

Table 4.6: Statistic analysis of model calculated PM_{10} components against daily observations in 2013. For explanation, see Table 4.2.

Site	Name	Obs	Mod	Bias	R	RMSE	IOA
$SO4$ in PM_{10}							
DE44	Melpitz	2.11	2.02	-4.0	0.63	1.45	0.78
ES01	Toledo	1.03	0.59	-43.0	0.66	0.69	0.63
ES06	Mahon	2.44	1.74	-29.0	0.78	1.04	0.80
ES07	Viznar	1.44	0.88	-39.0	0.71	0.86	0.76
ES08	Niembro	2.03	1.05	-48.0	0.42	1.67	0.56
ES09	Campisabalos	0.84	0.64	-24.0	0.68	0.47	0.77
ES10	Cabo de Creus	1.78	1.43	-20.0	0.76	0.79	0.85
ES11	Barcarrota	1.28	0.71	-45.0	0.67	0.93	0.61
ES12	Zarra	1.33	1.02	-23.0	0.84	0.55	0.88
ES13	Penausende	0.95	0.62	-35.0	0.71	0.54	0.73
ES14	Els Torms	1.43	1.11	-22.0	0.72	0.77	0.82
ES16	O Savinao	1.28	0.97	-24.0	0.80	0.62	0.85
ES17	Doana	2.22	1.09	-51.0	0.54	1.70	0.58
ES78	Montseny	1.34	1.58	18.0	0.76	0.77	0.86
$NO3$ in PM_{10}							
DE44	Melpitz	3.14	2.86	-9.0	0.60	2.79	0.75
ES01	Toledo	0.59	0.62	5.0	0.58	0.52	0.73
ES06	Mahon	1.57	1.34	-15.0	0.43	1.17	0.63
ES07	Viznar	0.82	1.01	23.0	0.36	0.95	0.52
ES08	Niembro	1.11	0.84	-24.0	0.43	1.22	0.65
ES09	Campisabalos	0.30	0.57	90.0	0.39	0.59	0.44
ES10	Cabo de Creus	1.75	1.34	-23.0	0.68	1.20	0.80
ES11	Barcarrota	0.84	0.71	-15.0	0.50	0.61	0.67
ES12	Zarra	1.15	1.28	11.0	0.59	1.03	0.68
ES13	Penausende	0.72	0.57	-21.0	0.65	0.58	0.77
ES14	Els Torms	0.92	1.30	41.0	0.53	1.36	0.65
ES16	O Savinao	0.73	0.73	0.0	0.62	0.61	0.76
ES17	Doana	1.44	0.97	-33.0	0.46	1.13	0.65
ES78	Montseny	0.87	2.22	155.0	0.35	2.27	0.39
$NH4$ in PM_{10}							
DE44	Melpitz	1.66	1.39	-16.0	0.67	1.20	0.77
ES01	Toledo	0.54	0.26	-52.0	0.44	0.41	0.51
ES07	Viznar	0.87	0.35	-60.0	0.33	0.82	0.50
ES08	Niembro	0.69	0.47	-32.0	0.31	0.76	0.55
ES09	Campisabalos	0.45	0.28	-38.0	0.25	0.37	0.53
ES14	Els Torms	0.82	0.42	-49.0	0.22	0.82	0.49
ES78	Montseny	0.42	1.02	143.0	0.40	0.92	0.39

Table 4.7: Continuation of Table 4.6

Site	Name	Obs	Mod	Bias	R	RMSE	IOA
EC in PM_{10}							
DE44	Melpitz	0.45	0.48	7.0	0.68	0.24	0.80
ES78	Montseny	0.22	0.61	177.0	0.20	0.51	0.27
GR02	Finokalia	0.34	0.13	-62.0	0.20	0.36	0.39
SE11	Vavihill	0.19	0.16	-16.0	0.16	0.16	0.48
SE12	Aspvreten	0.16	0.11	-31.0	0.51	0.10	0.63
OC in PM_{10}							
DE44	Melpitz	3.65	0.88	-76.0	0.40	3.74	0.46
ES78	Montseny	1.59	1.34	-16.0	0.74	0.63	0.84
GR02	Finokalia	1.79	1.17	-35.0	0.55	1.15	0.69
SE11	Vavihill	1.14	0.70	-39.0	0.24	0.83	0.50
SE12	Aspvreten	1.53	0.70	-54.0	0.60	1.26	0.58
Na in PM_{10}							
DE44	Melpitz	0.20	0.25	25.0	0.79	0.34	0.81
ES01	Toledo	0.29	0.15	-48.0	0.45	0.27	0.59
ES07	Viznar	0.33	0.20	-39.0	0.50	0.27	0.64
ES08	Niembro	1.67	0.48	-71.0	0.33	1.75	0.47
ES09	Campisabalos	0.17	0.12	-29.0	0.49	0.16	0.65
ES14	Els Torms	0.42	0.19	-55.0	0.66	0.36	0.66
ES78	Montseny	0.26	0.17	-35.0	0.81	0.21	0.87

Table 4.8: Statistic analysis of model calculated $PM_{2.5}$ components against daily observations in 2013. For explanation, see Table 4.4.

Site	Name	Obs	Mod	Bias	R	RMSE	IOA
SO4 in $PM_{2.5}$							
CY02	Ayia Marina	3.06	3.74	22.0	0.57	2.96	0.65
DE02	Langenbruegge/Waldhof	2.12	1.66	-22.0	0.44	1.89	0.59
DE03	Schauinsland	1.00	1.20	20.0	0.23	1.25	0.49
DE07	Neuglobsow	1.96	1.60	-18.0	0.66	1.48	0.77
DE08	Schmuecke	1.52	1.95	28.0	0.27	1.84	0.55
DE44	Melpitz	1.92	2.01	5.0	0.60	1.42	0.76
ES01	Toledo	0.67	0.59	-12.0	0.50	0.35	0.71
ES07	Viznar	1.29	0.91	-29.0	0.36	1.04	0.61
ES08	Niembro	1.05	1.04	-1.0	0.35	0.91	0.59
ES09	Campisabalos	0.63	0.59	-6.0	0.35	0.44	0.62
ES14	Els Torms	1.06	0.89	-16.0	0.41	0.87	0.64
ES78	Montseny	1.20	1.55	29.0	0.77	0.77	0.84
IT01	Montelibretti	1.59	1.48	-7.0	0.09	2.03	0.31
IT04	Ispra	1.92	1.10	-43.0	0.53	1.44	0.66
SI08	Iskrba	5.71	1.42	-75.0	0.65	6.03	0.50
NO3 in $PM_{2.5}$							
CY02	Ayia Marina	0.18	0.38	111.0	0.27	0.46	0.49
DE02	Langenbruegge/Waldhof	2.06	2.40	17.0	0.58	2.49	0.75
DE03	Schauinsland	0.97	2.31	138.0	0.33	2.81	0.50
DE07	Neuglobsow	1.40	2.12	51.0	0.54	2.21	0.69
DE08	Schmuecke	1.23	2.31	88.0	0.47	2.46	0.64
DE44	Melpitz	2.51	2.41	-4.0	0.60	2.57	0.75
ES07	Viznar	0.58	0.36	-38.0	0.00	0.76	0.30
ES08	Niembro	0.33	0.55	67.0	-0.06	1.13	0.13
ES09	Campisabalos	0.19	0.32	68.0	0.16	0.53	0.23
ES14	Els Torms	0.56	0.47	-16.0	0.19	0.99	0.40
ES78	Montseny	0.48	1.56	225.0	0.35	1.89	0.40
IT01	Montelibretti	1.15	0.92	-20.0	0.33	1.65	0.60
IT04	Ispra	3.66	4.96	36.0	0.37	6.90	0.59
SI08	Iskrba	1.23	1.08	-12.0	0.52	1.93	0.68
NH4 in $PM_{2.5}$							
CY02	Ayia Marina	0.92	1.13	23.0	0.54	0.76	0.70
DE02	Langenbruegge/Waldhof	1.28	1.24	-3.0	0.64	1.09	0.78
DE03	Schauinsland	0.70	1.08	54.0	0.34	1.11	0.55
DE07	Neuglobsow	1.13	1.14	1.0	0.62	0.97	0.77
DE08	Schmuecke	0.90	1.34	49.0	0.40	1.22	0.62
DE44	Melpitz	1.54	1.39	-10.0	0.64	1.13	0.77
ES01	Toledo	0.35	0.26	-26.0	0.49	0.22	0.65
ES07	Viznar	0.45	0.35	-22.0	0.35	0.32	0.60
ES08	Niembro	0.31	0.47	52.0	0.15	0.59	0.34
ES09	Campisabalos	0.26	0.28	8.0	0.30	0.25	0.55
ES14	Els Torms	0.66	0.42	-36.0	0.22	0.66	0.51
ES78	Montseny	0.44	0.96	118.0	0.46	0.81	0.45
IT04	Ispra	1.77	1.82	3.0	0.45	2.09	0.66
SI08	Iskrba	1.07	0.78	-27.0	0.57	0.82	0.72

Table 4.9: Continuation of Table 4.8

Site	Name	Obs	Mod	Bias	R	RMSE	IOA
EC in $PM_{2.5}$							
CH02	Payerne	0.41	0.31	-24.0	0.64	0.21	0.73
CH05	Rigi	0.21	0.30	43.0	0.67	0.17	0.67
CY02	Ayia Marina	0.24	0.13	-46.0	0.26	0.39	0.29
CZ03	Kosetice	0.46	0.34	-26.0	0.69	0.35	0.70
DE02	Langenbruegge/Waldhof	0.25	0.28	12.0	0.31	0.20	0.53
DE03	Schauinsland	0.09	0.28	211.0	0.14	0.23	0.32
DE07	Neuglobsow	0.26	0.28	8.0	0.19	0.24	0.43
DE08	Schmuecke	0.18	0.30	67.0	0.11	0.24	0.40
ES01	Toledo	0.09	0.09	0.0	0.72	0.05	0.81
ES09	Campisabalos	0.06	0.07	17.0	0.17	0.05	0.45
ES78	Montseny	0.20	0.59	195.0	0.25	0.50	0.27
IT04	Ispra	1.35	1.01	-25.0	0.59	1.13	0.66
NL44	Cabauw Wielsekade	2.57	0.54	-79.0	0.45	2.35	0.40
PL05	Diabla Gora	0.51	0.30	-41.0	0.53	0.39	0.64
SI08	Iskrba	0.27	0.39	44.0	0.64	0.26	0.70
OC in $PM_{2.5}$							
CH02	Payerne	2.41	0.78	-68.0	0.36	2.35	0.52
CH05	Rigi	1.36	0.96	-29.0	0.77	0.84	0.75
CY02	Ayia Marina	1.88	1.27	-32.0	0.28	1.38	0.55
CZ03	Kosetice	3.68	1.14	-69.0	0.31	3.30	0.49
DE02	Langenbruegge/Waldhof	2.40	0.74	-69.0	0.01	2.23	0.42
DE03	Schauinsland	1.27	0.83	-35.0	0.40	1.04	0.62
DE07	Neuglobsow	2.25	0.76	-66.0	0.01	2.31	0.43
DE08	Schmuecke	1.73	0.70	-60.0	0.03	2.20	0.35
ES01	Toledo	1.79	0.67	-63.0	0.81	1.29	0.62
ES09	Campisabalos	1.79	0.62	-65.0	0.18	1.92	0.43
ES78	Montseny	1.35	1.33	-1.0	0.73	0.60	0.85
IT04	Ispra	6.36	2.81	-56.0	0.34	6.31	0.49
NL44	Cabauw Wielsekade	0.36	0.77	114.0	0.43	0.58	0.37
PL05	Diabla Gora	3.04	1.07	-65.0	0.04	3.28	0.42
SI08	Iskrba	3.26	1.24	-62.0	0.34	2.54	0.48
Na in $PM_{2.5}$							
CY02	Ayia Marina	0.18	0.21	17.0	0.54	0.17	0.72
DE02	Langenbruegge/Waldhof	0.13	0.14	8.0	0.80	0.11	0.87
DE03	Schauinsland	0.04	0.03	-25.0	0.63	0.05	0.77
DE07	Neuglobsow	0.11	0.11	0.0	0.74	0.10	0.85
DE08	Schmuecke	0.05	0.06	20.0	0.52	0.10	0.69
DE44	Melpitz	0.06	0.08	33.0	0.67	0.11	0.75
ES01	Toledo	0.06	0.05	-17.0	0.12	0.05	0.45
ES07	Viznar	0.23	0.07	-70.0	-0.03	0.35	0.34
ES08	Niembro	0.22	0.16	-27.0	0.19	0.30	0.46
ES09	Campisabalos	0.06	0.04	-33.0	0.01	0.06	0.40
ES14	Els Torms	0.11	0.06	-45.0	-0.09	0.10	0.36
ES78	Montseny	0.06	0.06	0.0	0.77	0.08	0.77
SI08	Iskrba	0.03	0.02	-33.0	0.67	0.03	0.78